Restless Leg Syndrome and Sleep Disorders in Patients with Rheumatoid Arthritis and Its Relation with Anemia Parameters

Salih Demir[1], Adem Kucuk[2,*], Mustafa Altas[3], Erkan Cure[4]

ABSTRACT

Objectives: We aimed to investigate the prevalence of restless legs syndrome (RLS) and sleep disorders in patients with rheumatoid arthritis (RA), and the association of iron deficiency with them.

Materials and methods: The study included 72 patients with RA (59 females, 13 males), and 50 healthy control subjects (57 females, 15 males). Assessments were made using the International RLS Rating Scale, Pittsburgh Sleep Quality Index (PSQI), Epworth Sleepiness Scale, Fatigue Severity Scale (FSS), Beck anxiety and depression index and the SF-36 quality of life scores.

Results: We found that the frequency of RLS in RA patients was 29.1% and 13.8% in healthy control ($p = 0.021$). RA patients had 44.4% iron deficiency and 5.5% anemia of chronic disease. We found that 52.3% of patients with iron deficiency had RLS. There was an independent relationship between present of RLS and FSS (Beta [β] = 0.317, $p = 0.005$) and total iron binding capacity (TIBC) (β = 0.244, $p = 0.031$). There was an independent relationship between RLS severity score and PSQI (β = 0.264, $p = 0.025$) and social functionality (β = 0.302, $p = 0.009$).

Conclusion: The prevalence of iron deficiency is high in RA in the developing countries. Analysis obtained in patients with RA is suggestive of an association between iron deficiency and increased frequency of RLS. The presence of RLS in patients with RA negatively affects sleep quality, psychiatric status, and quality of life of patients with RA. TIBC value may be a predictive marker for early detection of RLS in patients with RA.

KEYWORDS

rheumatoid arthritis; restless legs syndrome; sleep disorders; iron deficiency; total iron binding capacity

AUTHOR AFFILIATIONS

[1] Department of Internal Medicine, Necmettin Erbakan University, Konya, Turkey
[2] Division of Rheumatology, Department of Internal Medicine, Necmettin Erbakan University, Konya, Turkey
[3] Department of Neurology, Necmettin Erbakan University, Konya, Turkey
[4] Department of Internal Medicine, Ota & Jinemed Hospital, Istanbul, Turkey
* Corresponding author: Division of Rheumatology, Department of Internal Medicine, Necmettin Erbakan University, Konya, Turkey; e-mail: drademk@yahoo.com

Received: 21 January 2021
Accepted: 15 May 2021
Published online: 11 November 2021

Acta Medica (Hradec Králové) 2021; 64(3): 137–144
https://doi.org/10.14712/18059694.2021.24

INTRODUCTION

Rheumatoid arthritis (RA) affects approximately 0.5% to 1% of the population worldwide (1). RA is a systemic, chronic autoimmune disease that symmetrically leads to arthritis in the joints. Environmental and genetic factors play a role in the pathogenesis of RA, and its etiology is unclear (1, 2). It is three to four times more common in women than in men. In RA, patients may develop joint deformities, loss of function, and workforce loss due to bone erosions (1, 2). RA can affect the central and peripheral nervous system and many organs. Anemia is common in patients with RA and has multifactorial pathogenesis (3). Although most types of anemia can be seen in RA patients, iron deficiency anemia (IDA) and anemia of chronic disease (ACD) are common (3). In patients with RA, IDA is mostly caused by chronic blood loss from the gastrointestinal tract due to gastritis (due to the use of non-steroidal anti-inflammatory drugs), peptic ulcer, or diaphragmatic hernia. Most patients with IDA are asymptomatic (4).

The psychological effects of RA can be seen in many areas of life such as family life and social relationships, therefore, it can lead to mood disorders (5). These mood disorders can cause pain, increased disease activity, cytokine release, immune-modulatory responses, and sleep disorders in patients. The sleep structure is usually normal, but sleep is interrupted with increased arousals and movements during sleep (6). Studies have reported that sleep disturbance and difficulty maintaining sleeping are seen in 50–75% (7).

Restless leg syndrome (RLS) is a common disease associated with chronic, sensorimotor motion disorder, especially holding the lower limb (8). In this syndrome, especially in the period when the patient is inactive, such as evening and night, paresthesia and restlessness occur. The patient is partially or completely relaxed with movement (8). Although RLS pathophysiology is not fully understood, dopamine dysfunction and a decrease of cerebral iron and ferritin levels play a critical role in the central nervous system (9). RLS is a common disease accompanying RA. The patient's quality of life can be improved by rapid diagnosis and treatment of RLS (10).

Several studies in the literature have proven the presence of RLS in patients with RA (10–14). In this study, we aimed to show the frequency of IDA and the relationship of iron deficiency with RLS in RA patients. Second, we aimed to investigate the effects of RLS on sleep disorder, psychological conditions, and quality of life in RA.

MATERIAL AND METHOD

Seventy-two patients diagnosed as RA according to ACR/EULAR 2010 Rheumatoid Arthritis Classification Criteria (15) and followed up in our hospital's Rheumatology Outpatient Clinic were included in the study. Seventy-two healthy people with sociodemographic characteristics similar to the group of patients without known systemic disease were included in the study as a control group. Patients with known liver, kidney, thyroid disease, hypertension, diabetes mellitus, other systemic connective tissue diseases, malignancy, chronic neurological disease, pregnancy, alcohol dependence were excluded in the study. The patient and the control group were interviewed face-to-face and evaluated for RLS symptoms. Patients who ensure four of the following criteria recommended by the International Working Group were diagnosed with RLS: (i) the urge to move limbs with senses of paresthesia/dysesthesia; (ii) the need to move and feel relaxed when moving; (iii) exacerbation of symptoms while resting and relief of symptoms when moving; (iv) exacerbation of symptoms in the evening/night. The severity of RLS was determined using the IRLSSG-RS scale in both groups (16, 17).

BECK DEPRESSION INVENTORY (BDI)

Depression levels were evaluated with the BDI comprising 21 items ranging from 0 to 3. The highest score is 63. One of the most commonly used self-rated depression scales, BDI is adaptable to any age group and considered highly reliable (18).

BECK ANXIETY INVENTORY (BAI)

BAI is a Likert-type self-report inventory applied to determine the prevalence and intensity of anxiety symptoms experienced by the individual. The BAI scale tests subjective anxiety and somatic symptoms such as dizziness, difficulty breathing, dizziness, flushing, and heartbeat. The highest score that can be obtained from this test is 63 and covers 21 symptoms (19).

FATIGUE SEVERITY SCALE

FSS is a questionnaire comprising 9 questions in total. Fatigue severity is assessed in different situations during the past week. Items are scored on a 7-point scale. 1 = strongly disagree and 7 = strongly agree. The average FSS score is found by dividing the total score by 9. The score is interpreted as ≥4 fatigue. Higher scores show a higher level of fatigue (20).

PITTSBURGH SLEEP QUALITY INDEX (PSQI)

PSQI is used to assess sleep quality for 1 month. Includes nineteen separate items and seven component points; by collecting these points, a general score between 0 and 21 is obtained. Higher scores represent subjective sleep quality disorder. PSQI score> 5 is considered sleep disturbance (21).

EPWORTH SLEEPINESS SCALE (ESS)

The ESS which includes eight items related to falling asleep or sleepiness in eight different daily living activities is used to assess daytime sleepiness. The ESS score ranges from 0 to 24, and higher scores show more be sleep state during the day (22).

36-ITEM SHORT-FORM HEALTH SURVEY (SF-36) QUESTIONNAIRE

SF-36 is a general health-related quality-of-life questionnaire used to score for eight subscales, including physical

function, role-physical, role-emotional, social functionality, general health, mental health, vitality, and physical pain. These subscales are combined to create two high-level summaries called physical and mental health component summaries (23).

ETHICAL ISSUE

Before the study, the voluntary patient consent form was obtained from the patient and control groups. We obtained approval for the study from the local ethics committee (2019/1823).

BIOCHEMICAL PARAMETERS

Venous blood samples from both patients and the control group were collected after 10 to 12 hours of fasting. Glucose blood urea nitrogen, creatinine, lipid panel, and ALT were studied with the photometric method of the Abbott Architect C16000 analyzer. C-reactive protein (CRP) was studied with the nephelometric method of Coulter Immage 800 device. HDL was analyzed using a direct enzymatic method without precipitation. Hematological tests were analyzed by the Abbott Cell Dyn Ruby analyzer. Erythrocyte sedimentation rate (ESR) was analyzed with the automated device Westerr (Eventus vacuplus ES 100).

The diagnosis of IDA and ACD was made according to the current guideline. According to the hemoglobin, ferritin, and transferrin saturation values, the patients and the control group were divided into three groups as IDA, ACD, and normal (24).

STATISTICAL ANALYSIS

All statistical analyzes were done with SPSS 20 program. Results are given as mean ± standard deviation, median (minimum-maximum), and n (percent). Whether the groups showed homogeneous distribution was evaluated with the Kolmogorov-Smirnov Test. Data showing homogenous distribution were evaluated by Student T-Test and non-homogeneous data were evaluated by Mann Whitney U Test. Categorical data were analyzed with Chi-square test. Pearson correlation test and Spearman Rank test were used for correlation analysis. Independent variables affecting the RLS severity score were analyzed by linear regression analysis. A p-value <0.05 was considered significant.

RESULTS

Age (51.9 ± 11.4 vs 49.5 ± 11.2 years, p = 0.215), gender (F/M: 59/13 vs 57/15, p = 0.417), and body mass index (29.0 ± 5.5 vs

Tab. 1 Sociodemographic data of the patient and control groups.

Parameters	RA (n = 72)	Control (n = 72)	P value
Age (years) (mean ± SD)	51.9 ± 11.4	49.5 ± 11.2	0.215
Gender (F/M) (n)	59/13	57/15	0.417
BMI (kg/m²) (mean ± SD)	29.0 ± 5.5	29.0 ± 4.9	0.941
DASH-28	2.8 ± 1.0		
Anti-CCP + (n, %)	40 (55.6)	0	
RF + (n, %)	37 (51.4)	0	
Disease duration (years)	3 (1–18)		
Smoking (n)	8	16	0.016
Drinking (n)	0	2	0.248
Hypertension (n)	23	16	0.130
Osteoporosis (n)	2	1	0.500
Hydroxychloroquine (n)	39		
Steroid (n)	31		
Methotrexate (n)	37		
NSAIDs (n)	12	3	0.012
Leflunomide (n)	25		
Salazopyrin (n)	27		
Infliximab (n)	1		
Etanercept (n)	0		
Golimumab (n)	4		
Certolizumab (n)	2		
Tocilizumab (n)	7		
Rituximab (n)	1		

Abbreviations: Ra, rheumatoid arthritis; F, female; M, male; BMI, body mass index; DASH-28, The Disease Activity Score-28 for Rheumatoid Arthritis; Anti-CCP, anti-cyclic citrullinated peptide; RF, rheumatoid factor; NSAIDs, non-selective non-steroidal anti-inflammatory agents.

29.0 ± 4.9 kg/m^2, p = 0.941) values of patients with RA were similar to the control group. Anti-CCP was positive in 55.6% of patients and RF was positive in 51.4% of patients. While 15 (20.8%) of the patients were using biological agents, the remaining patients were receiving DMARD therapy. All sociodemographic characteristics of the patients are given in Table 1.

The hemoglobin level of the patients (p = 0.011) was significantly lower than the control group. The patients' iron level (68.9 ± 36.1 vs 78.6 ± 34.3) was lower than the control group, but not significant. The ferritin (53.3 [4.0–655.0] vs 45.7 [2.0–432.0]) and total iron-binding capacity (TIBC) (266.4 ± 73.5 vs 261.2 ± 71.3) values of the patients were similar to the ferritin and TIBC values of the control group. The Vitamin D level (18.0 ± 8.8 vs 14.3 ± 8.2, p = 0.009) of the RA group was higher than the control group. ESR, and CRP values of RA patients were higher than the control group. The albumin value of RA patients was lower than the control group. All laboratory results of the patients are seen in Table 2.

Thirty-two patients had IDA, and 11 of them had RLS. Four patients had ACD, and 1 of them had RLS. In the control group, seventeen individuals had IDA, and 4 of them had RLS. Four of 10 RLS individuals had IDA (Figure 1).

The numbers of RLS positive patients were 2-fold more than the control group (29.1% vs 13.8%, p = 0.021). The RLS severity scale of both groups was similar. ESS was slightly higher in the RA group than control but were not significant. The PSQI value of the RA group was significantly higher than the control group. BAI and BDI values of RA patients were significantly higher than the control group. Physician visual analogue scales (VAS) and patient VAS values of the patient group were significantly lower than the control group. In the patient group, SF-36's physical function, physical role, vitality, social function, pain, general health perception scores were significantly lower than the control group. The emotional role, mental health, and health status change values of SF-36 in the patient group were also lower than the control group. But it was not statistically significant. All results and p values are seen in Table 3.

Tab. 2 Biochemical results of the patient and control groups.

Parameters	RA (n = 72)	Control (n = 72)	P value
WBC (×109/L)	7.7 ± 3.6	7.8 ± 2.1	0.852
Neutrophils	4.8 ± 3.0	4.6 ± 1.7	0.757
Lymphocytes	2.1 ± 0.8	2.3 ± 0.7	0.042
Hemoglobin (g/dL)	12.7 ± 1.7	13.5 ± 1.7	0.011
RDW	14.6 ± 2.1	13.6 ± 1.6	0.001
Platelets (×109/L)	294.1 ± 78.9	280.9 ± 75.5	0.272
CRP (mg/dL)	4.1 (0.5–96.0)	3.1 (0.5–37.0)	0.021
ESR (mm/h)	16.5 (2.0–72.0)	11.0 (2.0–48.0)	0.007
FPG (mg/dL)	97.4 ± 13.9	99.6 ± 16.6	0.380
Creatinine (mg/dL)	0.70 ± 0.1	0.74 ± 0.1	0.152
Sodium (mEq/L)	140.4 ± 2.3	140.0 ± 1.7	0.318
Potassium (mEq/L)	4.4 ± 0.5	4.4 ± 0.4	0.709
Calcium (mg/dL)	9.3 ± 0.4	9.4 ± 0.4	0.135
Total cholesterol (mg/dL)	183.4 ± 40.2	185.6 ± 41.0	0.742
Triglyceride (mg/dL)	144.6 ± 84.9	144.6 ± 72.0	0.999
HDL (mg/dL)	52.1 ± 16.1	48.4 ± 12.3	0.122
LDL (mg/dL)	101.5 ± 32.2	106.2 ± 36.4	0.413
Albumin (g/dL)	4.2 ± 0.3	4.4 ± 0.3	0.001
AST (IU/L)	17.3 ± 7.6	16.4 ± 6.1	0.447
ALT (IU/L)	18.8 ± 9.4	18.7 ± 8.8	0.934
Iron ((µg/dl)	68.9 ± 36.1	78.6 ± 34.3	0.099
TIBC (ug/dL)	266.4 ± 73.5	261.2 ± 71.3	0.663
Ferritin (ng/ml)	53.3 (4.0–655.0)	45.7 (2.0–432.0)	0.876
Transferrin saturation (%)	29.8 ± 22.4	34.0 ± 20.3	0.249
TSH (mU/L)	1.9 ± 1.2	1.9 ± 1.0	0.978
Vitamin B_{12} (pg/mL)	378.4 ± 207.5	341.3 ± 169.5	0.242
Folic acid (ng/ml)	9.0 ± 4.3	8.4 ± 3.6	0.395
Vitamin D (ng/mL)	18.0 ± 8.8	14.3 ± 8.2	0.009

Abbreviations: RA, rheumatoid arthritis; WBC, white blood cell count; RDW, red blood cell distribution width; CRP, C-reactive protein; ESR, erythrocyte sedimentation rate; FPG, fasting plasma glucose; HDL, high density lipoprotein; LDL, low-density lipoprotein; AST, aspartate aminotransferase; ALT, alanine aminotransferase; TIBC, total iron binding capacity; TSH, thyroid stimulating hormone.

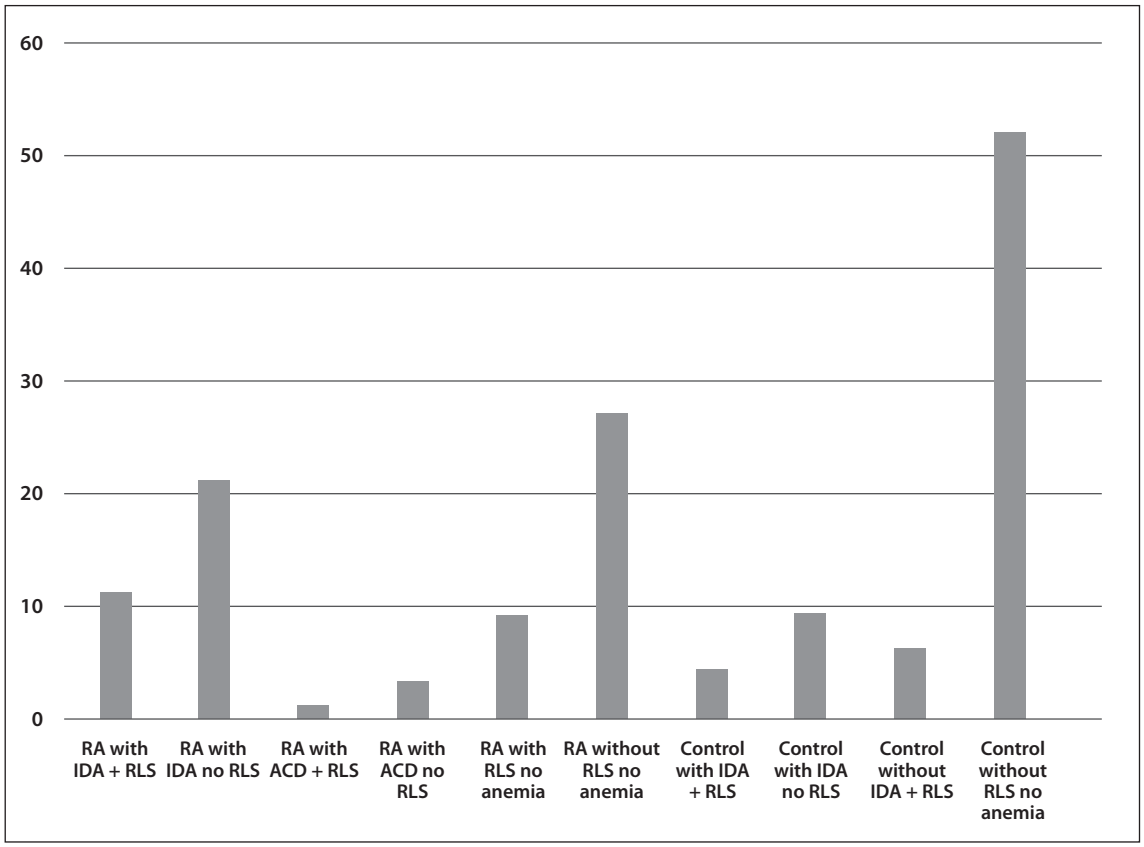

Fig. 1 Prevalence of RLS in RA patients with and without anemia.

Tab. 3 Evaluation of sleep and life quality of patient and control groups.

Parameters	RA (n = 72)	Control (n = 72)	P value
RLS (n, %)	21 (29.1)	10 (13.8)	0.021
RLS (F/M)	17/4	8/0	0.188
RLS severity score	12.5 ± 5.2	13.1 ± 6.4	0.830
ESS	5.3 ± 3.2	4.4 ± 3.4	0.141
PSQI	6.5 ± 3.5	4.3 ± 3.0	<0.001
PSQI ≥ 5, n (%)	43 (59.7)	23 (31.9)	0.001
ISI	9.0 (2.0–20.0)	2.0 (0.0–16.0)	0.001
FSS	3.3 ± 1.5	2.8 ± 1.6	0.094
BAI	8.5 ± 5.7	6.1 ± 4.8	0.008
BDI	9.7 ± 6.0	7.0 ± 5.6	0.007
Physical functioning	61.6 ± 21.2	75.9 ± 22.8	<0.001
Role physical	43.4 ± 41.5	63.1 ± 44.7	0.007
Role emotional	74.7 ± 32.1	83.4 ± 32.2	0.108
Vitality	45.6 ± 13.7	50.2 ± 14.3	0.049
Mental health	58.8 ± 10.0	61.7 ± 9.9	0.086
Social functioning	80.6 ± 19.7	89.5 ± 15.4	0.003
Bodily pain	68.8 ± 21.5	78.8 ± 24.2	0.010
General health	39.2 ± 16.1	47.1 ± 18.6	0.007
Change observed in health	45.2 ± 19.3	48.0 ± 25.1	0.458
Physician VAS	2.3 ± 1.4	1.2 ± 0.9	<0.001
Patients VAS	3.1 ± 1.5	1.8 ± 1.2	<0.001

Abbreviations: RA, rheumatoid arthritis; RLS, restless leg syndrome; ESS, Epworth Sleepiness Scale; PSQI, Pittsburgh Sleep Quality Index; ISI, Insomnia Severity Index; FSS, Fatigue Severity Scale; BAI, beck anxiety inventory; BDI, Beck Depression Index; VAS, visual analogue scale.

When correlation analysis was performed in the patient group, we found that the RLS severity score was positively associated with PSQI, Insomnia Severity Index, Fatigue Severity Scale, BAI, BDI, pain, and TIBC values. We found a negative correlation between the RLS severity score and energy/vitality, mental health, and social functionality. Correlation analysis results are seen in Table 4.

Tab. 4 Correlation analysis results of patients.

Parameters	RLS severity score	
	r value	p value
PSQI	0.456	0.001
ISI	0.367	0.003
FSS	0.431	0.001
BAI	0.430	<0.001
BDI	0.339	0.006
Vitality	-0.389	0.001
Mental health	-0.266	0.033
Social functioning	-0.412	0.001
Bodily pain	0.291	0.018
TIBC	0.268	0.031

Abbreviations: RLS, restless leg syndrome; PSQI, Pittsburgh Sleep Quality Index; ISI, Insomnia Severity Index; Fatigue Severity Scale; BAI, beck anxiety inventory; BDI, beck depression inventory; TIBC, total iron binding capacity.

In the multivariate regression analysis, there was an independent relationship between present of RLS and fatigue severity scale (Beta [β] = 0.317, p = 0.005) and TIBC (β = 0.244, p = 0.031). There was an independent relationship between RLS severity score and PSQI (β = 0.264, p = 0.025) and social functionality (β = 0.302, p = 0.009) (Table 5).

Tab. 5 Stepwise linear regression analysis.

Dependent variable	Independent Variables	Beta regression coefficient	P value
RLS	FSS	0.317	0.005
	TIBC	0.244	0.031
RLS severity score	PSQI	0.366	0.002
	Social functioning	0.302	0.009

Abbreviations: RLS, restless leg syndrome; FSS, Fatigue Severity Scale; TIBC, Total iron binding capacity; PSQI, Pittsburgh Sleep Quality Index.

DISCUSSION

In several studies, the frequency of RLS in RA patients was between 20–30%, and in healthy controls was found between 2–10% (10, 13, 14, 25). In our study, we found that the frequency of RLS in RA patients was 29.1% and 13.8% in healthy control. In the literature, only one study reported the frequency of RLS in RA as 63% (12). Since both diseases are more common in women, RLS is expected to be more common in female RA patients. Previous studies and our study reveal that RLS is more common in female RA patients (25).

RLS is also associated with other rheumatological diseases. The frequency of RLS was reported as 30.6% in systemic lupus erythematosus (SLE), 29.4% in Behçet's disease, 30.8% in ankylosing spondylitis, 40.7% in systemic sclerosis, and 64% in psoriatic arthritis (8,26). RLS is often associated with immune-based diseases such as Crohn, multiple sclerosis, psoriasis. In autoimmune diseases that damage the dopaminergic system such as Parkinson and SLE, the frequency of RLS has been reported to increase (27, 28). Previous studies suggest that symptoms in RLS patients occur because of damage to the dopaminergic pathway. In RLS patients, dopamine receptor agonists significantly relieve the patients' clinic (26–28). A better-known mechanism in RLS etiology is iron deficiency. The low iron level in the serum leads to an increase in the extracellular dopamine level, thereby reducing D2 dopaminergic receptors in the brain tissue (29). The formation of levodopa from tyrosine is catalyzed by the tyrosine hydroxylase enzyme, and this step is the rate-limiting step in dopamine synthesis. In iron deficiency, dopamine synthesis is reduced (30).

RA is a chronic inflammatory disease. Chronic inflammation causes iron to be trapped in macrophages and reduced iron supply to the bone marrow. A previous study reported the frequency of IDA in RA patients with RLS was 4.7% and the frequency of other anemia types was 3.1% (25). The frequency of IDA in patients with RA is between 30–60% in developing countries (4). Our RA patients had 44.4% IDA and 5.5% ACD. We found that 52.3% of patients with IDA had RLS and 25% of patients with ACD had RLS. When patients with both IDA and ACD were examined together, 57.1% of RA patients with RLS had anemia. In the current study, the control group had 23.6% IDA and individuals with IDA had 23.5% RLS. In the control group, 25% of individuals with RLS had DEA. While the TIBC level of our patients was like the control group, the iron level was lower than the control group. Although the ferritin values of our patients were not statistically significant, they were slightly higher than the control group. Ferritin is an acute-phase reactant. The ferritin values of our patients may be higher due to chronic inflammation than healthy control. Ferritin may not always be a good marker in demonstrating iron deficiency (24). Transferrin saturation is a more specific marker than ferritin in demonstrating iron deficiency (24). It is obtained by dividing the serum iron value by the serum TIBC value. TIBC increase alone is a strong marker in diagnosing IDA (31). In the regression analysis, we found an independent relationship between TIBC and RLS scores. In RA patients, TIBC can be a strong marker for the RLS severity score.

Vitamin D is an immune-modulating vitamin. Vitamin D is known to protect dopaminergic neurons against toxic substances. Therefore, vitamin D deficiency has been associated with RLS (32). In our study, vitamin D levels of RA patients were lower than normal, but higher than the control group. The relationship between RA and vitamin

D deficiency is known (33). We did not have any patients using vitamin D supplements; however, most RA patients may receive vitamin D therapy intermittently. It has been reported that vitamin D treatment does not improve RLS symptoms (34). We did not find a significant relationship between RLS and vitamin D in regression analysis.

Since RA is a disease with inflammation, many pro-inflammatory cytokine levels such as interleukin (IL)-1, IL-6, and tumor necrosis factor (TNF)-alpha an increase in RA patients (2). Some cytokines such as IL-4, IL-10, IL-13, and transforming growth factor (TGF)-beta have been reported to adversely affect the non-REM sleep phase and lead to sleep disturbance (35). Some cytokines, such as TNF-alpha, show the diurnal rhythm. In RA patients, improvement of sleep quality with TNF-alpha blockade suggests that TNF-alpha and other pro-inflammatory cytokines are responsible for sleep disturbance (36). Previous studies have reported between 62–63% sleep disturbance in RA patient's disturbance (12, 36). We found that 59.7% of our patients had sleep quality impairment. In the correlation analysis, we found a strong relationship between RLS score and PSQI, insomnia severity index, FSS, and vitality.

The presence of anxiety and depression in RA patients has been reported in the literature (37). RA is associated with psychological disorders due to pain, physical disabilities, and restricting one's work, family, and social life. This results in anxiety, depression, and a sense of helplessness. Depression and anxiety are psychiatric disorders frequently seen in RA (38). Quality of life disorder, anxiety, and depression are also associated with RLS (39). In the correlation analysis, we found a strong relationship between RLS score and BAI and BDI tests. We also found a negative relationship between the RLS severity score and mental health, social functionality, and pain. According to our results, RA and RLS coexistence significantly affect patients with RA psychologically and socially.

CONCLUSION

The prevalence of IDA is high in patients with RA in developing countries. Analysis obtained in patients with RA is suggestive of an association between iron deficiency and increased frequency of RLS. The presence of RLS in patients with RA negatively affects sleep quality, psychiatric status, and quality of life of patients with RA. TIBC value may be a predictive marker for early detection of RLS in patients with RA.

REFERENCES

1. Gibofsky A. Overview of epidemiology, pathophysiology, and diagnosis of rheumatoid arthritis. Am J Manag Care 2012; 18: S295–S302.
2. Tuzcu A, Baykara RA, Omma A, et al. Thiol/Disulfide homeostasis in patients with rheumatoid arthritis. Rom J Intern Med 2019 ;57: 30–6.
3. Padjen I, Öhler L, Studenic P, Woodworth T, Smolen J, Aletaha D. Clinical meaning and implications of serum hemoglobin levels in patients with rheumatoid arthritis. Semin Arthritis Rheum 2017; 47: 193–8.
4. Goyal R, Das R, Bambery P. Serum transferrin receptor-ferritin index shows concomitant iron deficiency anemia and anemia of chronic disease is common in patients with rheumatoid arthritis in north India. Indian J Pathol Microbiol 2008; 51: 102–4.
5. Katchamart W, Narongroeknawin P, Chanapai W, Thaweeratthakul P, Srisomnuek A. Prevalence of and factors associated with depression and anxiety in patients with rheumatoid arthritis: A multicenter prospective cross-sectional study. Int J Rheum Dis 2020; 23: 302–8.
6. Abad VC, Sarinas PS, Guilleminault C. Sleep and rheumatologic disorders. Sleep Med Rev 2008; 12: 211–28.
7. Pehlivan S, Karadakovan A, Pehlivan Y, Onat AM. Sleep quality and factors affecting sleep in elderly patientswith rheumatoid arthritis in Turkey. Turk J Med Sci 2016; 46: 1114–21.
8. Sandikci SC, Colak S, Aydoğan Baykara R, et al. Evaluation of restless legs syndrome and sleep disorders in patients with psoriatic arthritis. Z Rheumatol 2019; 78: 987–95.
9. Ekbom K, Ulfberg J. Restless legs syndrome. J Intern Med 2009; 266: 419–31.
10. Gjevre JA, Taylor Gjevre RM. Restless legs syndrome as a comorbidity in rheumatoid arthritis. Autoimmune Dis 2013; 2013: 352782.
11. Urashima K, Ichinose K, Kondo H, Maeda T, Kawakami A, Ozawa H. The prevalence of insomnia and restless legs syndrome among Japanese outpatients with rheumatic disease: A cross-sectional study. PLoS One 2020; 15: e0230273.
12. Mustafa M, Bawazir Y, Merdad L, et al. Frequency of sleep disorders in patients with rheumatoid arthritis. Open Access Rheumatol 2019; 11: 163–71.
13. Taylor-Gjevre RM, Gjevre JA, Nair BV. Increased nocturnal periodic limb movements in rheumatoid arthritis patients meeting questionnaire diagnostic criteria for restless legs syndrome. BMC Musculoskelet Disord 2014; 15: 378.
14. Ishaq M, Sualeh Muhammad J, Hameed K. Risk of restless legs syndrome in low socioeconomic rheumatoid arthritis patients. Mod Rheumatol 2013; 23: 705–8.
15. Villeneuve E, Nam J, Emery P. 2010 ACR-EULAR classification criteria for rheumatoid arthritis. Rev Bras Reumatol 2010; 50: 481–3.
16. Allen RP, Picchietti D, Hening WA, Trenkwalder C, Walters AS, Montplaisi J. Restless legs syndrome: diagnostic criteria, special considerations, and epidemiology. A report from the restless legs syndrome diagnosis and epidemiology workshop at the national institutes of health. Sleep Med 2003; 4: 101–19.
17. Walters AS, LeBrocq C, Dhar A, et al. Validation of the international restless legs syndrome study group rating scale for restless legs syndrome. Sleep Med 2003; 4: 121–32.
18. Beck AT, Ward CH, Mendelson M, Mock J, Erbaugh J. An inventory for measuring depression. Arch Gen Psychiatry 1961; 4: 561–71.
19. Beck AT, Epstein N, Brown G, Steer RA. An inventory for measuring clinical anxiety: psychometric properties. J Consult Clin Psychol 1988; 56: 893–7.
20. Valko PO, Bassetti CL, Bloch KE, Held U, Baumann CR. Validation of the fatigue severity scale in a Swiss cohort. Sleep 2008; 31: 1601–7.
21. Buysse DJ, Reynolds CF 3rd, Monk TH, Hoch CC, Yeager AL, Kupfer DJ. Quantification of subjective sleep quality in healthy elderly men and women using the Pittsburgh Sleep Quality Index (PSQI). Sleep 1991; 14: 331–8.
22. Johns MWA. New method for measuring daytime sleepiness: the Epworth sleepiness scale. Sleep 1991; 14: 540–5.
23. Ware JE Jr, Sherbourne CD. The MOS 36-item short-form health survey (SF-36). I. Conceptual framework and item selection. Med Care 1992; 30: 473–83.
24. Muñoz M, García-Erce JA, Remacha ÁF. Disorders of iron metabolism. Part II: iron deficiency and iron overload. J Clin Pathol 2011; 64: 287–96.
25. Taylor-Gjevre RM, Gjevre JA, Skomro R, Nair B. Restless legs syndrome in a rheumatoid arthritis patient cohort. J Clin Rheumatol 2009; 15: 12–15.
26. Kucuk A, Uslu AU, Yilmaz R, Salbas E, Solak Y, Tunc R. Relationship between prevalence and severity of restless legs syndrome and anemia in patients with systemic lupus erythematosus. Int J Rheum Dis 2017; 20: 469–73.
27. Kunas RC, McRae A, Kesselring J, Villiger PM. Antidopaminergic antibodies in a patient with a complex autoimmune disorder and rapidly progressing Parkinson's disease. J Allergy Clin Immunol 1995; 96: 688–90.
28. Ballok DA, Earls AM, Krasnik C, Hoffman SA, Sakic B. Autoimmune-induced damage of the midbrain dopaminergic system in lupus-prone mice. J Neuroimmunol 2004; 152: 83–97.
29. Earley CJ, Connor JR, Beard JL, Malecki EA, Epstein DK, Allen RP. Abnormalities in CSF concentrations of ferritin and transferrin in restless legs syndrome. Neurology 2000; 54: 1698–700.
30. Connor JR, Wang XS, Allen RP, et al. Altered dopaminergic profile in the putamen and substantia nigra in restless leg syndrome. Brain 2009; 132: 2403–12.

31. Hawkins RC. Total iron binding capacity or transferrin concentration alone outperforms iron and saturation indices in predicting iron deficiency. Clin Chim Acta 2007; 380: 203–7.
32. Wali S, Alsafadi S, Abaalkhail B, et al. The Association Between Vitamin D Level and Restless Legs Syndrome: A Population-Based Case-Control Study. J Clin Sleep Med 2018; 14: 557–64.
33. Kostoglou-Athanassiou I, Athanassiou P, Lyraki A, Raftakis I, Antoniadis C. Vitamin D and rheumatoid arthritis. Ther Adv Endocrinol Metab 2012; 3: 181–7.
34. Wali SO, Abaalkhail B, Alhejaili F, Pandi-Perumal SR. Efficacy of vitamin D replacement therapy in restless legs syndrome: a randomized control trial. Sleep Breath 2019; 23: 595–601.
35. Kapsimalis F, Richardson G, Opp MR, Kryger M. Cytokines and normal sleep. Curr Opin Pulm Med 2005; 11: 481–484.
36. Taylor-Gjevre RM, Gjevre JA, Nair BV, Skomro RP, Lim HJ. Improved Sleep Efficiency after Anti-Tumor Necrosis Factor α Therapy in Rheumatoid Arthritis Patients. Ther Adv Musculoskelet Dis 2011; 3: 227–33.
37. Lwin MN, Serhal L, Holroyd C, Edwards CJ. Rheumatoid Arthritis: The Impact of Mental Health on Disease: A Narrative Review. Rheumatol Ther 2020; 7: 457–71.
38. Isik A, Koca SS, Ozturk A, Mermi O. Anxiety and depression in patients with rheumatoid arthritis. Clin Rheumatol 2007; 26: 872–8.
39. Sevim S, Dogu O, Kaleagasi H, Aral M, Metin O, Camdeviren H. Correlation of anxiety and depression symptoms in patients with restless legs syndrome: a population based survey. J Neurol Neurosurg Psychiatry 2004; 75: 226–30.

A Comparison of the Neuroprotective and Reactivating Efficacy of a Novel Bispyridinium Oxime K870 with Commonly Used Pralidoxime and the Oxime HI-6 in Tabun-Poisoned Rats

Jiří Kassa[1,*], Jana Hatlapatková[1], Jana Žďárová Karasová[1], Vendula Hepnarová[1], Filip Caisberger[2], Jaroslav Pejchal[1]

ABSTRACT

Aim: The comparison of neuroprotective and central reactivating effects of the oxime K870 in combination with atropine with the efficacy of standard antidotal treatment in tabun-poisoned rats.

Methods: The neuroprotective effects of antidotal treatment were determined in rats poisoned with tabun at a sublethal dose using a functional observational battery 2 h and 24 h after tabun administration, the tabun-induced brain damage was investigated by the histopathological evaluation and central reactivating effects of oximes was evaluated by the determination of acetylcholinesterase activity in the brain using a standard spectrophotometric method.

Results: The central reactivating efficacy of a newly developed oxime K870 roughly corresponds to the central reactivating efficacy of pralidoxime while the ability of the oxime HI-6 to reactivate tabun-inhibited acetylcholinesterase in the brain was negligible. The ability of the oxime K870 to decrease tabun-induced acute neurotoxicity was slightly higher than that of pralidoxime and similar to the oxime HI-6. These results roughly correspond to the histopathological evaluation of tabun-induced brain damage.

Conclusion: The newly synthesized oxime K870 is not a suitable replacement for commonly used oximes in the antidotal treatment of acute tabun poisonings because its neuroprotective efficacy is only slightly higher or similar compared to studied currently used oximes.

KEYWORDS

tabun; acetylcholinesterase; neurotoxicity; functional observational battery; histopathology; oximes; rats

AUTHOR AFFILIATIONS

[1] Department of Toxicology and Military Pharmacy, Faculty of Military Health Sciences, University of Defense, Hradec Králové, Czech Republic

[2] Neurology, University Hospital Hradec Králové, Hradec Králové, Czech Republic

* Corresponding author: Faculty of Military Health Sciences, Třebešská 1575, 500 01 Hradec Králové, Czech Republic; e-mail: kassa@pmfhk.cz

Received: 16 March 2021
Accepted: 16 June 2021
Published online: 11 November 2021

Acta Medica (Hradec Králové) 2021; 64(3): 145–152
https://doi.org/10.14712/18059694.2021.25

INTRODUCTION

Nerve agents including tabun are highly toxic organophosphorus compounds that were developed and stockpiled for use as chemical warfare agents (1). Their main toxic mechanism is based on their covalent binding to the active site of acetylcholinesterase (AChE, EC 3.1.1.7) resulting in AChE irreversible inhibition and development of cholinergic crisis. As some nerve agents including tabun easily penetrate through the blood-brain barrier (BBB), they can cause centrally mediated seizure activity that can rapidly progress to status epilepticus and contribute to profound brain damage (2–4).

Tabun (O-ethyl-N,N-dimethyl phosphoramidocyanidate) is one of the most resistant nerve agents. It differs from other highly toxic organophosphates by its chemical structure and by the fact that commonly used antidotes (atropine in combination with an oxime) are not able to sufficiently eliminate tabun-induced acute toxic effects. Its acute toxic effects are extraordinarily difficult to counteract because of the existence of a free electron pair located on amidic nitrogen that makes the nucleophilic attack of oximes almost impossible (5, 6).

Severe intoxication with tabun usually leads to centrally mediated seizure activity and contribute to brain damage that is associated with long-lasting neurological and psychological injuries (7, 8). Therefore, the ability of antidotes to counteract acute neurotoxic effects of tabun and prevent tabun-poisoned organisms from irreversible lesions in the brain is very important for the successful antidotal treatment of acute tabun poisonings (2). However, all commonly used oximes are not able to sufficiently reactivate tabun-inhibited AChE and, in addition, their central reactivating efficacy is generally very low due to their low penetration through BBB (9–11).

Therefore, the development of new oxime or non-oxime reactivators of tabun-inhibited AChE has been a long-standing goal for the treatment of tabun poisoning. For this purpose, a novel dichlorinated bispyridinium oxime K870 with a double bond in the linker: *4-carbamoyl-1-[(2E)-4-{3.5-dichloro-4-[(hydroxyimino) methyl]-pyridinium-1-yl}but-2-en-1-yl]pyridinium dibromide* was synthesized to improve the efficacy of antidotal treatment in reactivating tabun-inhibited AChE and eliminating tabun-induced acute neurotoxic effects (12).

The aim of this study was to compare the potential neuroprotective and central reactivating effects of newly developed oxime K870 with the oxime HI-6 and pralidoxime in combination with an anticholinergic drug atropine in tabun-poisoned rats. The tabun-induced neurotoxic signs and symptoms were determined using a functional observational battery (FOB), the tabun-induced brain damage was investigated by the histopathological evaluation using hematoxylin-eosin staining.

MATERIAL AND METHODS

ANIMALS

Male Wistar albino rats (6-week-old, 240–270 g, VELAZ, Prague, Czech Republic) without genetic modification were kept in an accreditated animal facility (22 ± 2 °C and 50 ± 10% relative humidity, 12-h day-night cycle) and allowed access to standard food (VELAZ) and tap water *ad libitum*. Handling of the experimental animals was approved by the Ethics Committee of the Faculty of Military Health Sciences in Hradec Kralove (Czech Republic) and were conducted in accordance with the Animal Protection Law and Animal Protection Regulations.

CHEMICALS

Tabun was obtained from the Technical Institute in Brno (Czech Republic) and was 90% pure. Its purity was assayed by acidimetric titration. The basic solution of tabun (1mg/1mL) was prepared in propyleneglycol three days before starting the experiments. Actual solution of tabun was prepared from its basic solution with the help of saline immediately before its administration. Two oximes (pralidoxime, HI-6) were synthesized at the Department of Toxicology and Military Pharmacy of the Faculty of Military Health Sciences (University of Defence, Hradec Kralove, Czech Republic), the oxime K870 was synthesized at the Department of Chemistry of the Faculty of Science (University of Hradec Kralove, Czech Republic). Their purity was analyzed using HPLC technique with UV detection (310 nm) and they were more than 96% pure (13). All other drugs and chemicals of analytical grade were obtained commercially (Sigma-Aldrich, St. Louis, MO, USA) and used without further purification. The saline solution (0.9% NaCl, B Braun Melsungen AG, Melsungen, Germany) was used as a vehicle.

IN VIVO EXPERIMENTS

Animals were randomly divided into 6 groups (8 rats each): 1) a control group (administered with saline), 2) tabun-poisoned group ((220 μg/kg – 95% LD_{50}), 3) tabun- poisoned group treated with atropine sulphate alone (10 mg/kg), 4) tabun-poisoned group treated with atropine sulphate and K870 (100 mg/kg), 5) tabun-poisoned group treated with atropine sulphate and pralidoxime (197 mg/kg), 6) tabun-poisoned group treated with atropine sulphate and HI-6 (81 mg/kg).

Tabun was administered intramuscularly (i.m.) at a sublethal dose (220 μg/kg – 95% LD_{50}). One minute following tabun poisoning, the rats were treated i.m. with atropine (10 mg/kg b.w.) alone or in combination with the oxime HI-6 (81 mg/kg), pralidoxime (197 mg/kg) or K870 (100 mg/kg) at maximal tolerated doses (MTD, unpublished observations). All substances were administered intramuscularly (i. m.) at a volume of 1 mL/kg body weight (b.w.).

The neurotoxicity of tabun was monitored using FOB at 2 and 24 h following tabun poisoning. The evaluated markers of tabun-induced neurotoxicity in experimental animals were compared with the parameters obtained from control rats given saline instead of tabun and antidotes at the same volume (1 mL/kg b.w.). FOB consists of 42 measurements of sensory, motor and autonomic nervous functions. Some of them are scored (14), the others are measured in absolute units. The description of this method including statistical analysis has been already published (14, 15).

MEASUREMENT OF ACHE ACTIVITY IN THE BRAIN

To evaluate the reactivating efficacy of the oximes in the brain, the rats were decapitated after FOB test (24 h 30 min after intoxication), totally exsanguinated and the brain was rapidly removed, cut in half along the mid-sagittal plane and one half of the brain was immediately frozen at the temperature –70 °C. All experiments were perfomed in the same part of the day (from 08:00 h to 10:00 h). The spectrophotometric method of AChE activity determination and percentage of reactivation calculation including the statistical analysis was described previously (16, 17).

HEMATOXYLIN-EOSIN STAINING AND HISTOPATHOLOGY EVALUATION

To evaluate histopathological changes after tabun poisoning, second half of brain was fixed with a 10% neutral buffered formalin (Bamed s.r.o., Ceske Budejovic, Czech Republic). The description of sample preparation and the method of hematoxylin-eosin staining as well as histopathology evaluation including statistical analysis has been previously published (14, 18).

RESULTS

THE EVALUATION OF NEUPROTECTIVE EFFICACY OF OXIMES STUDIED IN TABUN-POISONED RATS

The results of the experiments related to the measurement of tabun-induced neurotoxicity at 2 hours following tabun poisoning are divided into three parts (activity and neuromuscular measures, sensorimotor and excitability measures and autonomic measures) (15) and summarized in Table 1a–c. While five non-treated tabun-poisoned rats, two tabun-poisoned rats treated with atropine alone and one tabun-poisoned rat treated with atropine and pralidoxime died before the evaluation of tabun-induced neurotoxicity by FOB, all tabun-poisoned rats treated with atropine in combination with K870 or the oxime HI-6 survived till the end of experiment. The evaluation of tabun-induced neurotoxic signs and symptoms at 2 h following intoxication proved significant alteration of practically all observed parameters with the exception of urination, defecation and himdlimb grip strength (Table 1a–c). All types of antidotal treatment of tabun poisoning including atropine alone were able to prevent some tabun-induced signs of neurotoxicity observed at 2 h following tabun challenge

Tab. 1a The values of tabun-induced activity and neuromuscular neurotoxic markers measured at 2 hours following tabun challenge by the functional observational battery (No 1–2, 4–14 – scored values, No 3, 15–18 – values in absolute units). Statistical significance: * $p \leq 0.05$ (comparison with the control values). Applied abbreviations: RRF, air righting reflex from back position; RRV, air righting reflex from vertical position; x/M, average or modus value; ± s, standard deviation; A, atropine; n, number of surviving animals.

2 hours		Controls		Tabun + A + pralidoxime		Tabun + A + HI-6		Tabun + A + K870		Tabun + atropine		Tabun	
No	**Marker**	**x/M**	**–/+s**	**x/M**	**–/+s**	**x/M**	**–/+s**	**x/M**	**–/+s**	**x/M**	**–/+s**	**x/M**	**–/+s**
1	posture	1.00		3.00		3.00		3.00		**3.00***		**7.00***	
2	muscular tonus	0.00		**–1.00***		0.00		0.00		0.00		**–2.00***	
3	rearing	10.13	6.73	**0.38***	1.06	**0.88***	1.36	**2.63***	2.88	**1.50***	2.00	**0.25***	0.71
4	hyperkinesis	0.00		**2.00***		**2.00***		0.00		0.00		**7.00***	
5	tremors	0.00		0.00		**3.00***		0.00		0.00		**5.00***	
6	clonic movements	0.00		0.00		0.00		0.00		0.00		**2.00***	
7	tonic movements	0.00		0.00		0.00		0.00		0.00		**5.00***	
8	gait	0.00		**1.00***		0.00		0.00		**1.00***		**7.00***	
9	ataxia	0.00		**1.00***		0.00		0.00		**1.00***		**2.00***	
10	paresis	0.00		0.00		0.00		0.00		0.00		**2.00***	
11	mobility score	1.00		1.00		1.00		1.00		1.00		**4.00***	
12	activity	4.00		3.00		3.00		4.00		4.00		**1.00***	
13	RRF	1.00		**2.00***		1.00		1.00		**2.00***		**7.00***	
14	RRV	1.00		**2.00***		1.00		1.00		**2.00***		**4.00***	
15	landing foot splay (mm)	9.70	1.61	5.73	3.97	7.05	3.09	8.76	1.88	8.34	1.20	**2.63***	3.81
16	forelimb grip strength (kg)	5.89	1.29	5.13	3.56	8.11	3.63	6.76	0.70	6.33	1.44	**2.21***	3.28
17	hindlimb grip strength (kg)	2.73	0.46	2.96	3.51	2.69	2.69	1.69	0.66	1.26	0.43	0.91	1.27
18	grip strength of all limbs (kg)	12.01	1.66	**3.86***	3.72	10.50	4.91	12.05	1.08	**9.55***	1.17	**4.18***	3.40
		n = 8		n = 7		n = 8		n = 8		n = 6		n = 3	

with the exception of a decrease in rearing activity, alteration of righting reflex, slight impairment of gait, the absence of pupil response to light, a decrease in forelimb and hindlimb grip strength, decrease in body temperature and respiration difficulties (Table 1a–c). Miosis was changed to mydriasis due to the effect of atropine. The ability of K870 to protect tabun-poisoned rats from tabun-induced acute neurotoxicity was slightly higher compared to other oximes studied. Pralidoxime was not able to eliminate fur abnormalities, unprovoked activity (arousal), a decrease in muscular tonus, the alteration of righting reflex, impairment of gait, absence of approach and tail-pinch reponse, a decrease in grip strength of all limbs while the other oximes (HI-6, K870) were able to do that. In addition, the oxime HI-6 was not able to eliminate hyperkinesis and tremors while the oxime K870 was able to do that (Table 1a–c).

Tab. 1b The values of tabun-induced sensorimotor and excitability neurotoxic markers measured at 2 hours following tabun challenge by the functional observational battery (scored values). Statistical significance: * $p \leq 0.05$ (comparison with the control values).

2 hours		Controls		Tabun + A + pralidoxime		Tabun + A + HI-6		Tabun + A + K870		Tabun + atropine		Tabun	
No	**Marker**	**x/M**	**–/+s**	**x/M**	**–/+s**	**x/M**	**–/+s**	**x/M**	**–/+s**	**x/M**	**–/+s**	**x/M**	**–/+s**
1	catch difficulty	2.00		2.00		2.00		2.00		2.00		**1.00***	
2	ease of handling	2.00		2.00		2.00		2.00		2.00		**1.00***	
3	arousal (GSC)	1.00		**2.00***		1.00		1.00		1.00		**4.00***	
4	tension	0.00		0.00		0.00		0.00		0.00		**2.00***	
5	vocalisation	0.00		0.00		0.00		0.00		0.00		**3.00***	
6	stereotypy	0.00		0.00		0.00		0.00		0.00		**5.00***	
7	bizzare behavior	0.00		0.00		0.00		0.00		0.00		**4.00***	
8	approach response	2.00		**1.00***		2.00		2.00		2.00		**1.00***	
9	touch response	2.00		2.00		2.00		2.00		2.00		**1.00***	
10	click response	2.00		2.00		2.00		2.00		2.00		**1.00***	
11	tail-pinch response	2.00		**1.00***		2.00		2.00		2.00		**1.00***	
		n = 8		n = 7		n = 8		n = 8		n = 6		n = 3	

Tab. 1c The values of tabun-induced autonomic neurotoxic markers measured at 2 hours following tabun challenge by the functional observational battery (No 1–7, 10–11, 13 – scored values, No 8–9, 12 – values in absolute units). Statistical significance: * $p \leq 0.05$ (comparison with the control values).

2 hours		Controls		Tabun + A + pralidoxime		Tabun + A + HI-6		Tabun + A + K870		Tabun + atropine		Tabun	
No	**Marker**	**x/M**	**–/+s**	**x/M**	**–/+s**	**x/M**	**–/+s**	**x/M**	**–/+s**	**x/M**	**–/+s**	**x/M**	**–/+s**
1	lacrimation	0.00		0.00		0.00		0.00		0.00		**4.00***	
2	palpebral closure	1.00		1.00		1.00		**2.00***		1.00		**5.00***	
3	endo/ exophtalmus	0.00		0.00		0.00		0.00		0.00		**1.00***	
4	fur abnormalities	0.00		**7.00***		0.00		0.00		0.00		**7.00***	
5	skin abnormalities	0.00		0.00		0.00		0.00		0.00		**4.00***	
6	salivation	0.00		0.00		0.00		0.00		0.00		**2.00***	
7	nose secretion	0.00		0.00		0.00		0.00		0.00		**3.00***	
8	urination	2.25	3.06	6.25	4.43	3.13	3.72	2.38	3.16	3.13	3.56	1.88	3.72
9	defecation	0.00		0.00		0.00		0.00		0.00		0.00	
10	pupil size	0.00		**2.00***		**2.00***		**1.00***		**2.00***		**-2.00***	
11	pupil response	1.00		**0.00***		**0.00***		**0.00***		**0.00***		**0.00***	
12	body temperature (°C)	37.50	0.22	**36.66***	1.47	**36.42***	1.38	**35.74***	0.37	**35.94***	0.53	**36.17***	1.76
13	respiration	0.00		**-1.00***		**-1.00***		0.00		**-1.00***		**-2.00***	
		n = 8		n = 7		n = 8		n = 8		n = 6		n = 3	

Tab. 2a The values of tabun-induced activity and neuromuscular neurotoxic markers measured at 24 hours following tabun challenge by the functional observational battery (No 1–2, 4–14 – scored values, No 3, 15–18 – values in absolute units). Statistical significance: * $p \leq 0.05$ (comparison with the control values). Applied abbreviations: RRF, air righting reflex from back position; RRV, air righting reflex from vertical position; x/M, average or modus value; ± s, standard deviation; A, atropine; n, number of surviving animals.

24 hours		Controls		Tabun + A + pralidoxime		Tabun + A + HI-6		Tabun + A + K870		Tabun + atropine		Tabun	
No	**Marker**	**x/M**	**–/+s**	**x/M**	**–/+s**	**x/M**	**–/+s**	**x/M**	**–/+s**	**x/M**	**–/+s**	**x/M**	**–/+s**
1	posture	1.00		1.00		1.00		1.00		1.00		**7.00***	
2	muscular tonus	0.00		0.00		0.00		0.00		0.00		**–2.00***	
3	rearing	0.75	0.71	3.25	2.76	3.38	6.32	0.63	1.06	3.88	7.61	0.25	0.46
4	hyperkinesis	0.00		0.00		0.00		0.00		**3.00***		**7.00***	
5	tremors	0.00		0.00		0.00		0.00		**3.00***		**5.00***	
6	clonic movements	0.00		0.00		0.00		0.00		0.00		**2.00***	
7	tonic movements	0.00		0.00		0.00		0.00		0.00		**5.00***	
8	gait	0.00		0.00		0.00		0.00		**1.00***		**7.00***	
9	ataxia	0.00		0.00		0.00		0.00		**2.00***		**2.00***	
10	paresis	0.00		0.00		0.00		0.00		0.00		**2.00***	
11	mobility score	1.00		1.00		1.00		1.00		**2.00***		**4.00***	
12	activity	4.00		4.00		**3.00***		**3.00***		**2.00***		**1.00***	
13	RRF	1.00		1.00		1.00		1.00		1.00		**7.00***	
14	RRV	1.00		1.00		1.00		1.00		1.00		**4.00***	
15	landing foot splay (mm)	9.51	0.86	**5.23***	3.91	**6.99***	3.19	**6.56***	0.94	8.20	1.70	**1.95***	3.70
16	forelimb grip strength (kg)	6.34	1.27	6.63	4.30	8.61	5.64	8.24	1.35	7.31	1.32	**1.89***	3.72
17	hindlimb grip strength (kg)	3.14	1.32	1.91	1.32	2.10	1.17	**1.84***	0.39	2.25	0.91	**0.53***	0.99
18	grip strength of all limbs (kg)	11.23	0.97	10.41	6.67	10.80	4.74	10.09	1.34	12.04	1.37	**2.76***	5.19
		n = 8		n = 6		n = 6		n = 6		n = 4		n = 2	

Tab. 2b The values of tabun-induced sensorimotor and excitability neurotoxic markers measured at 24 hours following tabun challenge by the functional observational battery (scored values). Statistical significance: * $p \leq 0.05$ (comparison with the control values).

24 hours		Controls		Tabun + A + pralidoxime		Tabun + A + HI-6		Tabun + A + K870		Tabun + atropine		Tabun	
No	**Marker**	**x/M**	**–/+s**	**x/M**	**–/+s**	**x/M**	**–/+s**	**x/M**	**–/+s**	**x/M**	**–/+s**	**x/M**	**–/+s**
1	catch difficulty	2.00		2.00		2.00		2.00		2.00		**1.00***	
2	ease of handling	2.00		2.00		**3.00***		2.00		2.00		**1.00***	
3	arousal (GSC)	1.00		1.00		1.00		1.00		**2.00***		**4.00***	
4	tension	0.00		0.00		0.00		0.00		0.00		**2.00***	
5	vocalisation	0.00		0.00		0.00		0.00		0.00		**3.00***	
6	stereotypy	0.00		0.00		0.00		0.00		0.00		**5.00***	
7	bizzare behavior	0.00		0.00		0.00		0.00		0.00		**5.00***	
8	approach response	1.00		1.00		1.00		1.00		1.00		1.00	
9	touch response	2.00		2.00		2.00		2.00		**1.00***		**1.00***	
10	click response	2.00		2.00		2.00		2.00		2.00		**1.00***	
11	tail-pinch response	2.00		**1.00***		2.00		2.00		2.00		**1.00***	
		n = 8		n = 6		n = 6		n = 6		n = 4		n = 2	

The results of the experiments related to the measurement of tabun-induced neurotoxicity at 24 hours following tabun poisoning are divided into three parts (activity and neuromuscular measures, sensorimotor and excitability measures and autonomic measures) (15) and summarized in Table 2a–c. Six non-treated tabun-poisoned rats, four tabun-poisoned rats treated with atropine alone and two tabun-poisoned rats treated with the oxime K870, HI-6 or pralidoxime in combination with atropine died before the evaluation of tabun-induced neurotoxicity by FOB. The evaluation of tabun-induced neurotoxic signs at 24 h following intoxication proved significant alteration of practically all observed parameters with the exception of rearing, urination, defecation and approach response (Table 2a–c).

All studied oximes in combination with atropine were able to prevent almost all tabun-induced signs of neurotoxicity observed at 24 h following tabun challenge with the exception of a slight decrease in activity, body temperature, landing foot splay and hindlimb grip strength. On the other hand, the ability of atropine alone to eliminate or at least reduce tabun-induced signs of acute neurotoxicity was lower compared to all oximes studied in combination with atropine. Atropine alone was not be able to eliminate hyperkinesis, tremors, slight impairment of gait in the form of ataxia, no reaction during a reflex testing consisting of recording each rat's response to the touch of the pen to the posterior flank and a decrerase in body temperature (Table 2a–c).

Tab. 2c The values of tabun-induced autonomic neurotoxic markers measured at 24 hours following tabun challenge by the functional observational battery (No 1–7, 10–11, 13 – scored values, No 8–9, 12 – values in absolute units). Statistical significance: * $p \leq 0.05$ (comparison with the control values).

24 hours		Controls		Tabun + A + pralidoxime		Tabun + A + HI-6		Tabun + A + K870		Tabun + atropine		Tabun	
No	**Marker**	**x/M**	**–/+s**	**x/M**	**–/+s**	**x/M**	**–/+s**	**x/M**	**–/+s**	**x/M**	**–/+s**	**x/M**	**–/+s**
1	lacrimation	0.00		0.00		0.00		0.00		0.00		**4.00***	
2	palpebral closure	1.00		1.00		1.00		1.00		1.00		**5.00***	
3	endo/ exophtalmus	0.00		0.00		0.00		0.00		0.00		**1.00***	
4	fur abnormalities	0.00		0.00		0.00		0.00		0.00		**7.00***	
5	skin abnormalities	0.00		0.00		0.00		0.00		0.00		**4.00***	
6	salivation	0.00		0.00		0.00		0.00		0.00		**2.00***	
7	nose secretion	0.00		0.00		0.00		0.00		0.00		**3.00***	
8	urination	0.00		0.00		0.00		0.00		0.00		0.00	
9	defecation	v0.00		0.00		0.00		1.00		0.00		0.00	
10	pupil size	0.00		0.00		0.00		0.00		0.00		**–2.00***	
11	pupil response	1.00		1.00		1.00		1.00		1.00		**0.00***	
12	body temperature (°C)	37.55	0.17	**36.48***	0.36	36.67	0.52	36.80	0.45	**36.41***	0.12	**36.90***	0.57
13	respiration	0.00		0.00		0.00		0.00		**–1.00***		**–2.00***	
		n = 8		n = 6		n = 6		n = 6		n = 4		n = 2	

THE EVALUATION OF REACTIVATING EFFICACY OF OXIMES STUDIED IN THE BRAIN OF TABUN-POISONED RATS

The ability of studied oximes to eliminate or reduce tabun-induced signs and symptoms of neurotoxicity does not correspond to their ability to reactivate tabun-inhibited AChE in the brain that was low. The highest reactivating efficacy was shown for the oxime K870 (5.5%) while the ability of pralidoxime to reactivate tabun-inhibited AChE in the brain was slightly lower compared to the oxime K870 (4.2%). The reactivating efficacy of the oxime HI-6 was not found. The differences among tested oximes were not significant (Table 3).

Tab. 3 Percentage of reactivation of tabun-inhibited AChE by oximes in rat brain *in vivo*.

TREATMENT	AChE activity (mkat/kg)
	Brain
Saline control	102.4 ± 2.44
Atropine control	39.56 ± 10.97[a]
Atropine + **K870** (% reactivation[b])	43.02 ± 10.91 (5.5)
Atropine + **pralidoxime** (% reactivation)	42.17 ± 6.35 (4.2)
Atropine + **HI-6** (% reactivation)	31.18 ± 6.40 (0)

[a] Means ± S.E.M., n = 4–8.
[b] % reactivation was determined using the AChE activity values: {1 – [((saline control) – (oxime + atropine))/((saline control) – (atropine control))]} × 100.

HISTOPATHOLOGICAL EVALUATION OF TABUN-INDUCED BRAIN DAMAGE

Significantly increased histopathological damage scores were only found in amygdaloid body ($p = 0.005$) of tabun-poisoned rats without treatment when compared to control animals. In this group, shrunken eosinophilic neurons were present, especially in basolateral and central nuclei of this brain region in 1 of 2 surviving animals. Administration of atropine alone or its mixture with K870, pralidoxime or HI-6 significantly reduced tabun-induced histopathological damage of amygdaloid body ($p = 0.016$, 0.008, 0.008, and 0.008).

No other significant changes were observed.

DISCUSSION

Severe poisoning with nerve agents including tabun can cause long-term overstimulation of the central muscarinic receptors leading to increased glutamatergic activity and subsequent excitotoxic damage of the brain (19, 20). Therefore, the antidotes with sufficient neuroprotective efficacy are important for the successful antidotal treatment of acute tabun poisonings.

It was found that atropine alone is not able to prevent tabun-induced seizures and subsequent neurotoxic effects including the brain damage following sublethal or lethal poisoning with tabun due to its low central antimuscarinic activity (21, 22). Thus, atropine should be combined with AChE reactivator in the antidotal treatment of tabun poisonings to improve its neuroprotective efficacy. However, the ability of commonly used oximes to eliminate tabun-induced acute neurotoxic effects is insufficient because of low reactivation of tabun-inhibited AChE and limited penetration through BBB (2, 9, 23–26). Therefore, new oximes with higher potency to reactivate tabun-inhibited AChE and to counteract tabun-induced acute neurotoxicity are still searched in order to increase the efficacy of antidotal treatment of acute tabun poisonings. Unfortunately, the presently available database on reactivators presented in the past few years gives no indication of a candidate which is clearly superior to the classic oximes.

The design of newly developed oximes should respect not only the goal to increase their reactivating efficacy via higher affinity to AChE but also the goal to increase their BBB penetration as much as possible. It was demonstrated that proper length between covalently connected proper peripheral site ligand and a non-ionic part containing nucleophilic aldoxime in the structure of AChE resulted in higher reactivation potency (27). The oxime K870 (dichlorinated bispyridinium AChE reactivator) has been developed based on aforementioned approach (12, 28–30).

Our results demonstrate that the neuroprotective efficacy of studied oximes is comparable. At 2 h after tabun administration, the ability of the oxime K870 to eliminate tabun-induced neurotoxic signs and symptoms was slightly higher than the neuroprotective efficacy of pralidoxime and similar to the efficacy of the oxime HI-6. No significant differences among all three groups (atropine with one of the tested oxime) at 24 h after tabun poisoning were found, either. On the other hand, the neuroprotective efficacy of atropine alone was markedly lower compared to the combination of atropine with one of studied oximes, especially at 24 h after tabun poisoning. This finding corresponds to the literature data (21). The differences in the neuroprotective efficacy of studied oximes do not correspond to their reactivating efficacy in the brain. Although the ability of K870 to reactivate tabun-inhibited AChE was the highest, the potency of all oximes studied to reactivate tabun-inhibited brain AChE was generally very low. This finding is supported by the fact that at least two tabun-poisoned rats died within 24 h after tabun challenge in all experimental groups. As the neuroprotective efficacy of all oximes studied is not possible to explain by their central reactivating efficacy that was very small, their neuroprotective efficacy could be also caused by their direct pharmacological effects such as inhibition of acetylcholine release, interaction with presynaptic cholinergic nerve terminals and/or with postsynaptic receptors (31–33).

Above mentioned data roughly correlate with histopathological evaluation. In comparison with our previous study (14), histopathological picture of tabun-poisoned rats without antidotal treatment was scarse. Significant damage was only found in amygdaloid body, which represents nuclei susceptible to excitotoxic damage (19). Nevertheless, these results are highly affected by a very low number of surviving animals that underwent the assessment. Regarding treated tabun-poisoned rats, no statistically significant differences were observed among all experimental groups as in case of the evaluation of neuroprotective and reactivating efficacy of all oximes studied.

CONCLUSIONS

It was found that neuroprotective and central reactivating efficacy of K870 did not prevail the effectiveness of currently available oximes studied and, therefore, it is not a suitable replacement for commonly used oximes in the antidotal treatment of acute tabun poisonings. Thus, a new structured, stepwise approach and a comprehensive set of *in vitro* and *in vivo* studies are required for the successful identification and downselection of new candidate reactivators with better entering into the active site of AChE-tabun complex and higher penetration through BBB.

ACKNOWLEDGEMENTS

The study was funded by the Ministry of Defence of the Czech Republic – "Long-term organization development plan – Medical Aspects of Weapons of Mass Destruction" of the Faculty of Military Health Sciences Hradec Králové, University of Defence, Czech Republic.

REFERENCES

1. Black R. Development, historical use and properties of chemical warfare agents. In: Worek F, Jenner J, Thierman H, eds. Chemical Warfare Toxicology, Royal Society of Chemistry, Cambridge, 2016: 1–28.
2. Bajgar J. Organophosphate/nerve agent poisoning: mechanism of action, diagnosis, prophylaxis, and treatment. Adv Clin Chem 2004; 38: 151–216.

3. Colovic MB, Krstic DZ, Lazarevic-Pasti TD, Bondzic AM, Vasic VM. Acetylcholinesterase inhibitors: pharmacology and toxicology. Curr Neuropharmacol 2013; 11: 315–35.
4. Delfino RT, Ribeiro TS, Figueroa-Villar JD. Organophosphorus compounds as chemical warfare agents: a review. J Braz Chem Soc 2009; 20: 407–28.
5. Cabal J, Bajgar J. Tabun – reappearance 50 years later (in Czech). Chem Listy 1999; 93: 27–31.
6. Ekström F, Akfur C, Tunemalm AK, Lundberg S. Structural changes of phenylalanine 338 and histidine 447 revealed by the crystal structures of tabun-inhibited murine acetylcholinesterase. Biochemistry 2006; 45: 74–81.
7. Hoffman A, Eisenkraft A, Finkelstein A, Schein O, Rotman E, Dushnitsky T. A decade after the Tokyo sarin attack: a review of neurological follow-up of the victims. Mil Med 2007; 172: 607–10.
8. Yamasue H, Abe O, Kasai K, et al. Human brain structural changes related to acute single exposure to sarin. Ann Neuro 2007; 61: 37–46.
9. Jokanovic M, Prostran M. Pyridinium oximes as cholinesterase reactivators. Structure-activity relationship and efficacy in the treatment of poisoning with organophosphorus compounds. Curr Med Chem 2009; 16: 2177–88.
10. Marrs TC, Rice P, Vale JA. The role of oximes in the treatment of nerve agent poisoning in civilian casualties. Toxicol Rev 2006; 25: 297–323.
11. Wilhelm CM, Snider TH, Babin MC, Jett DA, Platoff GEJr, Yeung DT. A comprehensive evaluation of the efficacy of leading oxime therapies in guinea pigs exposed to organophosphorus chemical warfare agents or pesticides. Toxicol Appl Pharmacol 2014; 281: 254–65.
12. Zorbaz T, Malinak D, Marakovic N, et al. Pyridinium oximes with ortho-positioned chlorine moiety exhibit improved physicochemical properties and efficient reactivation of human acetylcholinesterase inhibited by several nerve agents. J Med Chem 2018; 61: 10753–66.
13. Jun D, Kuca K, Stodulka P, et al. HPLC analysis of HI-6 dichloride and dimethanesulfonate – antidotes against nerve agents and organophosphorus pesticides. Anal Lett 2007; 40: 2783–7.
14. Kassa J, Misik J, Hatlapatkova J et al. The evaluation of the reactivating nad neuroprotective efficacy of two newly prepared bispyridinium oximes (K305, K307) in tabun-poisoned rats – a comparison with trimedoxime and the oxime K203. Molecules 2017; 22: 1152.
15. Moser VC, Tilson H, McPhail RC et al. The IPCS collaborative study on neurobehavioral screening methods: II. Protocol design and testing procedures. NeuroToxicology 1997; 18: 929–38.
16. Ellman GL, Courtney DK, Andres VJr, Feartherstone RM. A new and rapid colorimetric determination of acetylcholinesterase activity. Biochem Pharmacol 1961; 7: 88–93.
17. Clement JG, Hansen AS, Boulet CA. Efficacy of HLö-7 and pyrimidoxime as antidotes of nerve agent poisoning in mice. Arch Toxicol 1992; 66: 216–9.
18. Paxinos G, Watson C. The rat brain in stereotactic coordinates, 6th ed. Academic Press, San Diego, 2006: 307.
19. Chen Y. Organophosphate-induced brain damage: Mechanisms, neuropsychiatric and neurological consequences, and potential therapeutic strategies. NeuroToxicology 2012; 33: 391–400.
20. Shih TM, Duniho SM, McDonough JH. Control of NA-induced seizures is critical for neuroprotection and survival. Toxicol Appl Pharmacol 2003; 188: 69–80.
21. Kassa J, Kunesova G. Comparison of the neuroprotective effects of the newly developed oximes (K027, K048) with trimedoxime in tabun-poisoned rats. J Appl Biomed 2006; 4: 123–34.
22. McDonough JHJr, Zoeffel LD, McMonagle J, Copeland TL, Smith CD, Shih TM. Anticonvulsant treatment of nerve agent seizures: anticholinergics versus diazepam in soman-intoxicated guinea-pigs. Epilepsy Res 2000; 38: 1–14.
23. Jokanovic M. Structure-activity relationship and efficacy of pyridinium oximes in the treatment of poisoning with organophosphorus compounds: a review of recent data. Curr Topic Med Chem 2012; 12: 1775–89.
24. Kassa J, Krejcova G. Neuroprotective effects of currently used antidotes in tabun-poisoned rats. Pharmacol Toxicol 2003; 92: 258–64.
25. Worek F, Widmann R, Knopff O, Szinicz L. Reactivating potency of obidoxime, pralidoxime, HI-6 and HLö-7 in human erythrocyte acetylcholinesterase inhibited by highly toxic organophosphorus compounds. Arch Toxicol 1998; 72: 237–43.
26. Zdarova Karasova J, Pohanka M, Musilek K, Zemek F, Kuca K. Passive diffusion of acetylcholinesterase oxime reactivators through the blood-brain barrier: Influence of molecular structure. Toxicol in Vitro 2010; 24: 1838–44.
27. de Koning MC, van Grol M, Noort D. Peripheral site ligand conjugation to a non quaternary oxime enhances reactivation of nerve agent-inhibited human acetylcholinesterase. Toxicol Lett 2011; 206: 54–9.
28. Masson P, Nachon F, Lockridge O. Structural approach to the aging of phosphylated cholinesterases. Chem Biol Interact 2010; 187: 157–62.
29. Kuca K, Jun D, Musilek K. Structural requirements of acetylcholinesterase reactivators. Mini Rev Med Chem 2006; 6: 269–77.
30. Musilek K, Kuca K, Jun D, Dolezal M. Progress in synthesis of new acetylcholinesterase reactivators during the period 1990–2004. Curr Org Chem 2007; 11: 229–38.
31. Niessen KV, Tattersall JEH, Timperley CM, et al. Interaction of bispyridinium compounds with the orthosteric binding site of human α7 and Torpedo californica nicotinic acetylcholine receptors (nAChRs). Toxicol Lett 2011; 206: 100–4.
32. Sürig U, Gaal K, Kostenis E, Tränkle C, Mohr K, Holzgrabe U. Muscarinic allosteric modulators. Atypical structure-activity-relationships in bispyridinium-type compounds. Arch Pharm Chem Life Sci 2006; 339: 207–12.
33. Van Helden HPM, Busker RW, Melchers BPC, Bruijnzeel PLB. Pharmacological effects of oximes: how relevant are they? Arch Toxicol 1996; 70: 779–86.

Gene Expression of Antioxidant Enzymes in the Resected Intestine in Crohn's Disease

Otakar Sotona[1,2,*], Eva Peterová[3], Július Örhalmi[2], Tomáš Dušek[1,2], Alena Mrkvicová[3], Veronika Knoblochová[4], Petr Lochman[1,2], Ondřej Malý[1,2], Jiří Páral[1,2], Jan Bureš[4]

ABSTRACT

Introduction: The inflammatory process in Crohn's disease (CD) is closely associated with the formation of reactive oxygen species. Antioxidant enzymes can play an important role in the outcome of CD and may influence postoperative recurrence in these patients. The aim of our study was to evaluate gene expression of intracellular antioxidant enzymes in surgically resected intestinal specimens of patients with CD, both in macroscopically normal and in inflamed tissue.

Methods: A total of 28 patients referred for elective bowel resection were enrolled in the study. Full-thickness small intestinal specimens were investigated. Gene expression of antioxidant enzymes – superoxide dismutase (SOD), glutathione peroxidase (GPX), glutathione reductase (GSR) – was evaluated both in macroscopically normal and inflamed samples.

Results: There were significantly lower levels of SOD1 mRNA ($p = 0.007$) and GSR mRNA ($p = 0.027$) in inflamed tissue compared to macroscopically normal areas. No significant differences were found between affected and non-affected intestinal segments in mRNA for SOD2, SOD3 and GPX.

Conclusions: Our pilot data clearly showed that the gene expression of major antioxidant enzymes is not a uniform mechanism in the pathogenesis of Crohn's disease. Topically decreased gene expression of SOD1 and GSR might facilitate the segmental tissue injury caused by reactive oxygen species.

KEYWORDS

Crohn's disease; gene expression; intestine; antioxidant enzymes; superoxide dismutase; glutathione peroxidase; glutathione reductase

AUTHOR AFFILIATIONS

[1] Department of Field Surgery, Faculty of Military Health Sciences, University of Defence, Hradec Králové, Czech Republic
[2] Department of Surgery, Charles University, Faculty of Medicine in Hradec Králové and University Hospital Hradec Králové, Czech Republic
[3] Department of Medical Biochemistry, Charles University, Faculty of Medicine in Hradec Králové, Czech Republic
[4] 2nd Department of Internal Medicine – Gastroenterology, Charles University, Faculty of Medicine in Hradec Králové and University Hospital Hradec Králové, Czech Republic
* Corresponding author: Department of Field Surgery, Faculty of Military Health Sciences, University of Defence, Hradec Králové, Czech Republic; e-mail: otakar.sotona@seznam.cz

Received: 5 May 2021
Accepted: 22 July 2021
Published online: 11 November 2021

Acta Medica (Hradec Králové) 2021; 64(3): 153–157
https://doi.org/10.14712/18059694.2021.26

INTRODUCTION

Inflammatory bowel disease (IBD) is comprised of two entities: ulcerative colitis and Crohn's disease (CD). Ulcerative colitis affects the large bowel only, whereas CD can involve any part of the gastrointestinal tract (most commonly the ileum and proximal colon). These diseases have somewhat different pathologic and clinical characteristics, but with substantial overlap. CD is characterized by transmural inflammation and by segmental involvement of the bowel. The transmural inflammation may lead to fibrosis and strictures, and to obstructive clinical presentations, and may also result in sinus tracts, giving rise to microperforations and fistula formation (1, 2).

The pathogenesis of IBD still remains poorly understood. Several studies both in humans and in animal models suggest that genetically determined factors contribute to susceptibility to CD. However, only about 15 percent of those with CD have family history of IBD. The pathogenesis of CD results from dysregulated immune responses to luminal bacteria (and/or their products) and from the impact of various environmental factors (e.g., dietary factors, xenobiotics, smoking, drugs, oral contraceptives in women, and others). The components of immune response must be properly balanced. Either too strong or inadequate immune response to microbes in the intestinal lumen can ultimately result in intestinal inflammation (3).

Immune response in CD is a complex process, comprising dysregulated all innate-immune-, cytokine-, adaptive-immune-, epithelial-barrier- and microbial-clearance pathways. Inflammatory reaction, among others mediated by polymorphonuclear neutrophils, is associated with production of several products that can cause endothelial dysfunction and further worsen the structural intestinal injury. Reactive oxygen species (ROS) are key signalling molecules that play an important role in this process. Oxidative stress produced by polymorphonuclears leads to the opening of inter-endothelial junctions and promotes the migration of inflammatory cells across the endothelial barrier (4).

Antioxidant enzymes are proteins involved in the catalytic transformation of free radicals and reactive oxygen species and their by-products into stable nontoxic molecules. They represent an important defence mechanism against oxidative stress-induced cell damage. These enzyme systems include superoxide dismutase, glutathione peroxidase, glutathione reductase, lipoic acids, peroxiredoxins and catalases (5).

Although advances in medical therapy have been associated with decreased need for bowel resection in CD, surgical intervention is often required in the setting of bowel obstruction, abscesses or fistulas, or refractory disease. The 10-year risk of surgical resection for CD is nearly 50 percent (6).

Antioxidant enzymes may play an important role in the outcome of CD and may influence the postoperative recurrence in these patients. The aim of our current study was to evaluate gene expression of intracellular antioxidant enzymes in surgically resected intestinal specimens of patients with CD, both in macroscopically uninvolved and involved tissue.

METHODS

PATIENTS

A total of 28 individuals referred for bowel resection were included in the study. The group consisted of 12 males (mean age 37 ± 13; 6/12 were smokers) and 16 females (mean age 38 ± 13; 8/16 smokers).

SURGICAL PROCEDURE

All patients were indicated for intestinal resection according to the decision of a multidisciplinary team. All patients had L3B2 disease according to the Montreal classification (7). No preoperative bowel preparation was performed. A prophylactic dose of antibiotics was administered (amoxicillin/clavulanate 1.2 g i.v., metronidazole 500 mg i.v.). Patients underwent laparoscopic or open ileocecal resection or right hemicolectomy with a hand-sutured side-to-side or end-to-end anastomosis. For each patient, a full-thickness sample from small intestine was taken from the resected specimen by a surgeon from a macroscopically uninvolved and affected area. Samples were immediately stored in separate vials with RNAprotect Tissue Reagent (QIAGEN, Hilde, Germany) and were ready for further processing.

ANTIOXIDANT ENZYMES

Analysis of mRNA expression of major intracellular antioxidant enzymes was performed, both in macroscopically normal and in involved tissue. Analyses were carried out of superoxide dismutase (SOD) and its three isoforms – cytoplasmatic (SOD1), mitochondrial (SOD2) and extracellular (SOD3). Gene expression of glutathione peroxidase (GPX) and glutathione reductase (GSR) was also investigated.

RNA ISOLATION AND QPCR

Tissue samples were homogenized using a Precellys 24 homogenizer (Bertin Instruments, Bretonneux, France). Total cellular RNA was extracted using TRIzol reagent (Invitrogen, Carlsbad, CA, USA). RNA was reverse-transcribed using a cDNA Reverse Transcription Kit (Applied Biosystems, Foster City, CA, USA). Gene expression was quantified with TaqMan Gene Expression Assays (POLR2A Hs00172187_m1, SOD1 HS_00916176_m1, SOD2 Hs_00167309_m1, SOD3 Hs_00162090_m1, GSR HS_00167317_m1, GPX3 HS_01078668_m1. Gene expression was analysed using a QuantStudio 6 real-time PCR system (all purchased from Applied Biosystems, Foster City, CA, USA). Results were normalized to POLR2A RNA expression. mRNA levels were calculated using a comparative Ct method (ΔΔCt method) (8).

STATISTICAL ANALYSIS

Data had non-normal distribution and were tested by Mann-Whitney test and Kruskal-Wallis test. All statistics was performed using GraphPad Prism 8.0.1.244 (San Diego, CA, USA).

ETHICS

The project was carried out according to the Declaration of Helsinki and was approved by the Ethics Committee of University Hospital Hradec Králové (protocol number 201706S12P). All participants signed an informed consent.

RESULTS

There was a statistically significant difference between macroscopically non-pathological and pathological tissue in SOD1 mRNA level (p = 0.007; Figure 1.A) and GSR mRNA level (p = 0.026; Figure 1.D). No significant differences were found between macroscopically involved and non-involved intestinal samples in mRNA for SOD2 (Figure 1.B), SOD3 (p = 0.116; type 2 error beta: 0.783; power of the performed test 0.217; Figure 1.C), or GPX (Figure 1.E).

The mRNA for each enzyme in the non-pathological and pathological tissue of the males group was compared to the mRNA for each enzyme in females group. No statistically significant differences in the mRNA levels were found between male and female non-pathological tissue for SOD1 (p = 0.932), SOD2 (p = 0.819), SOD3 (p = 0.357), GSR (p = 0.948), or GPX (p = 0.765). No statistical differences were found between male non-pathological and pathological tissue in mRNA for SOD1 (p = 0.981), SOD2 (p = 0.999), SOD3 (p = 0.995), GSR (p = 0.893), or GPX (p = 0.769), nor were any differences identified between female non-pathological and pathological tissue in mRNA for SOD1 (p = 0.918), SOD2 (p = 0.593), SOD3 (p = 0.235), GSR (p = 0.525), or GPX (p = 0.340).

The mRNA for each enzyme in the non-pathological and pathological tissue of the smokers was compared to the mRNA for each enzyme in non-smokers. No statistically significant differences in the mRNA levels were found in non-pathological tissue for SOD1 (p = 0.950), SOD2 (p = 0.962), SOD3 (p = 0.613), GSR (p = 0.472), GPX (p = 0.738) between smokers and non-smokers. For non-pathological and pathological tissue in smokers, no statistical differences in mRNA levels for SOD1 (p = 0.999), SOD2 (p = 0.944), SOD3 (p = 0.240), GSR (p = 0.995), GPX (p = 0.993) were identified, nor were there any differences between non-smokers non-pathological and pathological tissue in mRNA for SOD1 (p = 0.783), SOD2 (p = 0.893), SOD3 (p = 0.985), GSR (p = 0.243), GPX (p = 0.925).

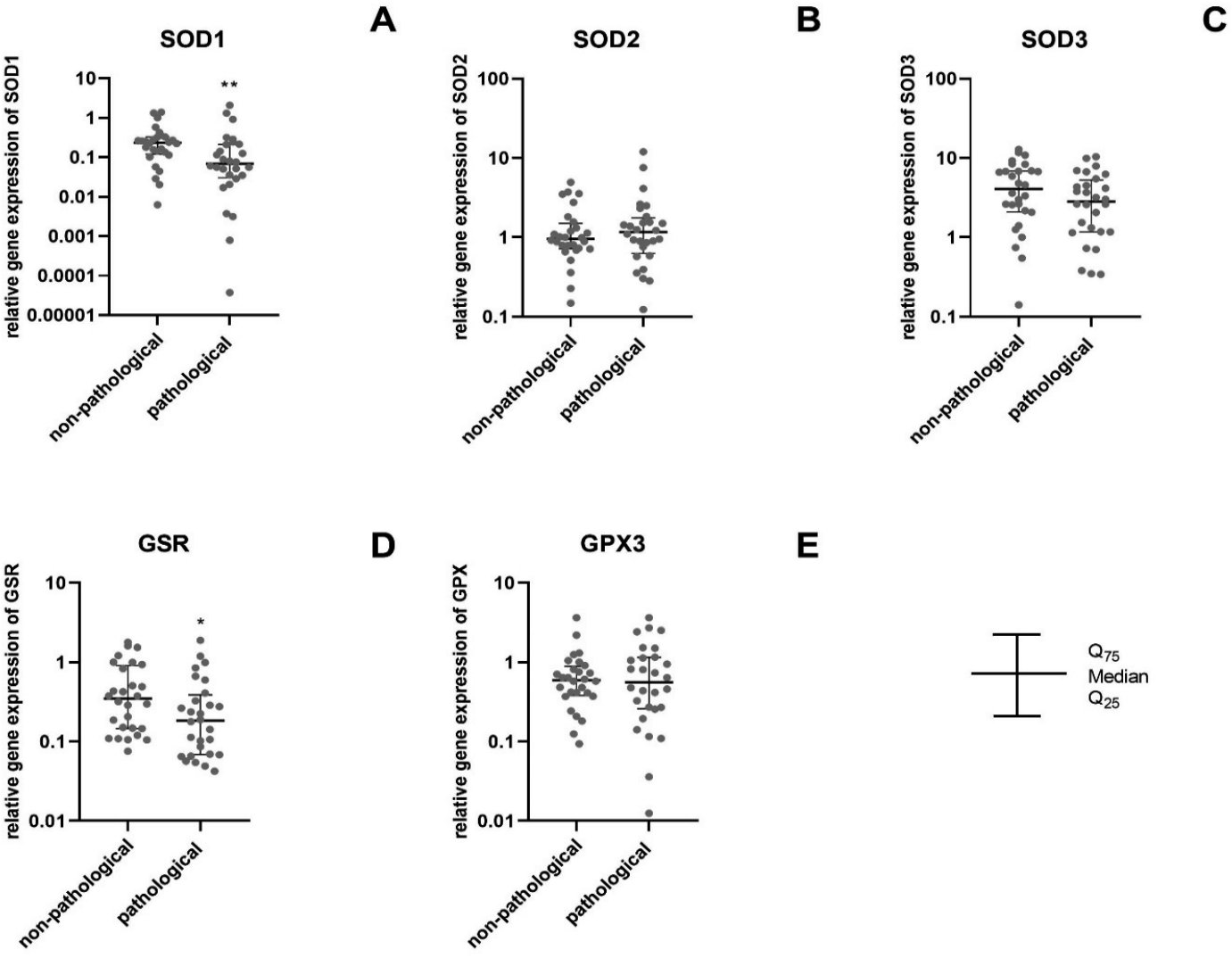

Fig. 1 mRNA expression of SOD1 (A), SOD2 (B), SOD3 (C), GSR (D), GPX (E) in macroscopically non-pathological tissue (n = 28) and macroscopically pathological tissue (n = 28).

DISCUSSION

Our study brought important insights into the role of gene expression of antioxidant enzymes in Crohn's disease (CD). From the analysis of pathologically altered and macroscopically uninvolved tissue samples, a statistically significant difference in mRNA level of SOD1 was found. A significantly reduced level of SOD1 was noted in the affected intestinal samples. Superoxide dismutase catalyses the disproportionation of superoxide radicals into H_2O_2 and O_2. SOD1 binds copper and zinc ions and is one of three superoxide dismutases. SOD1 deficiency in the dextran-sodium sulphate (DSS)-induced mouse model of colitis resulted in severe oxidative stress with body weight loss, epithelial barrier disruption, and decreased antioxidant enzyme activities (9). In CD, lipid peroxidation was found to correlate positively with SOD1 (10). The remaining two isoforms of SOD in our study failed to show a statistically significant difference in mRNA levels. However, Kruidenier et al. (11) demonstrated increased SOD2 expression in their work. SOD2 transforms toxic superoxide to clear mitochondrial reactive oxygen species, thus protecting against cell death. Mulder et al. (12) measured the content of superoxide dismutase in intestinal resection specimens from patients with Crohn's disease and ulcerative colitis and compared the concentrations with those obtained in the normal mucosa of a control group of patients with colorectal cancer. The superoxide dismutase content was similar in control mucosa and non-inflamed mucosa from that in patients with inflammatory bowel disease but was decreased in inflamed mucosa. The decreased SOD3 protein level in inflamed tissue compared to non-inflamed has been described in other studies (11, 13).

Our study also demonstrated a statistically significant decrease in glutathione reductase (GSR) mRNA levels. This enzyme regenerates the glutathione (GSH). GSR plays a key role in protecting cells from oxidative damage, it catalyses the reduction of H_2O_2 by GSH into H_2O and glutathione disulphide (GSSG). The inflamed ileum of patients with CD is characterized both by an increase of GSSG and decrease of GSH (14). The inflamed ileum in CD is not able to eliminate GSSG, probably due to a diminished GSR activity. Our results showed that such decrease is already evident at the gene level.

Glutathione peroxidase (GPX) was another enzyme whose gene expression was analysed in our study. GPX is involved in the protection of cells from damaging effects of reactive forms of oxygen. It follows the action of SOD. It catalyses the decomposition of H_2O_2 into water and oxygen (15). Our study did not confirm differences between inflamed and non-inflamed tissue in gene expression of GPX.

We have also investigated the possible influence of gender and smoking on the gene expression of antioxidant enzymes. Sex hormones, e.g. oestrogen, are thought to be associated with risk of IBD as variations in disease severity occur during pregnancy, menopause, or oral contraceptive use (16, 17). Unfer et al. (18) showed that serum oestrogen and progesterone levels positively correlated with blood SOD1 and SOD3 activity. Strehlow et al. (19) revealed that expression as well as activity of SOD2 and SOD3 are enhanced by oestrogens by transcriptional pathways, while GPX is not altered. In our study, we found no differences between the genders in gene expression of antioxidant enzymes.

Cigarette smoking in CD is put into context with accelerated disease, worse nutritional status, increased need for medical therapy (including biologics), and increased risk of recurrence following surgery, as well as a higher risk of postoperative complications (20–22). Contrarily, smoking has a protective effect for ulcerative colitis, and smokers are less likely to require colectomy (23, 24). However, our results showed no differences between smokers and non-smokers in CD, both in macroscopically normal and pathological tissue.

There is an increasing interest in miRNAs and exploring their possible role in the pathogenesis of CD. Current studies indicate that miRNA expression can be sensitive to the presence of intracellular H_2O_2 levels (25–27). Epigenetic regulation at the DNA level is an important mechanism involved in H_2O_2-mediated expression changes of multiple genes, indicating that miRNA expression is very sensitive to H_2O_2 stimulation. For example, in smooth muscle cells, cellular treatment with hydrogen peroxide resulted in an upregulation of microRNA-21 (10).

We are aware of possible limits of our study. We did not correlate our results with the histology of resected specimens (and tissue inflammatory grading). Due to the limited number of patients, we were not able to assess our data with respect to preoperative medical therapy. And last but not least, we did not evaluate other factors that can influence the gene expression of antioxidant enzymes and thus might create confounders. Nevertheless, our pilot data is an important basis for future research of this important topic.

CONCLUSIONS

Our pilot data clearly showed that the gene expression of major antioxidant enzymes is not a uniform mechanism in the pathogenesis of Crohn's disease. Topically decreased gene expression of SOD1 and GSR might facilitate the segmental tissue injury caused by reactive oxygen species.

ACKNOWLEDGEMENTS

This work was supported by the project PROGRES Q40-15 and Q40-01 from Charles University and by MH CZ – DRO (UHHK, 00179906).

The study was supported by A long-term organization development plan 1011 – Clinical fields (Faculty of Military Health Sciences 2016–2020).

The authors are grateful to Ian McColl, MD, PhD for assistance with the manuscript.

REFERENCES

1. Peppercorn MA, Cheifetz AS. Definitions, epidemiology, and risk factors for inflammatory bowel disease in adults. UpToDate on-line (Topic 4066, Version 38.0), Alphen aan den Rijn, Wolters Kluwer; accessed on 10th April 2021.
2. Lukáš M, et al. Idiopatické střevní záněty. Nové trendy a mezioborové souvislosti. Praha: Grada, 2020.

3. Snapper SB, Abraham C. Immune and microbial mechanisms in the pathogenesis of inflammatory bowel disease. UpToDate on-line (Topic 4077, Version 22.0), Alphen aan den Rijn, Wolters Kluwer; accessed on 10th April 2021.
4. Mittal M, Siddiqui MR, Tran K, Reddy SP, Malik AB. Reactive oxygen species in inflammation and tissue injury. Antioxid Redox Signal 2014; 20(7): 1126–67.
5. Sáez GT, Están-Capell N. Antioxidant Enzymes. In: Schwab M. (eds) Encyclopedia of Cancer. Berlin: Springer, 2014.
6. Frolkis AD, Dykeman J, Negrón ME, et al. Risk of surgery for inflammatory bowel diseases has decreased over time: a systematic review and meta-analysis of population-based studies. Gastroenterology 2013; 145(5): 996–1006.
7. Silverberg MS, Satsangi J, Ahmad T, et al. Toward an integrated clinical, molecular and serological classification of inflammatory bowel disease: report of a Working Party of the 2005 Montreal World Congress of Gastroenterology. Can J Gastroenterol 2005; 19, Suppl A: 5A–36A.
8. Rao X, Huang X, Zhou Z, Lin X. An improvement of the 2^(-delta delta CT) method for quantitative real-time polymerase chain reaction data analysis. Biostat Bioinform Biomath 2013; 3: 71–85.
9. Hwang J, Jing J, Sejin J, Shin HM, et al. SOD1 suppresses pro-inflammatory immune responses by protecting against oxidative stress in colitis. Redox Biology 37 (2020): 101760.
10. Moret-Tatay I, Ibora M, Cerrillo E, Tortosa L, Ns P, Beltrán B. Possible biomarkers in blood for Crohn's disease: Oxidative stress and microRNAs—Current evidences and further aspects to unravel. Oxidative medicine and cellular longevity 2016 (2016).
11. Kruidenier L, Kuiper I, van Duijn W, et al. Differential mucosal expression of three superoxide dismutase isoforms in inflammatory bowel disease. J Pathol 2003; 201: 7–16.
12. Mulder TP, Verspaget HW, Janssens AR, de Bruin PA, Peña AS, Lamers CB. Decrease in two intestinal copper/zinc containing proteins with antioxidant function in inflammatory bowel disease. Gut 1991; 32(10): 1146–50.
13. Kruidenier L, Kuiper I, Lamers CB, Verspaget HW. Intestinal oxidative damage in inflammatory bowel disease: semiquantification, localization, and association with mucosal antioxidants. J Pathol 2003; 201: 28–36.
14. Iantomasi T, Marraccini P, Favilli F, Vincenzini MT, Ferretti P, Tonelli F. Glutathione metabolism in Crohn's Disease. Biochemical Medicine and Metabolic Biology 1994; 53(2): 87–91.
15. Iborra M, Moret I, Rausell F, et al. Role of oxidative stress and antioxidant enzymes in Crohn's disease. Biochemical Society Transactions 2011; 39(4): 1102–6.
16. Godet PG, May GR, Sutherland LR. Meta-analysis of the role of oral contraceptive agents in inflammatory bowel disease. Gut 1995; 37(5): 668–73.
17. Khalili H, Higuchi LM, Ananthakrishnan AN, Richter JM, et al. Oral contraceptives, reproductive factors and risk of inflammatory bowel disease. Gut 2013; 62(8): 1153–9.
18. Unfer TC, Figueiredo CG, Zanchi MM, et al. Estrogen plus progestin increase superoxide dismutase and total antioxidant capacity in postmenopausal women. Climacteric 2015; 18(3): 379–88.
19. Strehlow K, Rotter S, Wassmann S, et al. Modulation of antioxidant enzyme expression and function by estrogen. Circulation Research 2003; 93(2): 170–7.
20. Underner M, Perriot J, Cosnes J, Beau P, Peiffer G, Meurice J-C. Smoking, smoking cessation and Crohn's disease**.** Presse Med 2016; 45(4 Pt 1): 390–402.
21. Kuenzig ME, Lee SM, Eksteen B, Seow CH, et al. Smoking influences the need for surgery in patients with the inflammatory bowel diseases: a systematic review and meta-analysis incorporating disease duration. BMC Gastroenterol 2016; 16(1): 143.
22. Lakatos PL, Szamosi T, Lakatos L. Smoking in inflammatory bowel diseases: good, bad or ugly? World J Gastroenterol 2007; 13(46): 6134–9.
23. Yamamoto, T, Keighley MR. Smoking and disease recurrence after operation for Crohn's disease. British Journal of Surgery 2000; 87(4): 398–404.
24. Bureš J, Fixa B, Komárková O, Fingerland A. Non-smoking: a feature of ulcerative colitis. Br Med J 1982; 285(6339): 440.
25. Lin Y, Liu X, Cheng Y, Yang J, Huo Y, Zhang C. Involvement of MicroRNAs in hydrogen peroxide-mediated gene regulation and cellular injury response in vascular smooth muscle cells. The Journal of Biological Chemistry 2009; 284(12): 7903–13.
26. Wang L, Huang H, Fan Y, et al. Effects of downregulation of microRNA-181a on H_2O_2-induced H9c2 cell apoptosis via the mitochondrial apoptotic pathway. Oxid Med Cell Longev 2014; 2014: 960362.
27. Christian P, Su Q. MicroRNA regulation of mitochondrial and ER stress signaling pathways: implications for lipoprotein metabolism in metabolic syndrome. American Journal of Physiology – Endocrinology and Metabolism 2014; 307(9): 729–37.

Obesity in Children with Leptin Receptor Gene Polymorphisms

Aleksandr Abaturov[1], Anna Nikulina[1,*]

ABSTRACT

Introduction: The study of single nucleotide polymorphisms (SNPs) of the leptin receptor gene (*LEPR*) based on next generation genomic sequencing (NGS) data is becoming an increasingly important aspect of diagnosis, treatment and prevention of both metabolically healthy (MHO) and metabolically unhealthy obesity (MUO) phenotypes.

Material and methods: 35 obese children 6-18 years old were examined by the NGS method with bioinformatic analysis. The main group (n = 18) was formed by children with MUO, according to the recommendations of the expert group of the National Heart, Lung, and Blood Institute. The control group (n = 17) was represented by children with MHO. Statistical methods were used: analysis of variance, Wald's sequential analysis, Spearman's correlation analysis, analysis of nominal data and multiple discriminant analysis.

Results: 10 types of non-synonymous SNPs (rs3790435, rs1137100, rs2186248, rs70940803, rs79639154, rs1359482195, rs1137101, rs1805094, rs13306520, rs13306522) of the *LEPR* gene in obese children have been identified. Multiple discriminant analysis demonstrated that the following *LEPR* SNPs are of greatest importance in the development of MUO: rs3790435, rs13306522, rs13306520. Analysis of nominal data revealed significant differences in the groups for Copy number variation (CNV) rs3790435 of the *LEPR* gene. Wald's analysis allowed us to identify 6 important predictors of MUO (I ≥ 0.5): 2 CNV rs3790435 (Relative Risk, RR = 2, Prognostic coefficient, PC = +2.76); male gender of the child (RR = 1.3, PC = +1.35); rs3790435 (RR = 1.9, PC = +2.76); hyperleptinemia more than 40.56 ng/ml (RR = 2, PC = +3); CNV rs1359482195 ≥ 3 (RR = 1.9, PC = +5.8); SNP of the *LEPR* gene ≥4 (RR = 3.8, PC = +5.8).

Conclusion: Children with the genotype rs3790435 gene *LEPR* had signs of MUO more often.

KEYWORDS

obesity phenotypes; children; leptin receptor gene; single nucleotide polymorphisms; next generation genomic sequencing

AUTHOR AFFILIATIONS

[1] Dnipro State Medical University (DSMU), Dnipro, Ukraine

* Corresponding author: Dnipro State Medical University (DSMU), Street 9, V. Vernadskogo, 49044, Dnipro, Ukraine; e-mail: anna.nikulina.201381@gmail.com

Received: 11 November 2020
Accepted: 13 September 2021
Published online: 11 November 2021

Acta Medica (Hradec Králové) 2021; 64(3): 158–164
https://doi.org/10.14712/18059694.2021.27

INTRODUCTION

The key role in the regulation of the body's energy metabolism is played by leptin (LEP) produced by adipocytes, which activates the leptin receptor (LEPR) of hypothalamic neurons (1, 2). Activation of the leptin receptor leads to increased transcription of anorexigenic pro-opiomelanocortin (POMC) and inhibition of the transcription of orexigenic neuropeptides agouti-related protein (AgRP) and neuropeptide Y (NPY) (3). Polymorphisms of the *LEPR* gene, which is located on chromosome 1 (1p31.3), associated with the development of obesity, are inherited in an autosomal recessive manner. Biallelic nonsynonymous polymorphisms of the *LEPR* gene located in exons can lead to dysfunction of the LEP/LEPR system by altering the structure of the leptin receptor protein. LEPR anomalies may be accompanied by the disturbance interaction of the receptor with LEP, the lack of LEPR excitation, the appearance of solute forms of LEPR that are not able to fix on the cell membrane, and the disturbance of interaction of the LEPR intradomain with components of intracellular signal conductivity cascades. The absence of the LEPR signal leads to the development of obesity, hyperphagia, and deficiency in the production of pituitary hormones already in the early period of childhood (4, 5). The prevalence of pathogenic *LEPR* mutations in a cohort of patients with severe monogenic early-onset obesity is 1.9% (6). There are currently 38 documented mutations in the *LEPR* gene associated with obesity. Most of the mutations are located in the region that encodes the extracellular domain, especially the leptin-binding site or activation domain of the receptor molecule (7). Missense mutations R612H, A409E, W664R, and H684P cause complete loss of leptin signaling, hyperphagia, severe obesity with early clinical manifestation, impairment of immune function and delay of puberty (8).

The detection of variants of leptin receptor gene polymorphisms based on next generation genomic sequencing (NGS) data is becoming an increasingly important aspect of diagnosis, treatment and prevention of both metabolically healthy (MHO) and metabolically unhealthy (MUO) obesity phenotypes associated with the formation of insulin resistance (9, 10). However, till now most studies have not examined the genetic effects of gene copies, including *LEPR*.

Objective: to determine the contribution of various SNPs of the *LEPR* gene and the CNV of gene regions to the development of metabolically unhealthy obesity and their importance in the diagnosis of various phenotypes of obesity in children.

MATERIAL AND METHODS

To accomplish the assigned tasks, a clinical and genetic examination was carried out in 35 children 6–18 years old with obesity, according to the recommendations of The American College of Medical Genetics and Genomics (ACMG) (11). The study was conducted among a Caucasian cohort of children with polygenic obesity.

Criteria for inclusion: all children enrolled in the study had a BMI greater than the 95th percentile or 2 SDS and underwent inpatient treatment in the endocrinology department.

Exclusion criteria: patients with hereditary syndromes accompanied by obesity and diseases, the treatment of which requires the use of drugs that affect the metabolism of carbohydrates and lipids; pregnant.

The main group included of 18 children with metabolically unhealthy obesity (MUO), according to the recommendations of the expert group of the National Heart, Lung, and Blood Institute, USA – NHLBI (12). The control group was formed of 17 children with metabolically healthy obesity (MHO). For inclusion in the main observation group, the presence of abdominal obesity and two of the presented criteria were taken into account: 1). Fasting glycemia ≥5.6 mmol/L (13); 2). High-density lipoprotein (HDL) ≤1.03 mmol/L or less than 10th percentile of the age norm; 3). Triacylglyceride (TAG) ≥1.7 mmol/L or more than the 90th percentile of the age norm; 4) Systolic blood pressure (SBP) above the 90th percentile for a given age, gender and height (12). The abdominal type of obesity was determined according to the consensus of the International Diabetes Federation (IDF), based on the excess of the waist circumference over the 90th percentile for children 6–15 years old or more than 94 cm for boys aged 16–18 years and more than 80 cm for girls 16–18 years old (14–16).

Laboratory examination for the formation of observation groups for obesity phenotypes included general clinical methods. Blood samples were obtained after an overnight fast by venipuncture in vacutainer gel tubes, and serum was separated from cells by centrifugation in a certified laboratory "Synevo" (Dnipro, Ukraine) using an analyzer and a Cobas 6000 test system; Roche Diagnostics (Switzerland). The analysis of serum glucose was carried out by the hexokinase method; the determination of triglycerides and high-density lipoproteins of blood plasma was carried out by the enzymatic – colorimetric method. HbA1c was analyzed using the immunoturbidimetric method, certified according to the National Glycohemoglobin Standardization Program (NGSP) and standardized according to the reference values adopted in the Diabetes Control and Complications Trial (DCCT). The level of HbA1c 4.8–5.9% of total hemoglobin in venous blood was considered normal. Insulin was analyzed using the electrochemiluminescence immunoassay method (ECLIA). The level of basal insulin in venous blood of 2.6–24.9 μIU/ml was considered normal. Insulin resistance was estimated using the Homeostasis Model Assessment for Insulin Resistance (HOMA-IR): Insulin (μIU/ml) × Fasting blood glucose (mmol/L)/22.5. An increase in insulin resistance was observed at HOMA-IR > 95th percentile according to the percentile curves recommended by the IDEFICS Consortium for the European population according to the age and sex of the child (17, 18).

Determination of serum leptin level was performed using radioimmunoassay using an analyzer and LDN test system (Germany), reference values for girls were 3.7–11.1 ng/ml, for boys 2.0–5.6 ng/ml.

Height (cm) was measured using Heightronic Digital Stadiometer® to the nearest 0.1 cm. Weight (kg) and body fat percentage was measured using Tefal Bodysignal body

composition analyzer (France). The calculation of the percentage of fat or body fat (BF) in the body was performed automatically with a discreteness of 0.1%, according to the requirements of Tefal Bodysignal, with the evaluation of results according to the unified centile scales for children of this age (19, 20). Waist circumference (WC), hip circumference (HC) was measured using a standardized anthropometric tape, measuring the circumference at the midpoint between the top of the iliac crest and the lower part of the lateral rib cage to the nearest 0.1 cm. BMI was converted to SDS by means of the current WHO growth references (21).

Systolic and diastolic blood pressure (SBP and DBP) were measured using a digital oscillimetric device, Dinamap ProCare (GE Healthcare).

Molecular genetic testing included complete genomic NGS with venous blood sampling in a certified CeXGat laboratory (Tubingen, Germany) using the Illumina CSPro® Certified service provider platform. Average amount of DNA (μg) in samples – 0.875. Library Preparation: Quantity used 50 ng. Library Preparation Kit: Twist Human Core Exome plus Kit (Twist Bioscience). Sequencing parameters: NovaSeq 6000; 2 × 100 bp. QC values of sequencing, Q30 value: 96.07%.

Bioinformatic analysis – demultiplexing of the sequencing reads was performed with Illumina bcl2fastq (version 2.20). Adapters were trimmed with Skewer, version 0.2.2 (22). DNA-Seq: Trimmed raw reads were aligned to the human reference genome (hg19-cegat) using the Burrows-Wheeler Aligner, BWA – mem version 0.7.17-cegat (23). ABRA, version 2.18 (24) was used for local restructuring of readings in target regions to improve more accurate detection of indels in the genome during mutagenesis. Proprietary readout tools, alignment with more than one locus with the same alignment score, were used; duplicate reads were discarded.

Variant calling: additional proprietary software was used to detect variants of polymorphisms, including variants with low frequencies (Observed frequency of the alternative allele in the range, OFA up to 2% of sequenced readings). The mutation variants were annotated based on various publicly available databases (Ensembl v100, RefSeq Curated (20200723), CCDS r22, dbSNP154, GnomAD 2.1 (exonic) and 3.0 (genomic), Gencode 34). Copy number variations (CNV) were found by comparing the number of reads that overlap the target genome regions ("coverage") with the expected number in the cohort of reference samples. All synonymous SNP types were excluded from the study.

The quality of FASTQ files was analyzed using FastQC, version 0.11.5-cegat (25). The plots were created with ggplot2 (26) in R version 3.6.1 (27). When interpreting the data of bioinformatic analysis, the combined annotated – dependent depletion (CADD) was calculated for each identified non-synonymous SNP of the *LEPR* gene (28, 29) and the software products FILTUS (30), SeqVISTA (31), Mutationassessor (32) were used.

Statistical processing of the results using parametric, nonparametric methods included: analysis of variance with the calculation of the Student's test (t); sequential Wald analysis with the calculation of the relative risk (Relative Risk – RR) and the prognostic coefficient (PC); Spearman correlation analysis with calculation of Spearman's rank correlation coefficient (ρ), analysis of nominal data with calculation of Chi-square test ($\chi 2$), $\chi 2$ test with Yates correction, $\chi 2$ test with correction for likelihood, Fisher's exact test (p), Cramer test (V), Pearson's contingency coefficient (C), normalized value of Pearson's coefficient (C'); multiple discriminant analysis with the calculation of the coefficients of the standardized canonical discriminant function (C_i MUO). The critical value of the level of statistical significance (p) for all types of analysis was taken at the level of $p < 0.05$ (5%). To reduce the sensitivity of computational procedures to the size of the sample presented, we used special methods that reduce the magnitude of computation errors by multivariate statistical processing of biometric data to obtain verified confidence coefficients (33). Statistical processing of the results was performed using Microsoft Excel (Office Home Business 2KB4Y-6H9DB-BM47K-749PV-PG3KT) and STATISTICA 6.1 software (StatSoftInc, no. AGAR909E415822FA).

RESULTS

The age distribution of polygenic obesity patients who took part in the survey was characterized by the following features. The proportion of children 6–10 years old (pre-pubertal period), in the main group, was 5.6% (1/18), 11–14 years old (early pubertal period) – 50% (9/18), 15–18 years old (late puberty period) – 44.4% (8/18). The proportion of children 6–10 years old in the control group was 5.8% (1/17), 11–14 years old – 47.1% (8/17), 15–18 years old – 47.1% (8/17), $p > 0.5$. The proportion of adolescents in the main group was 94.4% (17/18), in the control group – 94.2% (16/17), $p > 0.5$. The average age of patients in the observation groups was 12.06 ± 1.25 years. The proportion of boys in the main group was 61.1 ± 5.5% (11/18), while in the control group the proportion of boys in the study population was 47.06 ± 4.1% (8/17), $p = 0.049$.

Anthropometric examination revealed that in children with different phenotypes of obesity in the percentage of BMI, taking into account the age and sex of the child, no statistically significant difference in the comparison groups was observed. The absence of statistically significant differences in the frequency of obesity ($p > 0.05$) is due to the approach to the formation of survey groups, Table 1.

In order to take a part of children from BMI, but to surpass the 100th percentile in case of young variants of obesity phenotypes, and to the classification of extreme obesity in children, proponed by the American Heart Association and the Obesity Society (34). The MUO phenotype was detected in 64.5 ± 7.3% of children, the MHO phenotype – in 35.5 ± 6.9% of children with extreme obesity. The share of children with extreme obesity of class III (with body weight more than 140% of the 95th percentile) in those surveyed with the MUO phenotype was 25 ± 6.5%, while among those surveyed with the MHO phenotype – 7.3 ± 4.1%. Thus, children with the MUO phenotype have a higher genetic predisposition to develop severe obesity.

Tab. 1 Average values of anthropometric and manometric examination of children with different phenotypes of obesity.

Indicator	Children with MUO (M ± m)	Children with MHO (M ± m)	Probability, p
BMI in percentiles, %	98.8 ± 0.34	98.0 ± 0.4	p > 0.05
Proportion of children with extreme obesity of the III class (with body weight more than 140% from 95 percentile), %	26 ± 6.5	7.3 ± 4.1	p < 0.05
Physical development in percentiles	68.8 ± 4.7	74.3 ± 6.5	p > 0.05
BF in girls,%	38.2 ± 2.3	28.9 ± 0.8	p < 0.05
BF in boys, %	35.5 ± 2.5	25.0 ± 2.1	p < 0.05
WC in girls, cm	92.6 ± 4.2	74.5 ± 3.1	p < 0.05
WC in boys, cm	111.6 ± 3.2	91.7 ± 4.8	p < 0.05
Correlation WC/HC in girls	0.92 ± 0.04	0.74 ± 0.1	p < 0.05
Correlation WC/HC in boys	0.98 ± 0.04	0.84 ± 0.02	p < 0.05
Proportion of children with SBP exceeding the 95th percentile, %	27.3 ± 6,7	9.8 ± 4,6	p < 0.05

Mean WC levels and WC/HC ratios in both boys and girls had statistically significant differences ($p < 0.05$) in the comparison groups. In boys and girls with MUO phenotype, the average level of WC was 111.63 ± 3.21 and 92.55 ± 4.18 cm, respectively, the ratio of WC/HC was 0.98 ± 0.04 and 0.91 ± 0.04, respectively, associated with abdominal obesity according to IDF Consensus 2007 (35).

The proportion of children in the comparison subgroups who had a SBP higher than the 95th percentile, which is associated with hypertension among children with the MUO phenotype was almost three times higher than among children with the MHO phenotype, namely – 27.3 ± 6.3% and 9.8 ± 4.6%, $p < 0.05$. As a result of laboratory examination of carbohydrate metabolism in children with different phenotypes of obesity, the following results were obtained, Table 2.

Tab. 2 Features of carbohydrate and fat metabolism in children with different obesity phenotypes.

Indicator	Children with MUO (M ± m)	Children with MHO (M ± m)	Probability, p
Fasting blood glucose, mmol/L	4.9 ± 0.1	3.9 ± 0.2	p < 0.05
HbA1c, %	5.7 ± 0.1	4.9 ± 0.1	p < 0.05
HOMA-IR	6.2 ± 1.6	3.6 ± 0.4	p < 0.05
Proportion of children with HOMA-IR exceeding the 95th percentile, %	88.2 ± 0.1	36.4 ± 0.4	p < 0.05
Leptin in boys, ng/ml	39.3 ± 8.9	26.0 ± 6.4	*p* < 0.05
Leptin in girls, ng/ml	47.8 ± 4.4	32.5 ± 4.3	*p* < 0.05

As a result of NGS, 10 types of nonsynonymous SNPs (rs3790435, rs1137100, rs2186248, rs70940803, rs79639154, rs1359482195, rs1137101, rs1805094, rs13306520, rs-13306522) of the *LEPR* gene cohort were identified in 35 children.

Multiple discriminant analysis with the calculation of the coefficients of the standardized canonical discriminant function showed differences in the studied groups and the contribution of each of the 10 types of detected *LEPR* SNPs to the formation of MUO, Table 3.

The presented results of multiple discriminant analysis of 10 types of non-synonymous SNPs of the *LEPR* gene demonstrate that rs3790435, rs13306522, rs13306520, rs70940803, rs2186248, rs1359482195 make a certain contribution to the formation of MUO in children.

Analysis of nominal data on the criteria for assessing the significance of differences in outcomes depending

Tab. 3 Characteristics of SNP types of the *LEPR* gene and their contribution to the formation of metabolically unhealthy obesity.

dbSNP	Ref	Alt	Consequence	Codon Change	CADD	C_i MUO
rs3790435	T	C	5_prime_UTR	–/–	17.34	0.939
rs1137100 (exon-2) (K109R)	A	G	missense	aAgaca/aGgaca	17.74	-0.389
rs2186248	G	T	intronic	–/–	5.441	0.862
rs70940803	T	G	intronic	–/–	1.642	-0.894
rs79639154	T	G	intronic	–/–	2.884	–
rs1359482195	C	A	splice_region	–/–	21.70	-0.344
rs1137101 (exon-4) (Q223R)	A	G	missense	cAgtca/cGgtca	18.44	0.002
rs1805094 (exon 14) (K656N)	G	C	missense	aaGgag/aaCgag	9.128	–
rs13306520	A	G	intronic	–/–	4.568	-0.870
rs13306522	G	A	intronic	–/–	0.326	0.914

Comment: dbSNP – database identifier ("rs" number) of this variant in dbSNP. Ref – reference allele. Alt – alternative allele. Consequence – functional consequence of the variation in relation to the transcript. The nucleotide change and position relative to the coding sequence of the affected transcript in HGVS nomenclature: c. CDS Position Reference Base > Alternative Base. Example: c.223A>T. Codon Change – the affected base is written as a capital letter in both codons. Example: aAt/aCt. This column is empty if the variant is intergenic. CADD – Combined Annotation Dependent Depletion (19, 20). C_i MUO – coefficients of the standardized canonical discriminant function.

on the impact of a risk factor demonstrated significant differences in the observation groups in the CNV of the *LEPR* gene with rs3790435: Pearson Chi-Square ($\chi 2$) = 6.59, p = 0.01; $\chi 2$, Continuity Correction = 6.98, p = 0.009; Yates's correction $\chi 2$ (Likelihood Ratio) = 4.84, p = 0.03; Fisher's Exact Test (p) = 0.013, $p < 0.05$, with a minimum value of the expected phenomenon of 5.5. The assessment of the strength of the relationship between the risk factor and the outcome depending on the CNV of the *LEPR* gene c rs3790435 was relatively strong: Cramer's test (V) = 0.44, Pearson's contingency coefficient (C) = 0.4, normalized Pearson's coefficient (C') = 0.57, $p < 0.05$ (Table 4).

Analysis of the prognostic load of factors involved in the development of MUO, according to Wald's sequential analysis, allowed them to be distributed in descending order as follows ($I \geq 0.5$): 2 CNV rs3790435 (RR = 2, PC = +2.76); male gender of the child (RR = 1.3, PC = +1.35); rs3790435 (RR = 1.9, PC = +2.76); hyperleptinemia more than 40.56 ng/ml (RR = 2, PC = +3); 3 or more CNV rs1359482195 (RR = 1.9, PC = +5.8); more than 4 SNPs of the *LEPR* gene in an individual (RR = 3.8, PC = +5.8).

The presence of the rs70940803 polymorphism was associated with hyperleptinemia in both children with MHO ($\rho = +0.3$) and MUO ($\rho = +0.4$), $p < 0.05$. At the same time, the rs1137101 polymorphism in children with MHO had an inverse correlation with hyperleptinemia ($\rho = -0.62$), $p < 0.05$.

DISCUSSION

In this work, we demonstrated the role of CNV of genes of different genotypes of single nucleotide polymorphisms of the *LEPR* gene in the formation of polygenic obesity and proved their association with the possibility of the formation of certain phenotypes of MUO and MHO among the Caucasian population. Insulin resistance is the main criterion that distinguishes MUO from MHO. The HOMA-IR index exceeding the 95th percentile was recorded 2.4 times more often among patients with MUO compared with children with MHO, which was confirmed in a large number of previous studies that studied the effect of exposome on metabolic-associated diseases (10–17).

In our study, predictors of MUO were hyperleptinemia and male sex. A cross-sectional study by L. H. Barstad et al. (36) among Norwegian adolescents 12–18 years old seeking treatment for morbid obesity also showed similar gender differences. Namely, MUO signs were more often observed in boys (in 29% of cases) according to the following criteria: an increase in the level of triacylglycerides, systolic blood pressure, a decrease in the level of high-density lipoproteins compared with girls, in 19% of cases (17).

Our data are confirmed by the results of modern studies, which found that insulin resistance is associated with dysfunction of the LEP/LEPR system. Analysis of the scientometric PubMed database showed that the most studied association of obesity and type 2 diabetes with the following *LEPR* SNPs: rs3790435 and missense mutations rs1137100, rs1137101, rs1805094. The rs1137100 polymorphism is characterized by the replacement of Lys109Arg in the cytokine homology (CK) domain, rs1137101 – Gln223Arg in the loop of the CK-domain, rs1805094 – Lys656Asn in the domain of fibronectin type III of the LEPR molecule. It was shown that monogenic obesity is caused by homozygous mutations rs1137100, rs1137101, rs1805094, which are located in gene regions encoding functionally significant domains of the LEPR protein (38).

At the same time, there are conflicting data on the significance of mutations in the exons of the *LEPR* gene in the development of polygenic obesity. Thus, Aline Dos Santos Rocha et al. (39) demonstrated an association between rs1137100 (G) (OR = 1.92; 95% CI = 1.18–3.14) and overweight / obesity in children. Takuro Furusawa et al. (40) found no significant difference in the observation groups for this polymorphism. Ehab M.M. Ali (41) demonstrated that allelic frequencies of *LEPR* rs1137101 (Q223R) were significantly higher in obese subjects compared with non-obese ones in without obesity controls. At the same time, Malgorzata Roszkowska-Gancarz et al. (42) did not

Tab. 4 Genotypes and Copy number variation of the *LEPR* gene in individuals with MHO and MUO.

SNP (genotypes: HOM^P/HET/HOM^N)	Genotype (%)						CNV (%)					
	MHO			MUO			MHO			MUO		
	HOM^P	HET	HOM^N	HOM^P	HET	HOM^N	1	2	≥3	1	2	≥3
rs3790435 (TT/TC/CC)	5.9	41.2	52.9	0	83.3	16.7	58.9	41.1	0	16.7	83.3	0
rs1137100 (AA/AG/GG)	0	52.9	47.1	0	50.0	50.0	47.1	52.9	0	50.0	44.4	5.6
rs2186248 (TT/TC/CC)	5.9	5.9	88.2	0	0	100.0	5.9	0	94.1	0	0	100.0
rs70940803 (GG/TG/TT)	0	17.6	82.4	0	13.5	86.5	82.4	0	17.6	76.5	23.5	0
rs79639154 (GG/TG/TT)	0	5.9	94.1	0	0	100.0	94.1	5.9	0	100.0	0	0
rs1359482195 (AA/CA/CC)	0	5.9	94.1	0	11.1	88.1	94.1	0	5.9	88.1	0	11.1
rs1137101 (GG/AG/AA)	29.4	52.9	17.6	27.8	50.0	22.2	17.6	0	82.4	22.2	0	77.8
rs1805094 (TT/GT/GG)	0	23.5	76.5	0	22.2	77.8	76.5	0	23.5	22.2	0	77.8
rs13306520 (GG/AG/AA)	0	5.9	94.1	0	5.6	94.4	94.1	0	5.9	77.8	0	22.2
rs13306522 (GG/AG/AA)	0	0	100.0		5.6	94.4	100.0	0	0	94.4	0	5.6

Comment: HOM^P – homozygous variant (biallelic single nucleotide substitution), HET – heterozygous variant (single allelic single nucleotide substitution), HOM^N – homozygous variant (absence of nucleotide substitutions).

find a significant effect of rs1137100 on the probability of development of obesity.

According to our data, heterozygous missense mutations rs1137100, rs1137101, rs1805094 are not accompanied by an increase in the risk of developing MUO during childhood.

According to the results of our study, the CT genotype rs3790435 is more common in children with MUO (83.3%) and less often in children with MHO (41.2%).

It was found that a mutation located in the 5′-UTR may be associated with the development of some features in the course of obesity. Thus, Juan Li et al. (43), having examined 205 patients with physiological body weight and 117 obese patients, found that the presence of TT/CT rs3790435 genotypes in obese individuals was accompanied by an increased risk of obstructive sleep apnea syndrome, compared with individuals with the CC genotype (44).

It should be emphasized that in the absence of a difference in the frequency of occurrence of various exon and intron SNPs of the *LEPR* gene in groups of children with MHO and with MUO, however, according to the results of multiple discriminant analysis, these groups significantly differed from each other in terms of the set of studied polymorphisms. According to ENCODE (ENCyclopedia Of DNA Elements), not only exome, but also intronic or intergenic SNPs can represent functional significant variants (45). Thus, we can assume that the presence of several heterozygous SNPs of the *LEPR* gene is a significant pathogenic factor that determines the risk of developing MUO in children.

In contrast to the described studies, for the first time we obtained data on the presence of an association of two copies of the *LEPR* rs3790435 gene with the presence of MUO traits. It is believed that CNVs affect gene expression and are involved in the formation of the phenotype (46, 47). Maria Pettersson et al. (48) demonstrated an increase in CNV up to 19% in obese patients. It also presents evidence of the effect of changing the CNV of one gene on the likelihood of developing obesity. In particular, it was shown that a decrease in the CNV of the *AMY1* gene is associated with the development of overweight and low expression of IL-10 (49). In all likelihood, an increase in the CNV of the *LEPR* gene rs3790435 is associated with an increase in the activity of insulin resistance.

To determine the significance of *LEPR* gene polymorphisms in the development of MUO, it is necessary to further study their clinical associations in large cohorts of individuals with different obesity phenotypes.

CONCLUSIONS

Predictors of MUO formation in children are hyperleptinemia and male sex. The cumulative effect of the simultaneously present four or more SNPs of the *LEPR* gene predetermines the development of MUO. The greatest risk of MUO formation is associated with an increase in the CNV of the *LEPR* gene from rs3790435. The number of concurrently present different SNPs of the *LEPR* gene in one patient is associated with the level of the likelihood of MUO occurrence in childhood.

AUTHORS' CONTRIBUTIONS

AA was responsible for the idea and study design, looked over the articles, extracted the data, and interpreted bioinformatics analysis data. AN provided the collection of biological material using dried blood spot shipping kit, analyzed the data and interpreted it. Both authors reviewed the paper and approved the final manuscript.

COMPLIANCE WITH ETHICAL STANDARDS

Conflict of Interest: The authors declare that they have no conflict of interest.

Funding: The work is a fragment of the research work of the Department of Pediatrics 1 and Medical Genetics of the Dnipro State Medical University "Prediction of the development of childhood diseases associated with civilization" (state registration No 0120U101324). The study was carried out according to the budget program of the Code of program classification of expenses and crediting 2301020 "Scientific and scientific and technical activities in the field of health care", funded by the Ministry of Health of Ukraine from the state budget.

Ethical approval: All procedures performed in studies involving human participants were in accordance with the ethical standards of the institutional and/or national research committee and with the 2000 Helsinki declaration (52nd WMA General Assembly, Edinburgh, Scotland) and its later amendments or comparable ethical standards. The submissions were reviewed by the Ethics Committee of the Dnipro State Medical University (meeting minutes No. 7 of December 11, 2019 and minutes from meeting No. 5 of September 3, 2020).

Informed consent: Informed consent was obtained from all individual participants included in the study.

REFERENCES

1. Zhang Y, Chua S Jr. Leptin Function and Regulation. Compr Physiol 2017; 8(1): 351–69.
2. Izquierdo AG, Crujeiras AB, Casanueva FF, et al. Leptin, Obesity, and Leptin Resistance: Where Are We 25 Years Later? Nutrients 2019; 11(11): 2704.
3. Kleinendorst L, Abawi O, van der Kamp HJ, et al. Leptin receptor deficiency: a systematic literature review and prevalence estimation based on population genetics. Eur J Endocrinol 2020; 182(1): 47–56.
4. Thaker VV. Genetic and epigenetic causes of obesity. Adolesc Med State Art Rev 2017; 28(2): 379–405.
5. Kleinendorst L, Abawi O, van der Kamp HJ, et al. Leptin receptor deficiency: a systematic literature review and prevalence estimation based on population genetics. Eur J Endocrinol 2020; 182(1): 47–56.
6. Nordang GBN, Busk OL, Tveten K, et al. Next-generation sequencing of the monogenic obesity genes LEP, LEPR, MC4R, PCSK1 and POMC in a Norwegian cohort of patients with morbid obesity and normal weight controls. Molecular Genetics and Metabolism 2017; 1(121): 51–6.
7. Nunziata A, Funcke JB, Borck G, et al. Functional and Phenotypic Characteristics of Human Leptin Receptor Mutations. J Endocr Soc 2018; 3(1): 27–41.
8. Farooqi IS, Wangensteen T, Collins S, et al. Clinical and molecular genetic spectrum of congenital deficiency of the leptin receptor. N Engl J Med 2007; 356(3): 237–47.
9. Abaturov AE, Nikulina AA. (Phenotypes of obesity in children, clinical manifestations and genetic associations). Zdorov'e rebenka 2020; 4(15): 72–84. (In Ukrainian).

10. Abaturov AE, Nikulina AA. Genotype C/C 13910 of the Lactase Gene as a Risk Factor for the Formation of Insulin-Resistant Obesity in Children. Acta Medica (Hradec Králové) 2019; 62(4): 150–5.
11. ACMG Board of Directors. Clinical utility of genetic and genomic services: a position statement of the American College of Medical Genetics and Genomics. Genetics in Medicine 2015; 17(6): 505–7.
12. Elkins C, Fruh Sh, Jones L, et al. Clinical Practice Recommendations for Pediatric Dyslipidemia. Journal of Pediatric Health Care 2019; 33(4): 494–504.
13. American Diabetes Association. 2. Classification and Diagnosis of Diabetes: Standards of Medical Care in Diabetes – 2019. Diabetes Care Jan 2019; 42(Suppl. 1): 13–28.
14. Alberti KG, Zimmet P, Shaw J. International Diabetes Federation: a consensus on Type 2 diabetes prevention. Diabet Med 2007; 24(5): 451–63.
15. Weihe P, Weihrauch-Blüher S. Metabolic Syndrome in Children and Adolescents: Diagnostic Criteria, Therapeutic Options and Perspectives. Curr Obes Rep 2019; 8(4): 472–9.
16. Ranasinghe P, Jayawardena R, Gamage N, et al. The range of non-traditional anthropometric parameters to define obesity and obesity-related disease in children: a systematic review. Eur J Clin Nutr 2021; 75: 373–84.
17. Lissner L, Lanfer A, Gwozdz W et al. Television habits in relation to overweight, diet and taste preferences in European children: the IDEFICS study. 2012; 27(9): 705–15.
18. Peplies J, Börnhorst C, Günther K, et al. IDEFICS consortium. Longitudinal associations of lifestyle factors and weight status with insulin resistance (HOMA-IR) in preadolescent children: the large prospective cohort study IDEFICS. Int J Behav Nutr Phys Act 2016; 13(1): 97.
19. McCarthy HD, Cole TJ, Fry T, et al. Body fat reference curves for children. Int J Obes (Lond) 2006; 30(4): 598–602.
20. Schwandt P, von Eckardstein A, Haas G-M. Percentiles of Percentage Body Fat in German Children and Adolescents: An International Comparison. Int J Prev Med 2012; 3(12): 846–52.
21. WHO child growth standards: length/height-for-age, weight-for-age, weight-for-length, weight-for-height and body mass index-for-age: methods and development. Geneva: WHO; 2006.
22. Hongshan J, Rong L, Shou-Wei D, et al. Skewer: a fast and accurate adapter trimmer for next-generation sequencing paired-end reads. In BMC Bioinformatics 2014; 15: 182.
23. Li H, Durbin R. Fast and accurate short read alignment with Burrows-Wheeler transform. Bioinformatics 2009; 25(14): 1754–60.
24. Mose LE, Wilkerson MD, Hayes DN, et al. ABRA: improved coding indel detection via assembly-based realignment. Bioinformatics 2014; 30(19): 2813–5.
25. Wingett SW, Andrews S. FastQ Screen: A tool for multi-genome mapping and quality control. F1000Res 2018; 7: 1338.
26. Wickham H. ggplot2. Elegant graphics for data analysis. New York. 2016 Springer.
27. R Core Team: R: A Language and Environment for Statistical Computing. Vienna, Austria. 2015. (Accessed October 6, 2020, at https://www.R-project.org/).
28. Rentzsch P, Witten D, Cooper GM, Shendure J, Kircher M. CADD: predicting the deleteriousness of variants throughout the human genome. Nucleic Acids Res 2019; 47(D1): D886–D894.
29. The CADD webserver (Accessed September 11, 2020, at https://cadd.gs.washington.edu/snv).
30. FILTUS (Accessed October 6, 2020, at https://github.com/magnusdv/filtus).
31. SeqVISTA (Accessed October 6, 2020, at http://zlab.bu.edu/SeqVISTA).
32. Mutationassessor.org functional impact of protein mutations release (Accessed October 6, 2020, at http://mutationassessor.org/r3/).
33. Volchikhin VI, Ivanov AI, Serikova YuI. Compensation of methodological errors in calculating standard deviations and correlation coefficients arising from the small volume of samples. Izvestiya VUZov. Volga region. Technical Science 2016; 1(37): 103–10. (In Russian).
34. Chung ST, Onuzuruike AU, Magge ShN. Cardiometabolic risk in obese children. Ann N Y Acad Sci 2018; 1411(1): 166–83.
35. Zimmet P, Alberti GM, Kaufman F, et al. The metabolic syndrome in children and adolescents: the IDF consensus. Diabetes Voice 2007; 52(4): 29–32.
36. Barstad LH, Júlíusson PB, Johnson LK, et al. Gender-related differences in cardiometabolic risk factors and lifestyle behaviors in treatment-seeking adolescents with severe obesity. BMC Pediatr 2018; 18(1): 61.
37. Jamar G, Caranti DA, de Cassia Cesar H, et al. Leptin as a cardiovascular risk marker in metabolically healthy obese: Hyperleptinemia in metabolically healthy obese. Appetite 2017; 108: 477–82.
38. Fairbrother U, Kidd E, Malagamuwa T, Walley A. Genetics of Severe Obesity. Curr Diab Rep 2018; 18(10): 85.
39. Dos Santos Rocha A, de Cássia Ribeiro-Silva R, Nunes de Oliveira Costa G, et al. Food Consumption as a Modifier of the Association between LEPR Gene Variants and Excess Body Weight in Children and Adolescents: A Study of the SCAALA Cohort. Nutrients 2018; 10(8): 1117.
40. Furusawa T, Naka I, Yamauchi T, et al. The Q223R polymorphism in LEPR is associated with obesity in Pacific Islanders. Hum Genet 2010; 127(3): 287–94.
41. Ali EMM, Diab T, Elsaid A, et al. Fat mass and obesity-associated (FTO) and leptin receptor (LEPR) gene polymorphisms in Egyptian obese subjects. Arch Physiol Biochem 2021; 127(1): 28–36.
42. Roszkowska-Gancarz M, Kurylowicz A, Polosak J, et al. Functional polymorphisms of the leptin and leptin receptor genes are associated with longevity and with the risk of myocardial infarction and of type 2 diabetes mellitus. Endokrynol Pol 2014; 65(1): 11-6.
43. Li J, Yang S, Jiao X, et al. Targeted Sequencing Analysis of the Leptin Receptor Gene Identifies Variants Associated with Obstructive Sleep Apnoea in Chinese Han Population. Lung 2019; 197(5): 577–84.
44. Li J, Yang S, Jiao X, et al. Targeted Sequencing Analysis of the Leptin Receptor Gene Identifies Variants Associated with Obstructive Sleep Apnoea in Chinese Han Population. Lung 2019; 197(5): 577–84.
45. ENCODE Project Consortium. An integrated encyclopedia of DNA elements in the human genome. Nature 2012; 489(7414): 57–74.
46. Almal SH, Padh H. Implications of gene copy-number variation in health and diseases. J Hum Genet 2012; 57(1): 6–13.
47. Lauer S, Gresham D. An evolving view of copy number variants. Curr Genet 2019; 65(6): 1287–95.
48. Pettersson M, Viljakainen H, Loid P, et al. Copy Number Variants Are Enriched in Individuals With Early-Onset Obesity and Highlight Novel Pathogenic Pathways. J Clin Endocrinol Metab 2017; 102(8): 3029–39.
49. Selvaraju V, Venkatapoorna CMK, Babu JR, Geetha T. Salivary Amylase Gene Copy Number Is Associated with the Obesity and Inflammatory Markers in Children. Diabetes Metab Syndr Obes 2020; 13: 1695–701.

Laparoscopic Right Hemicolectomy for Appendiceal Mucocele

Eva Kudelová[1], Martin Grajciar[1,*], Marek Smolar[1], Michal Kalman[2], Ludovit Laca[1]

ABSTRACT
Appendiceal mucocele is a rare disease with an incidence of 0.07–0.63% of all appendectomies and was first described in 1842 by Carl von Rokitansky. It is defined as an abnormal intraluminal accumulation of mucin. The clinical picture of AM can vary from asymptomatic mass in the right lower quadrant to symptoms of acute appendicitis. In some cases, AM can be found accidentally on CT performed due to other reasons or during surgery. Diagnosis consists mainly of imaging methods such as ultrasound, CT, and MRI with the finding of encapsulated cystic mass with calcifications. The main goal of surgical treatment is to remove an intact mucocele and prevent spillage of mucin into the peritoneal cavity. We present a case of large mucocele treated with laparoscopic right hemicolectomy.

KEYWORDS
mucocele; laparoscopy; appendix; hemicolectomy

AUTHOR AFFILIATIONS
[1] Clinic of Surgery and Transplant Centre, Jessenius Faculty of Medicine, Martin, Comenius University Bratislava, Slovakia
[2] Department of Pathological Anatomy, Jessenius Faculty of Medicine, Martin, Comenius University Bratislava, Slovakia
* Corresponding author: Clinic of Surgery and Transplant Centre, Jessenius Faculty of Medicine, Comenius University in Bratislava, Kollárova 2, 03601, Martin, Slovak Republic; e-mail: martin.grajciar@unm.sk

Received: 20 February 2021
Accepted: 11 June 2021
Published online: 11 November 2021

Acta Medica (Hradec Králové) 2021; 64(3): 165–169
https://doi.org/10.14712/18059694.2021.28

INTRODUCTION

Appendiceal mucocele is a rare disease with an incidence of 0.07–0.63% of all appendectomies (1) and was first described in 1842 by Carl von Rokitansky (2). It is defined as an abnormal intraluminal accumulation of mucin (3). A mucocele is a result of the malignant transformation of goblet cells inside the lumen of the appendix (2). Previously, appendiceal mucocele (AM) was classified into four categories (simple/retention cyst, mucosal hyperplasia, mucinous cystadenoma, and mucinous cystadenocarcinoma) (4). A consensus for classification was reached in 2016 and it is suggested that AM should be used only as a clinical term, whereas diagnosis is based on histology (1).

The clinical picture of AM can vary from asymptomatic mass in the right lower quadrant to symptoms of acute appendicitis. Patients may also present with invagination, torsion, bleeding or AM can be misdiagnosed as an adnexal mass (5) or rarely as a chronic tubo-ovarian abscess (6). In some cases, AM can be found accidentally on CT performed due to other reasons or during surgery (5). Herein, we present a case report of appendiceal mucocele in a postmenopausal female patient.

CASE PRESENTATION

A 58-year-old female patient with a positive faecal occult blood test underwent colonoscopy with a finding of round shaped lesion with a diameter of 3 cm protruding into the caecal lumen. The mucosa of the caecum was without any pathological signs, although a compression was presented on the caecal wall due to an extraluminally localised lesion. Subsequently, a CT scan was performed, which showed a pathological fluid collection localised in the right lower quadrant. The lesion had features of a chronic abscess with calcifications in the wall. Other visceral organs were without any specific findings. The patient underwent magnetic resonance which revealed a cystic lesion in close contact with the caecal wall with the greatest diameter of 9 cm with internal septae.

In this patient, a laparoscopic revision was indicated and during the procedure, a whitish elastic well-bordered tumour with the size of 9.5 × 4 × 4 cm arising from appendix basis was found. There were no metastasis or ascites present in the peritoneal cavity. The tumour was fixed to the right colon, to the right lateral abdominal wall and retroperitoneum. The right hemicolectomy was performed due to the tumor fixation to the adjacent structures to avoid mucocele perforation. The surgery was performed by a laparoscopic approach using the no-touch technique with the ileo-transverso-anastomosis. The specimen was removed within the endo-bag through mini-laparotomy.

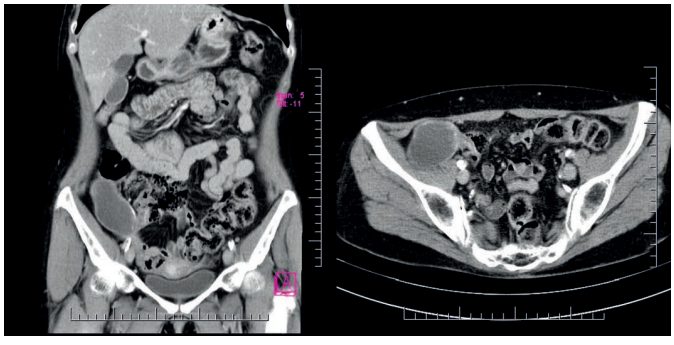

Fig. 1 Coronal and axial CT-scan showing cystic lesion with calcifications and in close contact with the caecal wall.

Fig. 2 Resected part of the right colon with appendiceal mucocele.

Fig. 3 Detail of appendiceal mucocele.

Histological examination confirmed low-grade mucinous neoplasm of the appendix (LAMN). The specimen was delivered to the pathology department en-block without perforation. The appendix was dilated and filled with gelatinoid material. The cystic tumour of the appendix was lined with flat and a few isolated cylindrical mucinous epithelia with focal low-grade dysplasia. The growth of the lesion had an expanding pattern with the loss of muscularis mucosae and fibrosis of submucous tissue and muscular layer without any signs of perforation or propagation of the tumour cells into the serous layer. Six lymph nodes were identified only with features of chronic antigen stimulation. Resection margins were without any neoplastic changes. Adjuvant chemotherapy was not indicated, and the patient was followed up during the first year after the surgery every 3 months and during the second year every

6 months and underwent regular imaging and laboratory examinations. The last follow up was in January 2021 with no signs of recurrence.

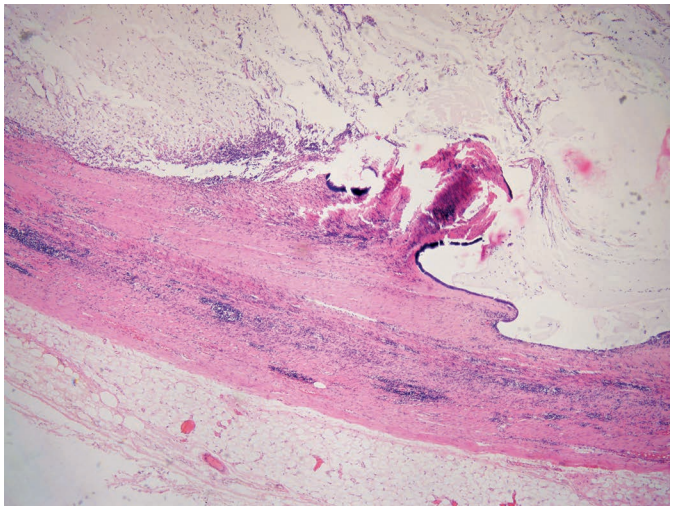

Fig. 4 Fibrosclerotic altered wall of the appendix with expansive tumour growth formed by a single-layer cylindrical epithelium with extracellular mucus formation. Most of the epithelium was denuded.

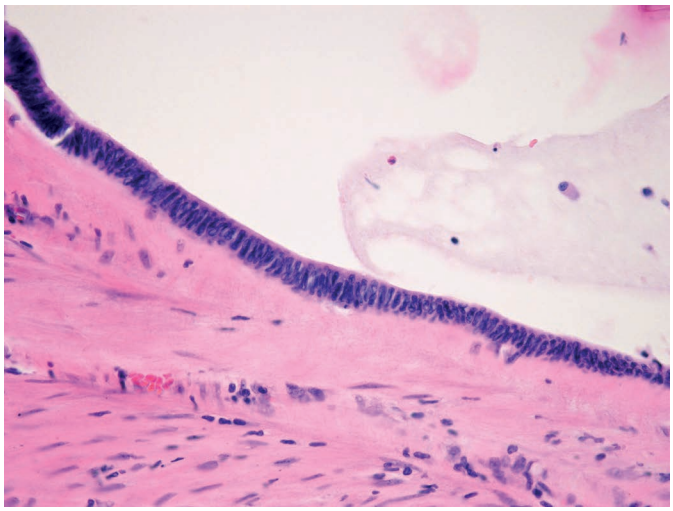

Fig. 5 Detail of a tumour lining formed by cylindrical cells with cigar-shaped hyperchromic nuclei corresponding to "low-grade" dysplasia.

DISCUSSION

Appendiceal mucocele represents an abnormal dilatation of the appendix with intraluminal mucin accumulation with an incidence of less than 1% (5). Mucocele is often diagnosed in patients over 50 years of age (4), whereas women are more often affected by this disease (7). Symptoms of AM are usually non-specific. Patients may complain of acute or chronic pain in the right lower abdominal quadrant and in some cases, a palpable mass can be present. Other common symptoms include also weight loss and changes in bowel habits (8). Some patients are admitted to the hospital due to symptoms of acute appendicitis and the diagnosis of AM is either established during surgery (6) or it can be found accidentally on imaging studies. Our patient did not have any specific symptoms except the positive faecal occult blood test.

Mucinous neoplasm represents a broad spectrum of tumours ranging from adenoma to mucinous adenocarcinoma. According to the recent classification from 2016, non-carcinoid epithelial tumours of the appendix are categorized into eight histomorphological groups which are summarized in Table 1 (9). Modified Delphi Consensus Protocol reviewed by Carr et al. states that lesions beyond the mucosa without infiltrative invasion are classified as LAMN or HAMN. High-grade appendiceal mucinous neoplasm (HAMN) has similar features as LAMN except the high-grade cytological atypia which is characteristic for HAMN. The infiltrative invasion characterized by discohesive cells, tumor budding and desmoplastic reaction are typical for the appendiceal adenocarcinoma. The presence of desmoplasia is referred as a diagnostic criterion for distinquishing adenocarcinoma from LAMN/HAMN (9).

Tab. 1 Modified Delphi Consensus Protocol 2016 reviewed by Carr et al. Abbreviation CRC, colorectal cancer (7, 9).

Terminology	Lesion
Tubular, tubovillous, villous adenoma	Adenoma (traditional CRC type)
Serrated polyp	Tumour with serrated features
Low-grade appendiceal mucinous neoplasm	Low-grade cytologic atypia and loss of the muscularis mucosa layer, pushing invasion, acellular mucin in the wall, mucin outside the appendix, submucosal fibrosis
High-grade appendiceal mucinous neoplasm	High-grade cytologic atypia without infiltrative invasion
Mucinous adenocarcinoma	Infiltrative invasion (single cells), desmoplasia
Mucinous adenocarcinoma with signet cells	Signet cells ≤50%
Signet cell carcinoma	Signet cells ≥50%
Adenocarcinoma	Adenocarcinoma (non-mucinous)

Appendiceal mucocele in some cases represents a diagnostic challenge. Abdominal ultrasound may reveal encapsulated cystic mass with or without acoustic shadowing caused by mural calcification. A pathognomonic for AM is the "onion skin sign" which refers to echogenic layers of mucin and acoustic shadowing caused by mural calcifications inside the lumen of a mucocele (2, 10). Furthermore, an appendix diameter of more than 1.5 cm and a wall thickness of more than 6 mm are considered to be the threshold values for AM diagnosis (10). Dilated low-attenuated encapsulated cystic lesion of the appendix is seen on CT. Intraluminal mucin accumulation causes chronic inflammatory changes which result in wall calcification which are characteristic for AM (2). In case of secondary intra-abdominal infection, there are signs such as peri-appendiceal fat stranding, free intraperitoneal fluid, calcification, and intraluminal air-fluid level shown on CT. Features such as wall irregularity and soft-tissue thickening highly support the malignant etiol-

ogy of AM. Magnetic resonance shows AM also as a cystic mass with various T1W1 intensity and hyperintense on T2W1 (10). Furthermore, mucocele of the appendix can be associated with synchronous colorectal neoplasms in 19–25% of cases (11). Therefore a colonoscopy should be performed before surgery to assess the extent of surgical resection (10, 12). A characteristic feature for AM can be found on colonoscopy known as "volcano sign" which is caused by fluctuation of protruded appendiceal ostium according to the respiratory movements (10). Tumour markers including CEA, CA 19-9 and CA-125 can be used in postoperative follow-up and their elevated levels may indicate recurrence (13), however, their diagnostic significance is low (2).

The goal of surgical treatment is to remove an intact mucocele, prevent spillage of mucin into the peritoneal cavity, and achieve negative resections margins (1). In case of spontaneous or iatrogenic perforation of AM, there is a high risk of pseudomyxoma peritonei development which is a severe complication with less than 20% of 5-years survival (14). Pseudomyxoma peritonei is a clinical syndrome characterized by the presence of mucin and neoplastic epithelial cells on the parietal and visceral peritoneum. This disease is a consequence of intraperitoneal dissemination from mucin-producing tumours (7). The treatment of PMP consists of cytoreductive surgery followed by hyperthermic intraperitoneal chemotherapy (15).

There are still no clear guidelines for surgical treatment of mucocele, however, Dhage-Ivatury et al. (16) and Kim et al. (17) created a scheme for the selection of the type of surgery. Several factors, which should be considered before the surgery, are summarized in table 1 (5). Frozen section examination of resection margins and sentinel lymph node (SLN) from mesoappendix is often useful and necessary to assess the extent of surgery. Right hemicolectomy is not indicated if SLN is without metastasis (18). Historically, laparotomy has been considered as the preferred surgical approach for mucocele treatment (4), however, there are several reports in the literature of successful laparoscopic mucocele resections. General principles of AM removal are the same regardless of the surgical approach. The operation should be performed carefully with an emphasis on the no-touch technique. An endo-bag must be used to prevent rupture of AM and port-site metastasis, while the surgeon should be experienced enough with laparoscopy (19). The prognosis of AM depends on several factors such as symptoms, histological parameters, perforation, increased tumour markers levels, and positive resection margins (20).

CONCLUSION

Appendiceal mucocele is a rare disease that can be asymptomatic or resembles acute appendicitis. Pre-operative diagnosis consists of imaging methods such as ultrasound, CT, MRI, or colonoscopy is used. The main goal of surgical treatment is to remove an intact mucocele and prevent spillage of mucin into the peritoneal cavity.

REFERENCES

1. Cestino L, Festa F, Cavuoti G, et al. Appendiceal mucocele: three cases with different clinical presentation and review of literature. J Surg Case Rep 2020; 2020(9): rjaa344.
2. Kwak HD, Ju JK. A prospective study of discrepancy between clinical and pathological diagnosis of appendiceal mucinous neoplasm. Ann Surg Treat Res 2020; 98(3): 124–9.
3. Sakata S, Moran BJ. What is a "mucocele" of the appendix and how are these lesions best managed? Beware the wolf in sheep's clothing. Colorectal Dis Off J Assoc Coloproctology G B Irel 2019; 21(11): 1237–9.
4. Şentürk M, Yavuz Y, Alkan S, Kafadar MT. The Investigation of 14 Appendiceal Mucocele Cases Encountered in 4850 Appendectomy Patients. J Gastrointest Cancer 2021; 52(2): 701–5.
5. Sun P, Jiang F, Sun H, et al. Minimally invasive surgery for appendiceal intussusception caused by mucocele of the appendix: case report and review of the literature. J Gastrointest Oncol 2020; 11(1): 102–7.
6. Cubro H, Cengic V, Burina N, Kravic Z, Beciragic E, Vranic S. Mucocele of the appendix presenting as an exacerbated chronic tubo-ovarian abscess: A case report and comprehensive review of the literature. Medicine (Baltimore) 2019; 98(39): e17149.
7. Gündoğar Ö, Kımıloğlu E, Komut N, et al. Evaluation of appendiceal mucinous neoplasms with a new classification system and literature review. Turk J Gastroenterol Off J Turk Soc Gastroenterol 2018; 29(5): 533–42.
8. Arnason T, Kamionek M, Yang M, Yantiss RK, Misdraji J. Significance of proximal margin involvement in low-grade appendiceal mucinous neoplasms. Arch Pathol Lab Med 2015; 139(4): 518–21.
9. Carr NJ, Cecil TD, Mohamed F, et al. A Consensus for Classification and Pathologic Reporting of Pseudomyxoma Peritonei and Associated Appendiceal Neoplasia: The Results of the Peritoneal Surface Oncology Group International (PSOGI) Modified Delphi Process. Am J Surg Pathol 2016; 40(1): 14–26.
10. Sharma P, Soin P, Chugh M, Goyal P. Dilated Appendix: Is There More to It? Case Report and Brief Review of Literature with Radiologic-Pathological Correlation. J Clin Imaging Sci 2019; 9: 9.
11. Alghamdi AO, Aldossary MY, Alsawidan M, AlBahar S. Low grade appendiceal mucinous neoplasm mimicking an ovarian cyst: A case report. Int J Surg Case Rep 2020; 70: 145–8.

Tab. 2 Factors determining the extent of surgery. Abbreviations AM, appendiceal mucocele; LN, lymph node (5, 16, 17).

	Type of Surgery		
	Appendectomy	**Partial cecectomy**	**Right hemicolectomy**
Factors	Non-perforated	Non-perforated	Non-perforated
	Intact appendiceal base	Broad, protruding AM into the caecal wall	AM invades the caecal wall or ileum
	Negative cytology	Negative/positive cytology	An adequate resection margin cannot be obtained
	Negative lymph nodes	Negative/positive margins of appendiceal stump	Positive cytology
		Negative appendiceal LN	Positive resection margin
			Positive margin of appendiceal stump
			Positive appendiceal LN
			Highly suspected malignancy

12. Foula MS, Alardhi AM, Othman SA, Mirza Gari MK. Laparoscopic management of appendicular mucinous cystadenoma, case report. Int J Surg Case Rep 2019; 54: 87–9.
13. Padmanaban V, Morano WF, Gleeson E, et al. Incidentally discovered low-grade appendiceal mucinous neoplasm: a precursor to pseudomyxoma peritonei. Clin Case Rep 2016; 4(12): 1112–6.
14. Pantiora EV, Massaras D, Koutalas J, Bagiasta A, Kontis EA, Fragulidis GP. Low-grade Appendiceal Mucinous Neoplasm Presenting as Adnexal Mass: A Case Report. Cureus 2018; 10(11): e3568.
15. Sullivan BJ, Bolton N, Sarpel U, Magge D. A unique presentation of superinfected pseudomyxoma peritonei secondary to a low-grade appendiceal mucinous neoplasm. World J Surg Oncol 2019; 17(1): 34.
16. Dhage-Ivatury S, Sugarbaker PH. Update on the surgical approach to mucocele of the appendix. J Am Coll Surg 2006; 202(4): 680–4.
17. Kim TK, Park JH, Kim JY, et al. Safety and feasibility of laparoscopic surgery for appendiceal mucocele: a multicenter study. Surg Endosc 2018; 32(11): 4408–14.
18. González-Moreno S, Sugarbaker PH. Radical appendectomy as an alternative to right colon resection in patients with epithelial appendiceal neoplasms. Surg Oncol 2017; 26(1): 86–90.
19. Park B-S, Shin DH, Kim D-I, Son GM, Kim HS. Appendiceal intussusception requiring an ileocecectomy: a case report and comment on the optimal surgery. BMC Surg 2018; 18(1): 48.
20. Shin R, Chai YJ, Park JW, et al. Ultimate Clinical Outcomes of Appendiceal Mucinous Neoplasm of Uncertain Malignant Potential. Ann Surg Oncol 2017; 24(4): 974–82.

Chondroblastoma of the Temporal Bone: A Case Report and Literature Review

Katarína Obtulovičová[1,*], Marián Sičák[1], Adrian Kališ[2,3], Tomáš Buday[4]

ABSTRACT

Introduction: Temporal bone chondroblastoma is a rare, locally aggressive tumour originating from immature cartilage, which recurs to a high degree. Treatment is surgical. Radiotherapy is reserved for recurrence. We describe a case of a 15-year-old-boy choosing a conservative surgical approach with reconstruction of the posterior canal wall. This study aims to report a rare pediatric case.
Methods: A literature review was performed to better understand temporal bone chondroblastomas, to describe their histopathological and radiological characteristics and to establish the optimal surgical and non-surgical treatments. The research of previous published data was done using PubMed with keywords mentioned below.
Results: Authors present a case of a 15-year-old boy with hearing impairment and facial nerve palsy. Conservative surgery with reconstruction of the tympanic membrane and posterior wall of the external auditory canal, restoring the hearing has been performed. We did not administer any adjuvant therapies. No sign of recurrence was observed 1 year after primary surgery. Facial nerve function is normal, and hearing is satisfactory.
Conclusion: Chondroblastomas account for less than 1% of primary bone tumours. Temporal bone chondroblastoma is rare, locally aggressive, with a high prevalence of recurrence. This study describes specific histopathological and radiological findings, the chosen surgical approach and follow-up to improve the management and the prognosis of patients affected with this particular clinical entity.

KEYWORDS

chondroblastoma; temporal bone tumour; facial nerve palsy

AUTHOR AFFILIATIONS

[1] Otorinolaryngology/Head & Neck Surgery Clinic, the Central Military Hospital – Faculty Hospital, Ružomberok, Slovakia
[2] Institute of Pathology, the Central Military Hospital – Faculty Hospital, Ružomberok, Slovakia
[3] Catholic University in Ružomberok, Slovakia
[4] The Jessenius Medical Faculty of Comenius University in Martin, Slovakia
* Corresponding author: Otolaryngology/Head & Neck Surgery Clinic, Central Military Hospital – Faculty Hospital, Generála M. Vesela 21, 034 26 Ružomberok, Slovakia, e-mail: obtulovicovak@gmail.com

Received: 28 May 2020
Accepted: 30 January 2021
Published online: 11 November 2021

Acta Medica (Hradec Králové) 2021; 64(3): 170–173
https://doi.org/10.14712/18059694.2021.29

INTRODUCTION

Temporal bone tumours represent a heterogeneous group of tumours with different biological behaviours. The specificity of this site represents a challenging surgical approach and often risk resection bringing postoperative morbidity. Histopathological findings, grading and staging in the case of malignant tumours determine the possibilities of non-surgical cancer therapy.

CASE REPORT

The ENT outpatient office is visited by a 15-year-old healthy boy due to buzz in his right ear since early April 2018. He had never had trouble with his ears before. At the initial examination, cerumen was partially removed, accompanied by haemorrhage from the ear canal. Ear drops, and systemic antibiotics were prescribed to the patient. During the check-up visit, otitis externa granulomatosa was diagnosed and the patient was sent to the clinic for further diagnosis and treatment. On April 18, 2018, an outpatient biopsy was collected from the granulation tissue of the ear canal with histopathological findings of non-specific granulation tissue, suspected of cholesteatoma. In the microbiological examination, *Staphylococcus aureus* and *Escherichia coli* were found. Audiometry, a slight conductive hearing loss with the air-bone gap of up to 20 dB on the right ear was diagnosed. From April 21, 2018, paresis of facial nerve of grade IV of House – Brackmann classification developed. An HRCT scan of the temporal bone was conducted with the finding of expansive intraosseal soft tissue with calcifications in the temporal bone to the right (Fig. 1). We proceeded with surgical treatment without delay. On April 27, 2018, temporal bone tumour resection with neuromonitoring of the facial nerve on the right in the range of canal-wall down mastoidectomy with retrofacial tympanotomy (modified Fisch A approach) and subsequent reconstruction was performed. A sample was sent for perioperative histology with the conclusion – mesenchymal malignant tumour.

The tumour tissue eroded the posterior wall of the ear canal – tumour masses filled the tympanic cavity and grew to the mastoid portion of the facial nerve (Fig. 2). The tympanic membrane was largely destructed, while the chain of ossicles remained complete but surrounded by tumorous mass. We removed the incus. We left the malleus and stapes in situ. The integrity of the facial nerve was intact. The jugular bulb was intact, the tumour did not grow from it. The ACI channel was intact (Fig. 3). We reconstructed the tympanic membrane and covered the cavity that arose in the hypotympanic area after drilling the bone by a cartilage graft. The facial nerve was covered by cartilage and muscle lobe. We have planned a second-look operation.

After definitive processing, the histopathological diagnosis of chondroblastoma was determined – a tumorous

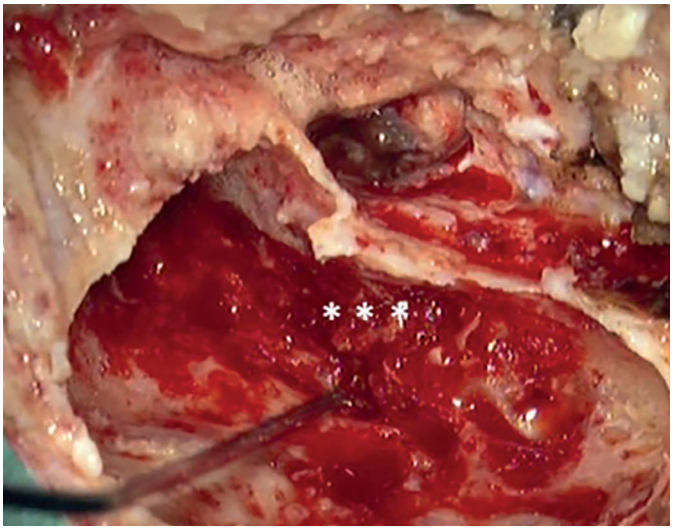

Fig. 2 A perioperative shot from primary surgery: evident destruction of the media third of the external ear canal (***). The neuromonitoring probe is attached to the mastoid region CN VII, right side. (NIM neuro 3 fi Medtronic).

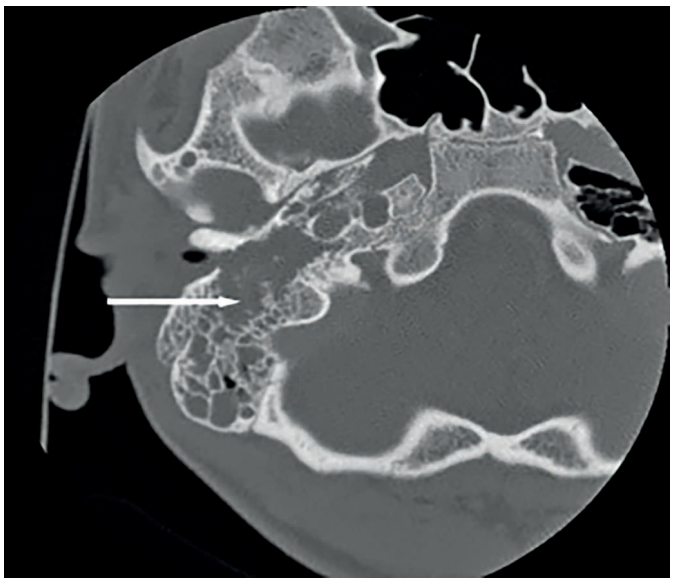

Fig. 1 A preoperative HRCT scan of the temporal bone with an expansive intraoseeal soft tissue with calcifications (white arrow).

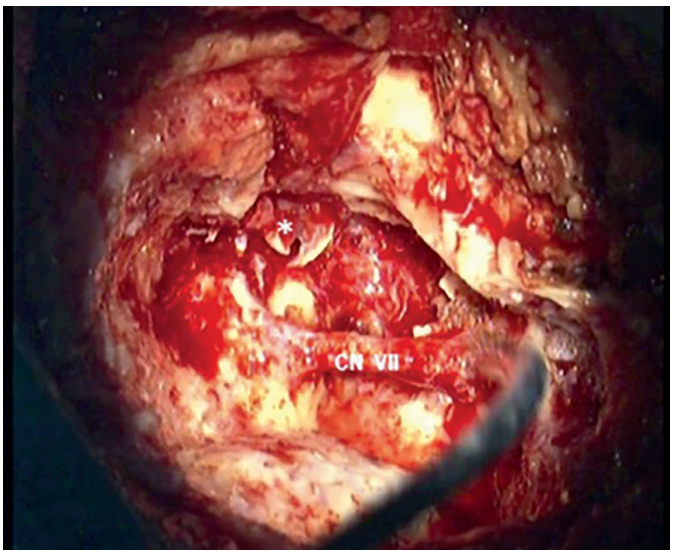

Fig. 3 A perioperative shot from primary surgery: after tumour remediation (* tympanic membrane). Completely denuded mastoid region CN VII, right side. (modified Fisch A).

lesion of the chondroosteoid appearance with round uniform S100+ cells, with the presence of gigantic multinuclear cells (CD68+).

After the surgery, the facial nerve function rapidly adjusted, with a slight conduction disorder with the air-bone gap of up to15dB.

On June 15, 2018, we carried out a control biopsy from granulation of the auditory canal, which was histologically negative. After complete healing, we found a favourable otomicroscopic finding – a solid ear canal without dehiscence and a solid neomyrinx in good standing.

In a post-operative follow-up an FDG-PET scan was performed on June 25, 2018, with the result being a slight focal elevation of FDG metabolism in the post-operative changes field to the right together with the recommendation of the dynamics follow-up due to a short time period since surgery (Fig. 5). In other localities, we did not find pathological lesions with increased FDG metabolism of the characteristics of tumour tissue.

In the further follow-up, MRI of the temporal bone was performed on July 10, 2018, and February 4, 2019, without finding a tumour recurrence.

On March 13, 2019, we performed a planned second-look operation with control biopsies, preceded by HRCT of the temporal bone – suspected residual tumour not confirmed (Fig. 4).

The original trepanation cavity was revised – samples were taken for perioperative histology – without tumour finding, as confirmed by definitive histology.

The trepanation cavity was freely ventilated through aditus ad antrum and retrofacial tympanotomy. Stimulation of CN VII, was functional. The in situ malleus and stapes in soft contact with the neomyrinx. Between the stapes and the neomyrinx, we inserted cartilage interposites. The original reconstruction of the tympanic membrane and the ear canal from the previous operation was preserved.

The patient remains without recurrence 2 years after surgery, in the dispensary care of our otologic outpatient office and the paediatric oncology outpatient office.

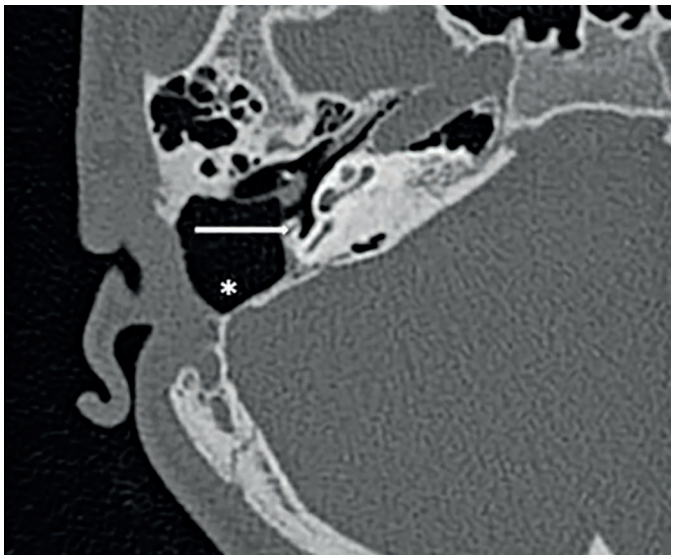

Fig. 4 A postoperative HR CT scan: the ventilated cavity of temporal bone (*) after chondroblastoma remediation without recurrence finding (CN VII – white arrow).

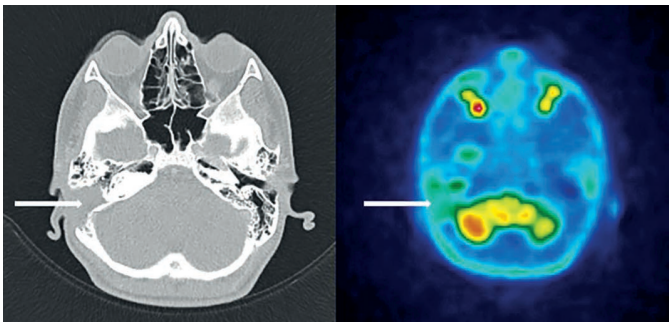

Fig. 5 A postoperative PET-CT scan of non-specific finding (white arrow) of the temporal bone after chondroblastoma remediation without recurrence finding.

DISCUSSION

Chondroblastomas represent less than 1% of primary bone tumours (1). The phenomenon was first described by Codman in 1931 as an "epiphyseal chondromatous large cell tumour of the proximal humerus". The term chondroblastoma was first used by Jaffe and Lichtenstein in 1942 (2).

It is a benign, cartilage-producing tumour most commonly occurring in the epiphyses of growing patients. A typical location is the knee, rib and pelvis. Most patients are 10–15 years old with male predominance. In the temporal bone, chondroblastoma is very rare. Patients with skull and temporal bone disease are older (40–50 years). It is a locally aggressive tumour (3).

From a histopathological point of view, chondroblastoma is a tumour from immature cartilage. It is a biological intermediate between chondroma and chondrosarcoma. Its biological behaviour ranks among low-grade tumours (4). Haematoxylin-eosin staining is characterized by cartilage with immature cells. The diagnosis of chondroblastoma is inevitably complemented by the positivity of CD-68, vimentin and S-100 protein (1).

In the preoperative diagnosis, there is a clear place for HRCT in the temporal bone and MRI imaging. Investigations will allow you to accurately determine the extent of disability and the choice of optimal surgery.

Typically, on HRCT, the tumour is shown as an expansive intraoseeal soft tissue with calcifications and postcontrast enhancement sites. Marginal and central calcifications are visible (Fig. 1). In a radiological study of 16 chondroblastoma patients Park found an invaded squamous portion of the temporal bone, temporal and infratemporal pits, temporomandibular joint, and the tympanic cavity (5).

In MRI imaging, chondroblastoma manifests itself as an expansive heterogeneous hypermetabolic mass with 2 distinct components – solid with predominantly low signal in T1 and T2 sequences and multilocular cystic with T1 and T2 elongation and presence of fluid-fluid signals at T2 imaging. Post-contrast saturation is present in the solid component and septum of the cystic component. Possible high signalling in T2 imaging depends on potential haemorrhage in the tumour mass. MRI better defines the infiltration of the dura, cerebral, intracranial, and soft tissue infiltration. There was no observed increase in the signal strength for DWI (5, 6).

In an FDG-PET examination, chondroblastoma is shown as a hypermetabolic lesion with strong uptake of deoxyglucose. Typically, there is increased FDG uptake, which increases from early to late phase. This type of dynamic increase in FDG uptake should lead to suspicion of bone tumour of the temporal bone (7). FDG-PET enables the identification of metastases, precise staging and diagnosis of tumour recurrence.

The treatment of choice is complete multidisciplinary tumour removal depending on the extent (3). In surgical resection, a conservative approach is recommended with a reduction of postoperative morbidity (2).

80–90% of chondroblastomas are treated with surgery. Local recurrence occurs between 14–18% and is often within two years. Temporal bone lesions have a higher incidence of recurrence (up to 50%) due to anatomical localization and difficult surgical extirpation (3). The role of radiotherapy is not clearly defined according to the current knowledge. Due to the low-grade character of the tumour and the absence of metastases, the postoperative radiotherapy is not indicated (2, 8).

The existence of a pure malignant variant of chondroblastoma is controversial. Mostly, it is a case of post-radiation sarcoma and misdiagnosis (3). The indication for radiotherapy is a recurrence. Chemotherapy is not indicated.

Reid reported a literary review of 81 cases of chondroblastoma of the temporal bone from 1950 to 2011. It gives a predilection of the incidence in men (1 : 1.2). The mean age of diagnosis was 41 years, with age ranges from 3 to 85 years. The symptomatology was very diverse, and its analysis did not prove a clear clinical picture that would lead to the diagnosis of chondroblastoma. Impaired hearing dominated (49.4%), followed by cranial nerve involvement (43.2%), facial swelling (22.2%), otalgia (19.8%), full ear feeling (14.8%), otorrhea (8.6%), tinnitus, temporomandibular pain, trismus and cephalea (2).

Reid et al. were able to evaluate follow-up in 61 (out of 81) patients. He was diagnosed with a recurrence in 8.2%, with an average time to recurrence of 12.9 months. All five patients diagnosed with recurrence have undergone surgical treatment and three postoperative radiotherapies (2).

Selesnick et al. analysing 21 patients with chondroblastoma of the temporal bone from the 1966–1998 literature review found 95% invasion of the middle cranial pit and 76% found erosion of the external auditory canal. It hypothesizes that chondroblastoma of the temporal bone may be the result of growth from the embryonic or cartilage base in the tympanosquamous suture of the middle cranial pit. It is a separate entity (8).

Adnot et al. report on the case of chondroblastoma, which manifested itself as a preauricular mass with temporal bone and temporomandibular joint invasion. Complete remission 4 years after surgical treatment has been reported (9).

Hatano et al. report on a 67-year-old female patient with right-sided mixed hearing impairment, finding granulation in the external ear canal, feeling full in the ear, otalgia and bloody otorrhea, and pain in the temporomandibular joint. Chondroblastoma with temporomandibular joint invasion, pterygopalatine fossa and infratemporal fossa were diagnosed in the patient. She underwent resection via infratemporal approach B, with a facial nerve function preservation. 7.5 years after surgery, there is no sign of recurrence (10).

To date, no case of temporal bone chondroblastoma with metastasis has been reported in the literature. In contrast, metastases in the abdomen and in the lungs have been described in pelvic chondroblastoma.

With adequate surgery, the prognosis is good. Long-term monitoring of the patient using imaging is recommended.

SUMMARY

Temporal bone chondroblastoma is a rare, locally aggressive tumour originating from immature cartilage, which recurs to a high degree. The diagnosis is based on detailed imaging and histopathological examination. Treatment is surgical. Its low-grade character makes it possible to select an operative performance in which the tumour is completely resected and, at the same time, a conservative approach with a reduction in postoperative morbidity. Radiotherapy is reserved for recurrence. Long-term patient follow-up using imaging examinations is indicated.

ACKNOWLEDGEMENTS

Mrs. Jana Plevková is acknowledged for her technical assistance.

FINANCIAL DISCLOSURE INFORMATION

None.

REFERENCES

1. Cotran R, Kumar V, Robbins S. Pathological basis of disease. Fifth edition. Pennsylvania: WB Saunders Company, 1994.
2. Reid LB, Wong DS, Lyons B. Chondroblastoma of the temporal bone: a case series, review and suggested management strategy. Skull Base Rep 2011; 1(2): 71–82.
3. Fletcher CDM, Bridge JA, Hogendoorn P, et al. WHO Classification of Tumours of soft tissue and bone. Fourth edition. Lyon: IARC Press, 2013.
4. Cabrera RA, Almeida M, Mendonca ME, Frable WJ. Diagnostic pitfalls in fine-needle aspiration cytology of temporomandibular chondroblastoma: report of two cases. Diagn Cytopathol 2006; 34(6): 424–9.
5. Park SW, Kim, JH, Park JH, et al. Temporal bone chondroblastoma: imaging characteristics with pathologic correlation. Head Neck 2017; 39(11): 2171–9.
6. Kobayashi Y, Murakami R, Toba M, et al. Chondroblastoma of the temporal bone. Skeletal Radiol 2001; 30(12): 714–8.
7. Toriihara A, Tsunoda A, Takemoto A, et al. Dual-time-point FDG-PET/CT Imaging of Temporal Bone Chondroblastoma: A report of two cases. Asia Ocean J Nucl Med Biol 2015; 3(2): 120–4.
8. Selesnick SH, Levine JM. Chondroblastoma of the temporal bone. Consistent middle fossa involvement. Skull Base Surg 1999; 9(4): 301–5.
9. Adnot J, Langlois, O, Tollard E, et al. Lateral skull base chondroblastoma resected with facial nerve posterior transposition. Neurochirurgie 2017; 63(2): 88–90.
10. Hatano M, De Donato G, Falcioni M, Sanna M. Chondroblastoma of the temporal bone. Acta Otolaryngol 2011; 131(8): 890–5.

Spindle Cell Lipoma Occurring in the Submandibular Space: Fifth Case Reported along with a Concise Review of the Literature

Manveen Kaur Jawanda[1], Harshaminder Kaur Grewal[2], Sonia Gupta[3,*], Vineet Sharma[4], Ravi Narula[5]

ABSTRACT

Spindle cell lipoma (SCL) is an uncommon histological variant of lipoma that accounts for 1.5% of all adipose tumors. It rarely occurs in the oral cavity. The most common sites of involvement are the buccal mucosa, tongue, lip, alveolar mucosa, gingiva, and palate. Submandibular space is a very rare site of occurrence for SCL. When occurs in this site, SCL mainly involves the 4th–7th decade with a female predominance. Due to wide communications of submandibular space, the actual extent and appearance of the lesions present here gets masked up especially those involving the deeper tissues leading to an inaccurate diagnosis. Wide overlap of clinical and histopathological features of SCL to other clinical pathologies leads to a challenging task for the clinicians to reach an accurate diagnosis. To our knowledge, only four cases of intraoral SCL involving the submandibular region directly or indirectly have been reported in the literature. Here we represent another rare case of SCL in an 18-year-old male patient along with a concise review of the literature. This case appears to be quite rare due to its location (submandibular space), age, and sex of the patient (18/M).

KEYWORDS

diagnostic challenge; intraoral; lipoma; spindle cell; submandibular space

AUTHOR AFFILIATIONS

[1] Dept. of Oral Pathology and Microbiology & Forensic odontology. Laxmi bai institute of dental sciences and hospital, Patiala, Punjab, India
[2] Waryam Singh Hospital, Yamunanagar, Haryana, India
[3] Dept. of Oral Pathology and Microbiology & Forensic odontology, Rayat Bahra Dental college and hospital, Mohali, Punjab, India
[4] Dept. of Conservative Dentistry, Laxmi bai institute of dental sciences and hospital, Patiala, Punjab, India
[5] Dept. of Oral and Maxillofacial surgery, Guru Nanak Dev Dental College and Research Institute, Sunam, Punjab, India
* Corresponding author: #95/3, Adarsh Nagar, Dera Bassi, Dist. Mohali, Punjab-140507, India; e-mail: Sonia.4840@gmail.com

Received: 12 November 2020
Accepted: 7 July 2021
Published online: 11 November 2021

Acta Medica (Hradec Králové) 2021; 64(3): 174–182
https://doi.org/10.14712/18059694.2021.30

INTRODUCTION

Enzinger and Harvey first reported on spindle cell lipoma (SCL) in 1975 (1), and this tumor is known to be a rare lipoma variant that represents about 1.5% of all adipocyte-origin tumors (2). Conventionally, depending upon the site, lipomas are classified into superficial, deep, and parosteal (3). Clinically they appear as non-tender, soft, mobile masses. Most of the time, the clinical detection of superficial lipomas is easy while the deep-seated or infiltrating lipomas may become difficult to diagnose and require further investigations such as imaging (4). Submandibular space is a very rare site of occurrence for SCL. We report a rare 5th case of SCL involving the submandibular space in an 18-year-old male patient with a concise review of the literature. A search of the online database yielded only four other case reports of SCL involving the submandibular space directly or indirectly till date (Table 1).

Tab. 1 Cases of Spindle cell lipoma in the submandibular space reported in the literature (1989–2020).

S. no.	Authors (Year)	Age/sex	Location of tumour mass
1.	Levy et al. (1989)	74/F	The palpation of mass through the submandibular triangle was without any fixation to the submandibular gland.
2.	Braumann et al. (2001)	45/M	Tender swelling of the right parotid area reaching the submandibular region.
3.	Coimbra et al. (2006)	29/F	Adjacent to the opening of the Wharton duct.
4.	Yalcin et al, (2015)	49/F	Superficially located in front of the sublingual caruncle.
5.	Present case******	18/M	Left submandibular region.

CASE REPORT

An 18-Year-old male patient reported with a painless swelling in the left submandibular region. He had been aware of the lesion for 3 months. He had difficulty in mastication without any associated pain. No history of trauma or inflammation of the area could be recalled. Patient was moderately built, with well orientation of the surroundings. All the vital signs were normal. He didn't reveal any relevant medical or habitual history.

Extraoral examination revealed a smooth surfaced, soft mass (4 cm × 5 cm) with well-defined margins in the left submandibular region (Figure 1A). The swelling was more prominent with the teeth clenching and reduced in size on relaxation. On palpation, the swelling was slightly tender, soft, and fluctuant. It raised the floor of the mouth on applying pressure on it from outside. Computerized tomography (CT) Scan and Magnetic resonance imaging (MRI) were advised, but patient refused to go for any of these due to poor socioeconomic status. Ultrasonography (USG) of the lesion showed a hyperechoic mass in the region of left neck anterolateral to the left submandibular gland with well-defined margins and homogeneous texture. The mass did not show any evidence of calcification or vascularity. No lymphadenopathy was observed.

The clinical differential diagnosis made for submandibular region swelling included ranula/dermoid cyst or salivary gland tumor. The tumor mass was partially above the mylohyoid muscle and the bulk of it was below the mylohyoid muscle in the submandibular space (Figure 2). So, the superficial part of the lesion was excised along with the sublingual gland by intraoral sublingual approach, and the bulk of the tumor mass below the mylohyoid muscle was removed extra orally by the standard submandibular approach. The specimen (Figure 1B) in toto was sent for histopathological examination.

Fig. 1 A) Clinical photograph showing swelling in the left submandibular region. B) Photograph of gross excisional tissue.

On histopathological examination, H & E stained sections revealed the presence of well -circumscribed tumor mass composed of lobules of normal mature adipocytes with clear cytoplasm and a peripheral nucleus giving a signet ring appearance. The lipocytes were separated by spindle cells and fibrous tissue (Figure 3A,B). Cellular areas were composed of spindle cells with elongated nuclei and scant cytoplasm along with bundles of dense ropey collagen fibers (Figure 4A,B). While excised sublingual gland revealed the presence of lobules of mucus acini separated by connective tissue septa. Based on these features, a histopathological diagnosis of SCL along with normal sublingual gland was given. Immunohistochemical (IHC) Staining with CD34 demonstrated strong intracytoplasmic

reactivity in many spindle cells (Figure 5A,B), confirming the histopathological diagnosis of SCL (Figure 6). SCL being a benign lesion is treated with surgical excision only without need of any other therapy. And the recurrence rates have been reported very rare. In the present case also, surgical excision was done. Postoperative healing was uneventful and 4 years after surgery the patient was free of Postoperative healing was uneventful and 4years after surgery the patient was free of recurrence.

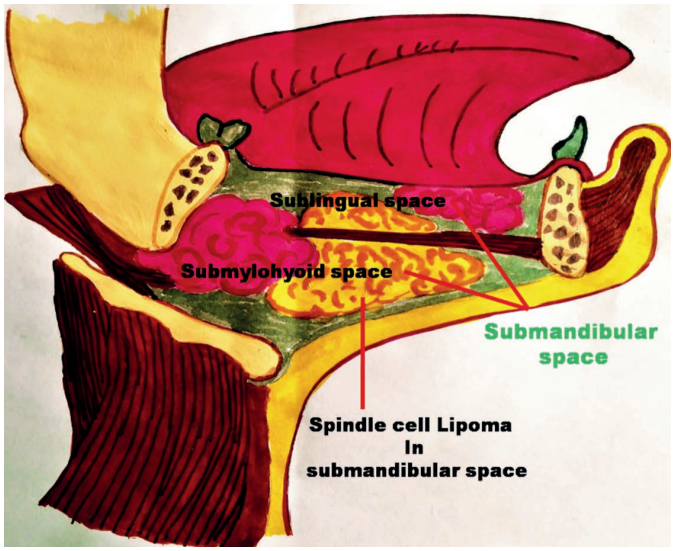

Fig. 2 Tumor mass occupying the submandibular space, partially above the mylohyoid muscle (sublingual space) and the bulk of it in the sub mylohyoid space.

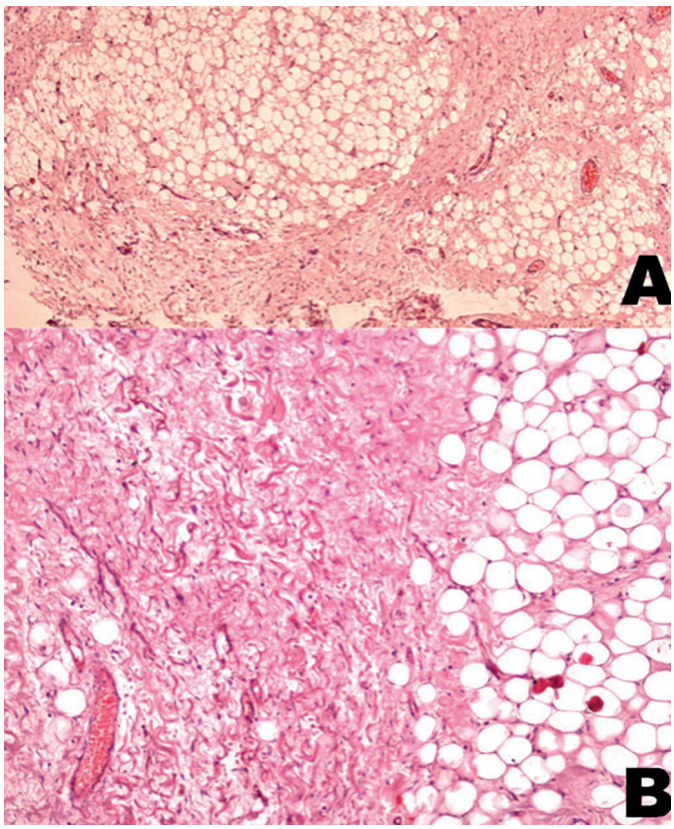

Fig. 3 A) Photomicrograph showing lobules of normal mature lipocytes separated by spindle cells and fibrous tissue (H&E stain, 40×); B) (H&E, 100×).

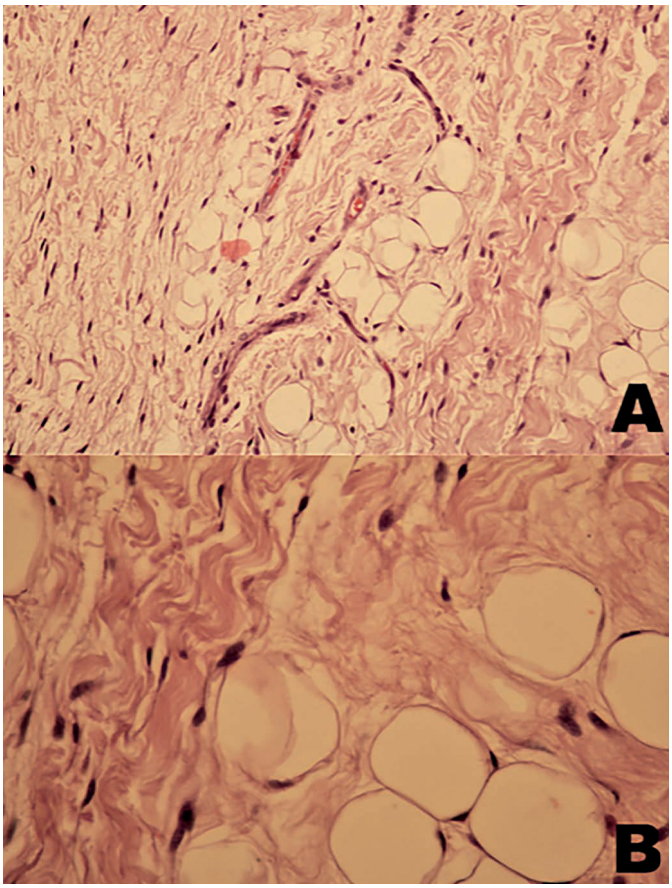

Fig. 4 A) Spindle cells with elongated nuclei and scant cytoplasm along with bundles of dense ropey collagen fibers along with mature adipocytes (H&E stain, 200×); B) (H&E stain, 400×).

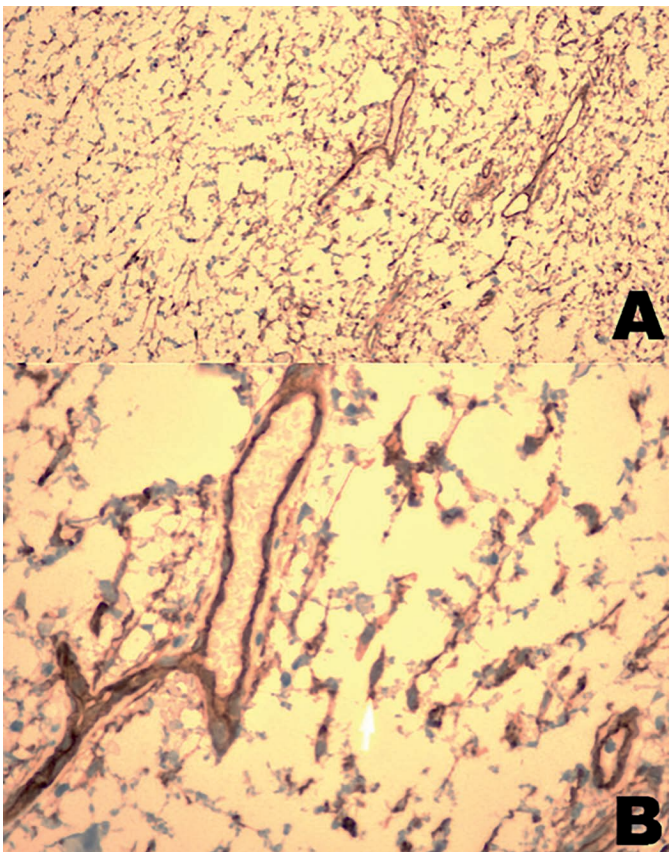

Fig. 5 A) Immunopositivity for CD34 by spindle cells (100×); B) (400×).

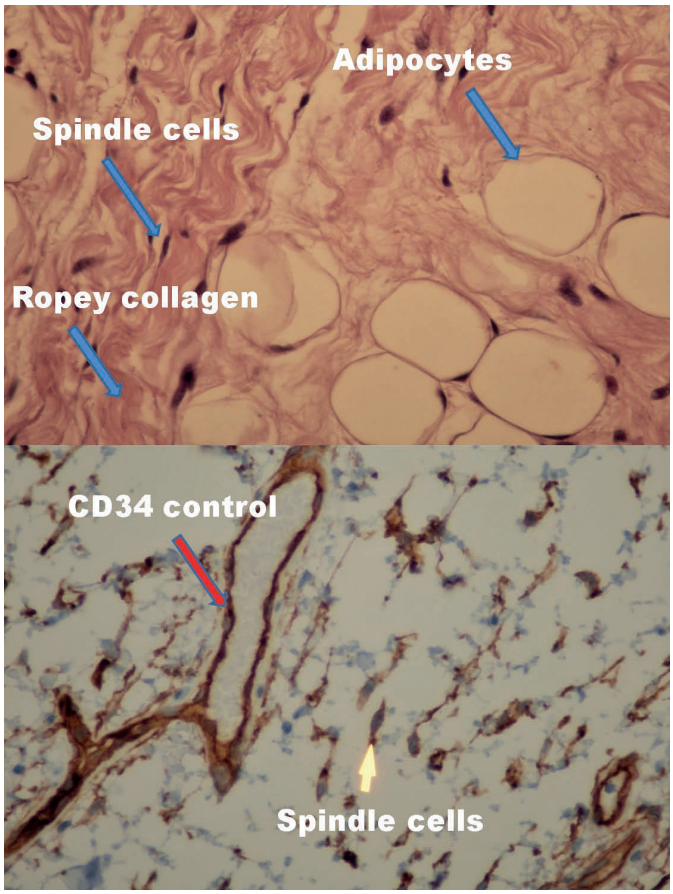

Fig. 6 Co-relation of CD34 immunopositivity with the histological H&E staining slide confirming the final diagnosis of spindle cell lipoma.

DISCUSSION

Lipomas are the benign mesenchymal tumors occurring mostly in the subcutaneous tissues of the head and neck (5). These tumors are very rare in the oral region. Histologically, many variants of lipoma have been described based on the type of tissue present (6) (Table 2). SCL is a rare histological subtype of lipoma which was first described by Enzinger and Harvey in 1975 based on its characteristic histological findings (1).

CLINICAL FEATURES

SCL occurs mostly in the 4th–6th decade with male predominance (male : female = 2 : 1) (7). Familial occurrence has also been reported (8). Most exclusively SCL involves subcutaneous tissue of the upper back, shoulders, and posterior neck (9). Intraoral SCL is very rare, and the main site of occurrence is buccal mucosa followed by tongue, gingiva, palate, alveolar ridge, and lip. This pattern corresponds closely to the quantity of fat deposits in the oral cavity. A few cases have been reported in parotid gland too (10–12). Submandibular space is a very rare site of involvement for SCL (13). In the literature only four cases of SCL involving the submandibular space directly or indirectly have been reported. Levy et al., in 1989, presented the first case of SCL in 74-year female patient occurring on the floor of mouth, in which palpation of mass through the submandibular triangle was noticed without any fixation to the submandibular gland (14). Baumann et al., in 2001 reported a case of SCL in a 45-year-old male with a tender

Tab. 2 Histological variants of Lipoma.

S. no.	Type	Features
1.	Fibrolipoma (most common)	Fibrous component + Adipose tissue.
2.	Angiolipoma	Vascular component + Adipose tissue.
3.	Myolipoma	Smooth muscles + Adipose tissue.
4.	Spindle cell lipoma	Variable amounts of uniform appearing spindle cells + adipose tissue
		Subtypes:
		Classic — Spindle cell, rope-like collagen, adipose tissue.
		Fibrous — Massive collagen fibers.
		Myxoid — Myxoid stroma.
		Low-fat — Little or almost no adipose tissue.
		Fat-rich — A large amount of adipose tissue.
		Pseudo angiomatous — Highly vascular with staghorn type bloodvessels.
5.	Pleomorphic lipoma	Pleomorphic spindle cells.
6.	Intramuscular/Infiltrating lipoma	Muscle gets replaced by mature adipose tissue. More deeply situated and having an infiltrative growth pattern.
7.	Chondroid lipoma	Chondrocytes + Adipose tissue.
8.	Perineural Fibro lipoma	Abundant adipose tissue surrounding the nerves displaying concentric perineural fibrosis.
9.	Myxolipoma	Myxoid stroma + Adipose tissue.
10.	Myelolipoma	Bone marrow component + Adipose tissue.
11.	Osteolipoma	Osseous component + Adipose tissue.
12.	Adenolipoma	Ductal component + Adipose tissue.

swelling of the right parotid area that had reached the submandibular region (15). Coimbra et al., in 2006 described a case of SCL in a 29 yr female occurring on the floor of the mouth in which the lesion was located adjacent to the opening of the Wharton duct of the submandibular gland (16). Yalcin et al., in 2015 published a case of SCL in a 49-yr. old female in which the tumour was superficially located and non-infiltrating in front of the sublingual caruncle (opening of the submandibular and sublingual duct) on the floor of the mouth (17).

Though SCL involves mostly males, surprisingly the reported cases of SCL occurring in the submandibular region have revealed the female predominance (13–19). Out of 4 cases, only 1 occurred in a male. Our case is involving an 18-year male patient reflecting a rare feature of SCL in submandibular space. Clinically, intraoral SCL appears as a yellow coloured, soft, painless, well-circumscribed submucosal, slow growing mass of appx 1 cm in diameter. The size may extend up to 5–10 cm too (9). In our case, the lesion was soft, fluctuant, slightly tender, slow-growing, appx 5 cm in diameter with normal skin colour. The swelling raised the floor of the mouth on pressing from outside.

CLINICAL DIFFERENTIAL DIAGNOSIS

Lesions occurring in the submandibular space are of great clinical importance because this space has numerous tightly netted vital structures in contiguity with each other. The submandibular space extends from the hyoid bone to the mucosa of the floor of the mouth and is bounded anteriorly and laterally by the mandible, medially by the anterior belly of the digastric muscles, superiorly by the mylohyoid muscle. Space is enclosed by the superficial layer of the deep cervical fascia, except along the posterior margin of the mylohyoid muscle, permitting continuity with the sublingual space and potential communication with the parapharyngeal space through a buccopharyngeal gap created by the styloglossus muscle. Mylohyoid muscle plays a key role in determining the direction of the spread of tumor mass. The lesion that is in the sublingual space i.e. above the mylohyoid muscle has got the potential to grow into the sub mylohyoid space i.e. below the mylohyoid muscle, thus involving the whole of submandibular space (Figure 2) and presenting as a swelling in the neck (i.e. having both oral and cervical components). The primary contents include the superficial portion of the submandibular gland, submandibular lymph nodes, and fat. The facial artery and vein, as well as a portion of the hypoglossal nerve, course through space.

Pathologies occurring in the submandibular region are very challenging to diagnose because most of these entities manifest as swelling that can mimic many other lesions clinically (Table 3). The lesions in this region range from the most benign forms such as ranula to the sinister malignant neoplasms. Due to wide communications of this space, the actual extent and appearance of the lesions get masked up especially those occurring in deeper tissues leading to an inaccurate diagnosis (20). Various clinical differential diagnosis of lipoma occurring in submandibular region can be as follow:

1. Ranula: It represents as a mucocele that involves the sublingual glands. As the cystic lesion enlarges, it can rupture through its sublingual space boundaries extending into the submandibular space referred to as a plunging ranula and raises the floor of the mouth on putting pressure from outside. But ranula mostly occurs in the young age group of 1st to 2nd decade with female predominance, while lipoma has different age predilection. Moreover, Ranula appears as a bluish swelling whereas lipoma is mostly yellowish (21).

2. Oral lymphoepithelial cysts: They appear as a movable yellow or yellowish white, painless submucosal nodule which is usually small as compared to those seen in lipoma. And these cysts usually occur in the first to third decade of life while lipoma occurs in 4th to 6th decades (22).

3. Dermoid & Epidermoid cysts: These cysts are considered to be a variation of teratomas and arise from entrapment of epithelial remnants during the closure of the branchial arches or as a result of trauma. These appear as soft to rubbery swelling mainly located on the floor of the mouth superficially within submandibular and sublingual spaces either in midline or latterly, where they may cause tongue elevation, submental protrusion, or both (23) but they may also produce another mass in the neck from where they originally arose due to the sequestration of cutaneous tissue along cervical embryonic lines of closure, later extending to the mouth. These cysts mostly involve the young age groups whereas lipoma occurs mostly in the old age.

4. Benign salivary gland tumors: Any small lesion especially pleomorphic adenoma occurring in the submandibular region with slow growth, non-infiltration, without evidence of pain, induration, ulceration, and mucosal changes may be mistaken for lipoma but their other characteristic features help distinguishing them from lipoma which are described in table 3 (16).

5. Malignant salivary gland tumors: Some of the malignant salivary gland tumours involve the submandibular space such as Adenoid cystic carcinoma (AdCC), Mucoepidermoid carcinoma (MEC), Carcinoma-ex-PA, Acinar cell carcinoma, Mucinous adenocarcinoma, and Squamous cell carcinoma (24). But as compared to lipoma, they may be associated with other clinical features such as pain, ulceration, perineural invasion, more distant metastasis, high recurrence rate, worse prognosis, and different line of treatment.

6. Benign mesenchymal neoplasms: Lymphatic malformations such as lymphangioma occurring most commonly in the submandibular space may mimic lipoma. The characteristic appearance is a non-enhancing multiloculated cystic lesion with fluid-fluid levels without calcifications. Vascular tumours such as haemangioma occurring rarely in the submandibular space can also resemble sometimes to lipoma but it appears to be reddish or bluish, highly vascular and may produce blanching of tissue on compression and is mostly congenital (25). Schwannomas and neurofibromas are rare within the submandibular space. Arising from peripheral and sympathetic nerves, schwannomas involving the lingual and hypoglossal nerves can occur on the floor of the mouth and can resemble lipoma.

DIAGNOSTIC AIDS

ROLE OF IMAGING

Imaging modalities such as CT, MRI, and USG are recommended in certain cases especially which extend from the neck to deeper tissues, to know the extent, location, and delimitation of the margins of the mass. Lipomas do not show characteristic pathognomic features on imaging (26). They may show a homogeneous appearance with the same density as subcutaneous fat in CT scan. On MRI these lesions may show a strikingly high-intensity signal, equal to that of the subcutaneous adipose tissue on both T1- and T2-weighted images (27). USG findings suggest hypoechoic masses in the majority of the cases with small echogenic lines. Some cases also reported lipomas as isoechoic masses (19). In the present case, USG was performed which revealed the presence of a hyperechoic mass in the region of left neck anterolateral to the left submandibular gland with clear well defined anterior and posterior margins. The mass did not show any evidence of calcification or vascularity. No lymphadenopathy was observed. Thyroid glands were normal.

Tab. 3 Clinical differential diagnosis of spindle cell lipoma occurring in submandibular space.

Lesion	Age (decades)	Sex	Clinical features
Spindle cell lipoma	4th–6th	Females	Yellow, soft, painless, well-circumscribed submucosal slow-growing mass of appx 1–5 cm in diameter.
Ranula	1st–2nd	Females	Bluish grey, soft, may raise the floor of the mouth on applying pressure.
Lymphoepithelial cyst	1st–3rd	Not specific	Soft submucosal nodules, small in size, yellow.
Dermoid/ epidermoid cysts	1st–3rd	Not specific	Soft rubbery swellings, small size, cause tongue elevation, submental protrusion.
Benign salivary gland tumour	3rd–5th	Females	Soft painless swelling of normal skin colour, may be associated with facial nerve palsy.
Malignant tumours	2nd–9th	Females	Painful swelling associated with ulceration, perineural invasion, distant metastasis, poor prognosis.
Benign mesenchymal tumour	3rd–5th	Females	Vary depending on the tissue involved. Soft to firm, swelling may be highly vascular, multiloculated cystic lesions.

1. Histopathological investigations

It is difficult to differentiate clinical lesions without histopathological investigations. To reach out at the accurate diagnosis, histopathological examination is essential. The lesions which are similar to spindle cell lipoma clinically, show different histological features that help to reach an accurate diagnosis (Table 3).

2. Macroscopic features

Grossly, SCL is well encapsulated and well-circumscribed appearing as classic lipoma with few differences. Cut surface may be nodular with grayish-white to grayish-yellow gelatinous foci representing the area of spindle cell formation (28). Due to the admixture of collagen fibers and the adipose tissue the surface texture may be soft to touch. No evidence of necrosis or vascularity has been reported (6). In the present case also the tumor mass was well encapsulated with cut surface showing yellowish nodular areas along with grayish-white gelatinous foci.

3. Microscopic features

Microscopically, SCL is composed of mature adipocytes along with mitotically inactive spindle cells associated with ropey collagen fibers surrounded by a clear fibrous capsule. Also, scattered mast cells, lymphocytes, multinucleated giant cells, and blood vessels are also observed. The spindle cells are characterized by pale staining vesicular, oval, or compressed nuclei, with a sparse, poorly defined, eosinophilic cytoplasm and, sometimes they demonstrate nuclear palisading (8). Spindle cells are bland, with uniform staining, without obvious atypia, pleomorphism, or nuclear mitoses, and are arranged in bundles between the collagen fibers (29). Sometimes infrequent variations can also be found in these classical features, giving rise to various other subtypes such as fibrous, myxoid, fat-rich, low-fat, and pseudo angiomatous types (30) (Table 2). In the present case, the H&E stained section of the lesion represented classical histological features of SCL characterized by the presence of well-circumscribed tumor mass composed of lobules of normal adipose tissue separated by connective tissue septa and areas of loose myxoid matrix containing bland spindle-shaped cells along with the bundle of dense ropey collagen fibers. The cells had elongated nuclei and scant cytoplasm. Numerous thick-walled blood vessels and mast cells were also seen in the connective tissue stroma. Based on these features, a histopathological diagnosis of SCL was given.

The exact origin of spindle cells is not clear, but it has been reported to be fibroblastic in origin rather than lipoblastic (31). They may also be derived from adipocytic lineage or immature mesenchymal cells. Another possible origin from dendritic interstitial cells has also been mentioned (32). It is suggested that spindle cells are analogs to the nonlipoblastic stellate mesenchymal cells of the primitive fat lobules (33), which have lost their ability to differentiate to lipocytes but are capable of collage synthesis (34). The presence of mature lipocytes and fibroblastic cells in SCL probably reflects the potential to tumor cells to differentiate to both fat-storing and collagen-producing cells (35).

Tab. 4 Histopathological differential diagnosis of spindle cell lipoma.

Tumour	Adipocytes	Spindle cells	Ropey Collagen	Vascularity	Infiltration
SCL	+	Bland, uniform, Isomorphic nuclei, No pleomorphism and hyperchromasia, no mitotic figures.	+	Not highly vascular.	–
Classic lipoma	Localized.	–	–	Not highly vascular.	–
Fibro lipoma	Mature.	–	–	Not highly vascular.	–
SFT	–	–	–	Highly vascular.	–
Neurofibroma	–	Wavy nuclei.	–	Not highly vascular.	–
Leiomyoma	–	Same as SCL.	–	Not highly vascular.	–
Fibrosarcoma	–	Arranged in fascicles, herringbone pattern, pleomorphic, hyperchromatic, mitotic figures.	–	Not highly vascular.	+
WDL	–	Pleomorphic nuclei, hyperchromatic, mitosis.	–	Highly vascular.	+
Vascular tumours	–	–	–	Highly vascular.	+
DFS	–	May resemble the fascicular type of SCL.	–	Not highly vascular.	+

DFS: Dermatofibrosarcoma protuberans, SCL: Spindle cell lipoma, SFT: Solitary fibrous tumour, WDL: Well-differentiated liposarcoma.

HISTOPATHOLOGICAL DIFFERENTIAL DIAGNOSIS

Histopathologically, many features of SCL can resemble other lesions making it difficult to distinguish it from those entities. (Table 4) The following are the possible microscopic differential diagnosed lesions for SCL.

Classic lipoma: The spindle cells sometimes are so localized that they can be overlooked letting the tumour be diagnosed as an ordinary lipoma (9).

Fibro lipoma (FL): FL are characterized by an admixture of mature fat cells and fibrous connective tissue devoid of bundles of spindle cells and mast cells. Even IHC can't distinguish between SCL and FL because both tumors stain positive for vimentin and CD34 (36).

Solitary fibrous tumour (SFT): Spindle cells and collagen fibers in SCL and SFT seem to be similar, but the absence of adipocytes and the presence of abundant vascularity in SFT differentiates the two lesions. Ropey collagen fibers are the feature of SCL, not SFT. SCL is characterized by hypocellular stroma as compared to SFT which has hypercellular activity. Also, SFT occurs rarely in the oral cavity as compared to SCL (37).

Neurofibroma: Presence of spindle cells and mast cells may lead to a diagnosis of neurofibroma. But in neurofibroma, spindle cells have wavy nuclei and the lesions can be distinguished based on IHC investigations (38). Immunonegativity of spindle cells for S-100 helps to exclude the diagnosis of neurofibroma in which spindle cells are S-100 immunopositive.

Leiomyoma: Spindle cells of SCL & Leiomyoma can resemble each other and both tumours being benign can result in difficulty to diagnose based on histological features (1).

Fibrosarcoma: Sometimes the spindle cells in SCL, are pleomorphic exhibiting hyperchromasia resembling fibrosarcoma like pattern (9).

Well-differentiated Liposarcoma (WDL) and Myxoid Liposarcoma (MLS): SCL with pseudolipoblastic change secondary to atrophy may mimic WDL/ atypical lipomatous tumor and myxoid liposarcoma (39, 40). In WDL, lipoblasts are rarely seen (41). The diagnostic lesional cell of well-differentiated liposarcoma is an atypical hyperchromatic tumor cell, typically without a cytoplasmic fat vacuole. These atypical hyperchromatic cells are often found in dense fibrous bands rather than the wiry ropy collagen of SCL. Also, pseudo lipoblasts are arranged in a lobular arrangement rather than the more random distribution seen in liposarcoma (41). WDL is immunonegative to CD34. Clinically, SCL is superficially located, well-circumscribed as compared to WDL which is deep seated and ill-defined (18). Myxoid Liposarcoma unlike SCL with myxoid stroma, typically shows prominent lipoblastic differentiation and have a characteristic "Chicken wire" vascular pattern rather than the wirey collagen characteristic of SCL. MLS is CD34 negative as compared to SCL which shows wide CD34 positivity (41).

Vascular tumours: Normally SCL is not vascular but the presence of high vascularity can mislead to the diagnosis of any vascular tumours (9).

Dermatofibrosarcoma protuberans (DFS): There is an overlap of histological features seen in DFS with SCL. The fascicular pattern of spindle cells may be seen in both the lesions. However, DFS is a cutaneous tumour exceptionally found in the oral region. And it also exhibits infiltrative nature as compared to SCL which is not infiltrative (42).

Due to the overlap of histological features of SCL with the above lesions, it becomes difficult to reach exact diagnosis. And that can be confirmed with help of IHC. The same was performed in our case too.

IMMUNOHISTOCHEMICAL INVESTIGATIONS

Immunohistochemical investigations can help resolving the conflicts of overlapping features of SCL with other lesions (Table 5). Studies have revealed that the spindle cells in SCL show intense immunopositivity for CD34, vimentin & bcl-2 and immunonegativity for Alpha-smooth mus-

Tab. 5 Immunohistochemical markers for differentiating various lesions from spindle cell lipoma.

S.no	Name of lesion	CD 34	Bcl2	F-VIII	S-100	CD-99	Alpha SMA	Ki67
1.	**Spindle cell lipoma**	+	+	–	–	–	–	–
2.	Solitary fibrous tumour	+	+	–	–	–/+	–	–
3.	**Neurofibroma**	–	–	–	+	–	–	–
4.	**Leiomyoma**	–	–	–	–	–	+	–
5.	**Liposarcoma**	–	–	–	–	–	–	+
6.	Dermatofibrosarcoma protuberans	+	–	–	–	–	–	–

cle actin (SMA), Factor VIII, Cytokeratin (CK), and S-100 which eliminates the evidence of the muscular, neurogenic or endothelial origin of spindle cells found in SCL and helps to distinguish it from other neural, muscular and vascular tumours (35, 43). Ki67 expression is found to be very low in SCL which helps to distinguish it from malignant neoplasm like Liposarcoma in which tumour cells show a high proliferative index of Ki67 (44). In the present case, spindle cells showed immunopositive reaction with CD34 that is consistent with the findings reported in the literature.

MANAGEMENT & PROGNOSIS

SCLs are mostly treated by surgical excision. These are benign lesions with a good prognosis. Recurrences are rare and are encountered only when the lesion is infiltrating and invading the surrounding muscles and tissues. However, surgical manipulation of spindle cell lipoma in the submandibular region must be cautioned as the lesion may be contiguous with vital structures such as the salivary glands and their respective ducts along with nerves and vessels mainly lingual nerves and vessels, hypoglossal nerves, and glossopharyngeal nerve. Malignant transformation is thought to be almost non-existent with very few cases reported. Long term follow up is necessary (45, 46). In the present case surgical excision was done and good post-operative healing was observed after 4 years of follow up with no recurrence.

CONCLUSION

Intraoral lipomas are rare as compared to other lipomas. SCL is a histological variant of lipoma that infrequently occurs in the submandibular region. Due to wide communications of submandibular space, the actual extent and appearance of the lesions present here get masked up especially those occurring in deeper tissues leading to an inaccurate diagnosis. Also, the slow expansile growth of lipoma probably allows neighboring structures to adapt to the increasing pressure, thus leaving the patient unaware of the growth. The wide overlap of clinical and histopathological features of SCL leads to a challenging task for the clinicians to reach an accurate diagnosis. Thorough investigations and evaluations are mandatory to frame out a proper diagnosis for providing preferential treatment to avoid further complications.

REFERENCES

1. Enzinger FM, Harvey DA. Spindle cell lipoma. Cancer 1975; 36: 1852–9.
2. Fletcher CD, Martin-bates E. Spindle cell: a clinicopathological study with some original Histopathology 1987; 11: 803–17.
3. Pusiol T, Franceschetti I, Scialpi M, Piscioli I. Oncocytic sialolipoma of the submandibular gland with sebaceous differentiation: A new pathological entity. Indian J Pathol Microbiol 2009; 52: 379–82.
4. El-Monem MH, Gaafar AH, Magdy EA. Lipomas of the head and neck. Presentation variability and diagnostic work up. J Laryngol Otol 2006; 120: 47–55.
5. Miloro M, Haupt A, Olsson AB, Kolokythas A. Oral spindle cell lipoma: a rare occurrence and review of the literature. Oral Maxillofac Surg Cases 2015: 12–14.
6. Shafer WG, Hine MK, Levy BM. Shafer's textbook of oral pathology .6th ed. Elsevier publications: Noida, India 2009, p. 138.
7. Milhan NVM, Cavalcante ASR, Marques YMFS, Carvalho YR, Anbinder AL. Spindle cell lipoma occurring in the buccal mucosa: an unusual location of this benign lipomatous neoplasm. Case Reports Pathol 2015: 805730.
8. Kempson RL, Fletcher CDM, Evans HL, Hendrickson MR, Sibley RK. Tumors of the soft tissues Atlas of tumor pathology. Bethesda: Third Series Armed Forces Institute of Pathology, 2001, p. 203–8.
9. Piatteli A, Perrotti V, Fioroni M. Spindle cell lipoma of the floor of the mouth: report of a case. Auris Nasus Larynx 2005; 32: 205–7.
10. Amore FF, Musumeci G, Castrogiovanni P, Longo FR, Magro G. Spindle cell lipoma of peri-parotid soft tissues. Report of a case and histogenetic considerations. J Histol Histopathol 2015; 2: 7.
11. Fasig JH, Robinson RA, McCulloch TM, Fletcher MS, Miller CK. Spindle cell lipoma of the parotid: fine-needle aspiration and histologic findings. Arch Pathol Lab Med 2001; 125: 820–1.
12. Rosenthal LS, Garzon S, Setty S, Yao M. Left-sided facial mass. Spindle cell lipoma of the parotid gland. Arch Pathol Lab Med 2006; 130: 875–6.
13. McDaniel RK, Newland JR, Chiles DG. Intraoral spindle cell lipoma: case report with correlated light and electron microscopy. Oral Surg Oral Med Oral Pathol 1984; 57: 52–7.
14. Levy FE, Goding Jr GS. Spindle cell lipoma: an unusual oral presentation. Otolaryngol Head Neck Surg 1989; 101: 601–3.
15. Baumann I, Dammann F, Horny HP, Plinkert PK. Spindle cell lipoma of the parapharyngeal space. First report of a case. Ear, Nose, & Throat Journal 2001; 80(4): 247–50.
16. Coimbra F, Lopes JM, Figueiral H, Scully C. Spindle cell lipoma of the floor of the mouth. A case report. Med Oral Patol Oral Cir Bucal 2006; 11: 401–3.
17. Yalçin M, Atilgan SS, Laçin N, Atalay Y. Spindle Cell Lipoma on the Floor of the Mouth. J Dent App 2015; 2(8): 291–4.
18. Billings SD, Henley JD, Summerlin DJ, Vakili S, Tomich CE. Spindle cell lipoma of the oral cavity. Am J Dermatopathol 2006; 28: 28–31.
19. Malthiery E, Costes-Martineau V, Fauroux MA, Torres JH. A 37mm Spindle Cell Lipoma on the Floor of the Mouth. Case Reports in Dentistry 2019: 2138928.
20. Tan MS, Singh B. Difficulties in diagnosing lesions in the floor of the mouth – Report of Two Rare Cases. Ann Acad Med Singapore 2004; 33(Suppl): 72S-76S.
21. Kokong D, Iduh A, Chukwu I, Mugu J, Nuhu S, Augustine S. Ranula: Current Concept of Pathophysiologic Basis and Surgical Management Options. World J Surg 2017; 41: 1476–81.
22. Joshi B, Rajesh G, Shivani B. Oral Lipoma-a Rare Clinical Anomaly-A Case Report. Acta Scient Dent Sci 2018; 2(7): 114–7.
23. Sabhalok SS, Shetty LS, Sarve PH, Setiya SV, Bharadwaj SR. Epidermoid and dermoid cysts of the head and neck region. PlastAesthet Res 2016; 3: 347–50.

24. Kessler AT, Bhatt AA. Review of the Major and Minor Salivary Glands, Part 2: Neoplasms and Tumor-like Lesions. J Clin Imaging Sci 2018; 8: 48.
25. Egido-Moreno S, Lozano-Porras AB, Mishra S, Allegue-Allegue M, Marí-Roig A, López-López J. Intraoral lipomas: Review of literature and report of two clinical cases. J Clin Exp Dent 2016; 8(5): e597–e603.
26. Lee HK, Hwang SB, Chung GH, Hong KH, Jang KY. Retropharyngeal Spindle Cell/Pleomorphic Lipoma. Korean J Radiol 2013; 14(3): 493–6.
27. Upadhyay S, Sharma A, Mhashal S, Dabholkar JP. Spindle cell lipoma of the anterior triangle of the neck: a rare entity. Braz J Otorhinolaryngol 2011; 77(3): 401.
28. Darling M, Thompson I, Schneider J. Spindle cell lipoma of the alveolar mucosa: a case report. Oral Surg Oral Med Oral Pathol Oral Radiol Endod 2002; 93: 171–3.
29. Said-Al-Naief N, Zahurulla FR, Sciubba JJ. Oral spindle cell lipoma. Ann Diagn Pathol 2001; 5: 207–15.
30. Chen S, Huang H, He S, et al. Spindle cell lipoma: clinicopathologic characterization of 40 cases. Int J Clin Exp Pathol 2019; 12(7): 2613–21.
31. Miettinen MM, Mandahl N. Spindle cell lipoma/pleomorphic lipoma. In: Fletcher CDM, Unni KK, Mertens F, editors. Pathology and genetics of tumours of soft tissue and bone. Lyon: World Health Classification of Tumours International Agency for Research of Cancer (IARC) IARC Press; 2002: 31–2.
32. Horiuchi K, Yabe H, Nishimoto K, Nakamura N, Toyama Y. Intramuscular spindle cell lipoma: case report and review of the literature. Pathology Int 2001; 51: 301–4.
33. Bole JW, Thorning D. Spindle-cell lipoma. A clinical, light-and electron-microscopical study. Am J Surg Pathol 1981; 5: 435–41.
34. BehanA, Schmid C, Hodl S, Fletcher CDM. Spindle cell and pleomorphic lipoma:an immunohistochemical study and histogenetic analysis. J Pathol 1989; 157: 219–22.
35. Lombardi T, Odell Ew. Spindle cell Lipoma of the oral cavity: report of a case. J Oral Pathol Med 1994; 23: 237–9.
36. Templeton SF, Solomon AR Jr. Spindle cell lipoma is strongly CD34 positive. An immunohistochemical study. J CutanPathol 1996; 23: 546.
37. Wood L, Fountaine TJ, Rosamilia L, et al: Cutaneous CD34+ spindle cell neo- plasms: histopathologic features distinguish spindle cell lipoma, solitary fibrous tumor, and dermatofibrosarcoma protuberans. Am J Dermatopathol 2010; 32(8): 764–8.
38. Bajpai M, Pardhe N, Kumar M. Immunohistochemical differentiation between spindle cell lipoma and neurofibroma of oral cavity using CD34 and SOX10. Indian J Pathol Microbiol 2018; 61: 561–3.
39. Dominguez FV, Guglielmotti MB, Flores MC. Myxoid liposarcoma of the cheek. J Oral Maxillofac Surg 1990; 48: 395–7.
40. Nascimento AF, Mc Menamin ME, Fletcher CD. Liposarcomas/atypical lipomatous tumors of the oral cavity: a clinicopathologic study of 23 cases. Ann Diagn Pathol 2002; 6: 83–93.
41. Weiss SW, Goldblum JR. Enzinger and Weiss's soft Tissue Tumors. St. Louis: Mosby; 2001.
42. Jaeger F, Capistrano HM, de Castro WH, et al. Oral spindle cell lipoma in a rare location: a differential diagnosis. Am J Case Rep 2015; 16: 844–8.
43. Manor E, Sion-Vardy N, Brennan PA. Spindle cell lipoma of the oral cavity: a clinicopathologic analysis of 35 reported cases. Surgical Science 2013; 4: 196–201.
44. Linares MF, Leonel ACLS, Carvalho EJA, de Castro JFL, de Almeida OP, Perez DEC. Intraoral lipomas: A clinicopathological study of 43 cases, including four cases of spindle cell/pleomorphic subtype. Med Oral Patol Oral Cir Bucal 2019; 24(3): e373–8.
45. Manor E, Sion-Vardy N, Josua BZ, Bodner L. Oral lipoma: analysis of 58 new cases and review of the literature. Ann Diagn Pathol 2011; 15: 257–61.
46. Julliasse LE, Nonaka CF, Pinto LP, Freitas Rde A, Miguel MC. Lipomas of the oral cavity: clinical and histopathologic study of 41 cases in a Brazilian population. Eur Arch Otorhinolaryngol 2010; 267: 459–65.

Guillan-Barré Syndrome after First Vaccination Dose against COVID-19: Case Report

Daniel Čenščák[1], Leoš Ungermann[2], Ivana Štětkářová[3], Edvard Ehler[4,*]

ABSTRACT

A number of neurological complications have been reported after the administration of flu vaccine, including Guillain-Barré syndrome (GBS), especially after vaccination against swine flu. Only facial nerve neuropathy has thus far been reported after vaccination against COVID-19. More recently, there was a case of an elderly woman with GBS. In our report, we describe a case of a 42-year-old, previously almost healthy male who developed sensory symptoms 14 days after the first dose of Pfizer vaccine. One week later, the patient developed right facial nerve palsy and lower limb weakness and was no longer able to walk. Albuminocytological dissociation was detected in the cerebrospinal fluid, and there were inflammatory radicular changes in MRI scans of the lumbosacral spine. EMG indicated significant demyelinating polyradiculoneuritis and no antibodies against gangliosides were demonstrated. A 5-day course of immunoglobulins at a dose of 2 g/kg lead to a significant improvement and the patient was soon able to walk. In conclusion, we report a case of Guillan-Barré syndrome after COVID-19 vaccine in a young patient with a rapid diagnosis and prompt administration of immunoglobulins.

KEYWORDS

vaccines; polyradiculoneuritis; ataxia; nerve conduction studies; COVID-19; Guillain-Barré syndrome; immunoglobulins

AUTHOR AFFILIATIONS

[1] Department of Neurology, District Hospital Pardubice, Czech Republic
[2] Department of Radiology, Faculty of Health-Care study, Pardubice University, District Hospital Pardubice, Czech Republic
[3] Department of Neurology, 3rd Medical Faculty Charles University, Prague, and University Hospital Královské Vinohrady, Prague, Czech Republic
[4] Department of Neurology, Faculty of Health-Care Study, Pardubice University, District Hospital Pardubice, Czech Republic
* Corresponding author: Department of Neurology, Faculty of Health-Care Study, Pardubice University, District Hospital Pardubice, Czech Republic; e-mail: edvard.ehler@nempk.cz

Received: 5 April 2021
Accepted: 10 August 2021
Published online: 11 November 2021

Acta Medica (Hradec Králové) 2021; 64(3): 183–186
https://doi.org/10.14712/18059694.2021.31

INTRODUCTION

Many vaccines can provoke autoimmune diseases, including GBS (Guillain-Barré syndrome). Flu vaccines, especially for swine flu, lead to multiple cases of vaccination-induced GBS, polyneuritis cranialis and other forms of peripheral or autonomic neuropathy (1). Facial nerve neuropathies and other peripheral nerve disorders have thus far been described in temporal occurrence after COVID-19 vaccination (2). GBS has been reported in only one 82-year-old woman after the mRNA vaccine (3). Later on some other papers were published on GBS and vaccines, which confirmed only temporal occurrence and not causality (4–6). In our report, we present the next case of a young 42-year-old male who also developed autoimmune inflammation of peripheral nerves (GBS) after the first vaccination dose against COVID-19 (Comirnaty, Pfizer), with a favourable course.

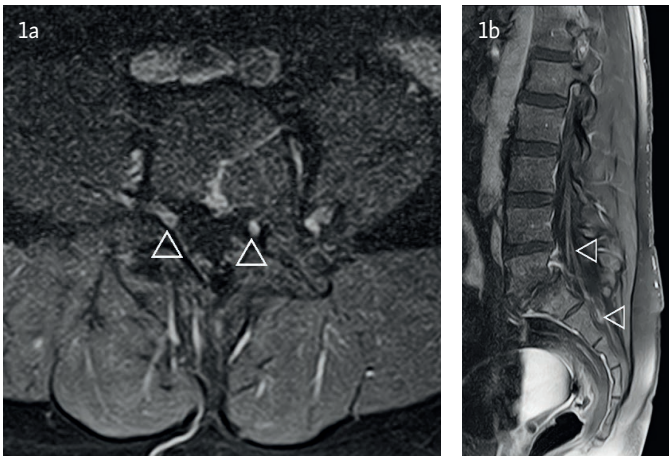

Fig. 1 In the axial (1a) and sagittal (1b) T1 weighted images after gadolinium there is mild thickening and enhancement of spinal roots in lumbosacral region.

CASE REPORT

A 42-year-old male developed paraesthesia of the soles of his feet 14 days after the first vaccine dose against COVID-19 (mRNA vaccine, Comirnaty, Pfizer). The patient works as a nurse in a retirement home, he has been managed for bronchial asthma (budesonium, ipraproium, fenoterol inhalation twice a day) for 8 years.

Paraesthesia worsened the next day and spread to his hands as well. After a week, the patient developed gait problems; he had unsteady gait and weak knees. After 3 more days, he started to complain of right-sided mimic muscle weakness and lumbalgia. He was admitted to our neurological department 18 days after the onset of neurological problems (32 days after the first dose of vaccine).

In the clinical finding, there was right-side mimic muscle weakening, lagophthalmos on the right side up to 2 mm, the philtrum was mildly pulled to the right side, there were no taste disturbances, he was ameningeal, was able to raise his head while lying on his back, the exteroceptive reflexes of the abdominal muscles were symmetric, handgrip strength 45 kPa at the right side, 40 kPa at the left side (median value per 42 years – 141.7 kPa), slight weakening in the elevation of the right arm, reflexes C5-8 minimal, L2-S2 not elicitable, lower limbs with a slow descent from rectangle elevation while lying on his back within 6 seconds on both sides, hypoesthesia 10 cm above the wrist and from the middle of the shanks for thermal and tactile qualities, vibration sense 6/8 on both sides. The patient was able to take 3–4 steps leaning on the furniture with ataxia and knees buckling.

Spirometry in a sitting position was performed (FVC (forced ventilation capacity): 0.62 l, FEV1 (forced expiratory volume in 1 second): 0.46 l), cerebrospinal fluid was collected, detecting albuminocytological dissociation (proteins 2.24 g/l, 6 leukocytes – all mononuclears), MRI of LS spine with post-contrast signal increase in the roots of cauda equina (Figures 1a and 1b). Antigen and PCR COVID-19 tests were repeatedly negative. Anti-ganglioside antibodies have not been detected.

Autonomic functions (handgrip test and Valsalva test) indicated a disorder of the autonomic nervous system with a decrease of heart rate variability.

Nerve conduction studies (NCS) and electromyography (EMG) examinations were performed immediately after admission to the neurological department, the results of which are presented in Table 1. Sensitive nerve action potentials (SNAP) were not elicitable in the lower limbs and low amplitude of SNAP (2.6 uV) was found in the upper limbs (median nerve) with a significant reduction in the conduction velocity through sensitive fibres (SCV = 18.2 m/s). Acute inflammatory demyelinating polyneuropathy (AIDP) with significant involvement of motor and sensitive fibres was confirmed based on the clinical findings and NCS/EMG examinations. NCS pointed to motor impairment both in the distal (DML – distal motor latency) and in the proximal section (F-waves) of the peripheral nervous system.

Tab. 1 Results of EMG examination at admission.

Nerve (muscle)	DML (ms)	A-CMAP (mV)	d-CMAP (ms)	MCV	F-lat (ms)	F-wave persistence
Median (APB)	9.20 /13.70	2.6/2.6	12.10	39.50	46.3	70%
Ulnar (ADM)	5.60/10.45	2.9/1.9	11.30	41.20	39.5	60%
Peroneal (EDB)	7.45/16.30	2.6/2.2	9.15	46.30	71.2	20%
Tibial (AH)	8.10/16.30	0.7/0.2	19.35	54.90	84.4	100%

Note: DML = distal motor latency, A-CMAP = amplitude of compound muscle action potential, d-CMAP duration of compound muscle action potential, MCV = motor conduction velocity, F-lat = F wave latency, APB = abductor pollicis brevis muscle, ADM = abductor digiti minimi muscle, EDB = extensor digitorum brevis muscle, AH = abductor hallucis muscle.

The treatment started with intravenous administration of immunoglobulins (2 g/kg over 5 days, at a total dose of 140 g) on the day of admission. Paraesthesia in the limbs already improved during the treatment, only partially thus far, but gait and handgrip strength improved significantly. The patient was transferred to a rehabilitation institution, able to walk with minimal assistance (leaning on furniture), mild facial weakness remained, but without lagophthalmos. He was able to close his eyes actively and smile. There were no problems with breathing and swallowing. Vigorimetry (55 and 54 kPa) and spirometry (FVC 3.73 l, FEV1 1.62 l) parameters improved.

DISCUSSION

About 70% of patients with GBS have a clear trigger in the history (infection, surgery, stress, vaccination). Swine-flu vaccination has led to individual GBS cases (1). Facial nerve palsy and later other peripheral nerv disorders were detected in a individuals after COVID-19 vaccination (2). It was not until February 2021 that a case of an 82-year-old woman who developed leg aches within a week of the first dose of vaccine (Pfizer) was published, followed by lower limb weakness the next week, leading to a fall and admission to neurology. Only hyperproteinorachia (0.88 g/l) was found in the cerebrospinal fluid. MRI of the LS spine detected root enhancement after gadolinium administration. IVIG administration lead to slow improvement of lower limb mobility and the patient regained gait ability (3). We are presenting the second case – a young male patient with GBS after COVID-19 vaccination. Fortunately, his problems regressed very quickly after immunomodulatory treatment. Our patient also had significant sensory disturbances and lower limb ataxia combined with mimic muscle weakness on the right side, inflammatory root changes in the lumbar region in MRI scans, and a closer examination revealed autonomic dysfunction (handgrip, Valsalva test). Anti-ganglioside antibodies were not detected. The clinical condition of this patient rapidly improved after the administration of intravenous immunoglobulins.

GBS, including its focal forms, may develop during COVID-19 infection (8). GBS has been published in 72 patients, presenting with sensory dysfunction in the lower limbs, ascending forms with upper limb involvement, either alone or in combination with paraparesis or tetraparesis (2). Ataxia was common, cranial nerve lesions occurred in 50% and dysphagia in 24% cases. About 36% of patients had respiratory muscle weakness (6). Autonomic dysfunction was uncommon in these patients. Peak clinical disability occurred 4 days after admission to hospital. EMG detected a demyelinating form of GBS in 77.4%. The axonal form of GBS occurred in 14.5%; the remainder were mixed forms (2). The clinical findings in patients with COVID-19 who develop GBS are similar, but the pathophysiological mechanisms are different. The absence of anti-ganglioside antibodies was unusual for patients with GBS prior to the COVID-19 pandemic. Patients with COVID-19-related GBS have typically more severe sensory impairment, less frequent involvement of the cranial nerves, marked ataxia, dysphagia is present in 50%, and respiratory symptoms in 36% of patients. Autonomic symptoms are less common, and radicular gadolinium enhancement in lumbar region MRI scans is also rare. Our patient presented with peripheral quadriparesis with sensory disturbances and marked ataxia. EMG detected a demyelinating type of the disease. We proved the involvement of autonomic fibres was evident. An additional MRI scan was performed, detecting enhancement in inflamed and thickened roots in the lumbar region. The clinical findings improved rapidly and significantly after acute immunoglobulin treatment. Our patient differed from typical GBS forms, including post-COVID-19 GBS, since he presented with marked ataxia, absence of anti-ganglioside antibodies, and rapid clinical improvement after the administration of immunoglobulins.

Treatment of GBS is the same in patients with COVID-19 as in patients without COVID-19. Plasmapheresis provides the advantage of removing antibodies and cytokines. Nevertheless, the better tolerated administration of an immunoglobulin, which is also more comfortable for the patient, is preferred. Antibodies against COVID-19 could be included in current formulations.

There were some papers describing GBS after administration of vaccines – COVID-19 and influenza (9–12). Ogbebor et al. (4) described a case of GBS after vaccine administration against COVID-19. The first symptoms of GBS occurred the next day after first dose of vaccine (Pfizer). If the vaccine was the trigger, the symptoms developed 1–4 weeks after the trigger. The authors emphasise that temporal association should not be translated into causality. Patel et al. (5) presented a 37-year old man who developed GBS with ascending muscle weakness 3 weeks after the first dose of vaccine. Treatment with immunoglobulins lead to slow improvement. The authors suggested that GBS after Covid-19 vaccine is an extremely rarely reported side effect. Lunn et al. (13) looked at the development of GBS after vaccines. Approximately 1 billion people will be vaccinated, and an expert would expect 17,000 cases of GBS to occur sporadically per annum, of which 1,962 would occur in any 6-week period. It is therefore inevitable that many thousands of sporadic cases of GBS caused by other factors will appear temporally associated with COVID-19 vaccination. But this cannot be considered causal. Li et al. (14) presented a big multi-national network cohort study with potential incidence rates of potential adverse events of special interest. The calculated incidence rates are stratified by age, sex and database. Patients with GBS are on the lists published by regulators.

Only sporadic cases of GBS after administration of COVID-19 vaccines are published. According to larger epidemiological studies and meta-analysis of vaccines and development of GBS, we are convinced that vaccination against COVID-19 is not the cause of acute polyradiculoneuritis development, but there is only temporal association. A sporadic occurrence of GBS is in temporal association with vaccine administration.

REFERENCES

1. Hampton LM, Aggarwal R, Evans SJW, Las B. General determination of causation between Covid-19 vaccines and possible adverse events. Vaccine 2021; 39: 1478–80.
2. Abu-Rumeileh S, Abdelhak A, Foschi M, Tuman H, Otto M. Guillain-Barré syndrom spectrum associated with COVID-19: an up-to-date systematic review of 73 cases. J Neurol 2021; 268(4): 1133–70.
3. Waheed S, Bayas A, Hindi F, Rizvi Z, Espinosa PS. Neurological Complications of COVID-19: Guillain-Barre Syndrome Following Pfizer COVID-19 Vaccine. Cureus 2021; 13(2): e13426.
4. Ogbebor O, Seth H, Min Z, Bhanot N. Guillain-Barré syndrome following the first dose of SARS-CoV-2 vaccine: A temporal occurrence, not a causal association. IDCases 2021; 24: e01143.
5. Patel SU, Khurram R, Lakhani A, Quirk B. Guillain-Barre syndrome following the first dose of the chimpanzee adenovirus-vectored COVID-19 vaccine, ChAdOx1. BMJ Case Rep 2021; 14(4), e242956.
6. Márquez Loza AM, Holroyd KB, Johnson SA, Pilgrim DM, Amato AA. Guillain- Barré Syndrome in the Placebo and Active Arms of a COVID-19 Vaccine Clinical Trial: Temporal Associations Do Not Imply Causality. Neurology 2021: 10.1212/WNL.0000000000011881.
7. Merkies I. Assessing grip strength in healthy individuals and patients with immune-mediated polyneuropathies. Muscle Nerve 2000; 23: 1393–401.
8. Dufour C, Co TM, Liu A. GM1 ganglioside antibody and COVD-19 related Guillain Barre Syndrome: A case report, systemic review and implication for vaccine development. Brain Behav Immun Health 2021; 12: 100203.
9. Park YS, Lee KJ, Kim SW, Kim KM, Su BC. Clinical features of post-vaccination Guillain-Barré Syndrom in Korea. J Korean Med Sci 2017; 32: 1154–9.
10. Soni R, Heindl SE, Wiltshire DA, Vahora IS, Khan S. Antigenic variability a potential factor in assessing the relationship between Guillain Barré syndrome and influenza vaccine – up to date literature review. Cureus 2020; 12(9): e10208.
11. Dotan A, Muller S, Kanduc D, David P, Halpert G, Shoenfeld Y. The SARS-CoV-2 as an instrumental trigger of autoimmunity. Autoimmune Rev 2021; 20(4): 102792.
12. Kochkar S, Salmon DA. Planning for COVID-19 vaccines safety surveillance. Vaccine 2020; 38(40): 6194–8.
13. Lunn MP, Cornblath DR, Jacobs BC, et al. COVID-19 vaccine and Guillain-Barré syndrome: let's not leap to associations. Brain 2021; 144(2): 357–60.
14. Li X, Ostropolets A, Makadia R, et al. Characterizing the incidence of adverse events of special interest for COVID-19 vaccines across eight countries: a multinational network cohort study. Preprint. medRxiv 2021; 2021.03.25.21254315.

Oral Ibandronate Therapy in Three Patients with Osteogenesis Imperfecta

Štěpán Kutílek[1,2,3,*], Ivana Plášilová[2,3], Sylva Skálová[3], Milan Bayer[3,4], Erika Ondrušová[3]

ABSTRACT

Introduction: Treatment with orally administered ibandronate is an effective way to increase bone mineral density (BMD) and reduce fracture rate in post-menopausal women and in men with osteoporosis. There are only very few reports concerning ibandronate therapy in children and adolescents, and in patients with osteogenesis imperfecta (OI), as bisphosphonates are not registered for therapeutic use in pediatrics.

Case Report: We present three patients with OI, where once-monthly oral ibandronate increased spinal BMD after two and four years, respectively, of therapy without any occurrence of new fractures and no adverse reactions. Somatic growth was not affected by the ibandronate treatment.

Conclusion: Once-monthly oral ibandronate increased BMD and most probably improved bone quality in young patients with OI.

KEYWORDS

ibandronate; osteogenesis imperfecta; bone mineral density

AUTHOR AFFILIATIONS

[1] Department of Pediatrics, Klatovy Hospital, Klatovy, Czech Republic
[2] Department of Pediatrics, Pardubice Hospital, Pardubice, Czech Republic
[3] Department of Pediatrics, Faculty of Medicine and Faculty Hospital in Hradec Králové, Charles University, Hradec Králové, Czech Republic
[4] Department of Pediatrics, 3rd Faculty of Medicine and University Hospital Královské Vinohrady, Charles University in Prague, Czech Republic
* Corresponding author: Department of Pediatrics, Klatovy Hospital, Klatovy, Czech Republic; e-mail: kutilek@nemkt.cz

Received: 13 December 2019
Accepted: 12 August 2021
Published online: 11 November 2021

Acta Medica (Hradec Králové) 2021; 64(3): 187–192
https://doi.org/10.14712/18059694.2021.32

INTRODUCTION

Osteogenesis imperfecta (OI) is a group of genetic skeletal disorders with high bone turnover, low bone mass and increased bone fragility with multiple low-energy trauma fractures. Bisphosphonates, such as intravenous pamidronate or zoledronate, oral alendronate or risedronate are used to increase bone mineral density and reduce number of fractures in patients with OI (1, 2), several studies also reported improved function and mobility after bisphosphonate treatment (1–3).

Ibandronate, an effective antiresorptive agent, is widely used in the treatment of postmenopausal and male osteoporosis (4, 5). So far, it has been only scarcely used in children with low bone mineral density (BMD) and recurrent fractures (6–11). We present three patients with OI treated with once monthly oral ibandronate.

CASE REPORTS

CASE REPORT 1

The first patient was a male with type IV OI, based on clinical features (recurrent fractures, blue sclerae, dentinogenesis imperfecta, stunted growth, hyperkyphosis of the thoracic spine, long bone deformities). His father was also suffering from OI, with multiple fractures of the extremities and vertebrae. Our patient suffered 40 low-energy trauma fractures until the age of 11 years (i.e. mean 3.6 fractures/year) (Figure 1a). Afterwards, he was started on weekly oral 70 mg alendronate, together with calcium and vitamin D. This treatment, performed at a different healthcare facility, translated into a rapid drop in number of fractures and impressive increase in spinal BMD (Figure 1a, b). After nine years of treatment, alendronate was discontinued, due to occassional gastrointestinal discomfort (heartburn) and possible risks of long term bisphosphonate therapy (potential risks of jaw osteonecrosis and atypical femoral fractures). After the withdrawal of alendronate, alleviation of heartburn followed. However, after 12 months of drug holliday, at the age of 21 years, he complained about severe pain in the extremities and backpain. X-rays did not reveal any signs of atypical femoral fractures, neither new vertebral fractures. There was a 5% drop in spinal bone mineral density (L1–L4 BMD; g/cm^2; DXA Lunar), and in relevant Z-score (Figure 1b). Shortly afterwards he suffered a low-energy trauma fracture of the right tibia, infraction of the 5th metacarpal bone of the right hand and fracture of the rib after an episode of coughing. He was restarted on bisphosphonates, this time on oral ibandronate (150 mg tablet) once monthly. He was also receiving oral calcium (1000–1500 mg/day) and vitamin D (cholecalciferol 1000–1500 IU/day). This was followed by an alleviation of pain within two months and another increase in spinal BMD (g/cm^2) after one (+4.1%) and two years (+6.5%), respectively, and a corresponding increase in Z-score (Figure 1b). Blood count, basic biochemical parameters (serum levels of sodium – S-Na, potassium – S-K, chloride – S-Cl, calcium – S-Ca, phosphate – S-P, magnesium – S-Mg, creatinine, parathyroid hormone – S-PTH and activity of alkaline phosphatase – S-ALP, aspartate-aminotransferase – S-AST, alanin-aminotransferase – S-ALT, urinary calcium/creatinine ratio – U-Ca/U-creat and serum bone turnover markers osteocalcin – S-OC and crosslinked C-terminal telopeptide – S-CTx) were evaluated every three months. These were within normal reference ranges. In the course of ibandronate treatment there was no significant shift in laboratory markers and we noticed oscillating values of S-OC, CTx. No new fractures occurred (Fig. 1a), he did not experience any adverse events.

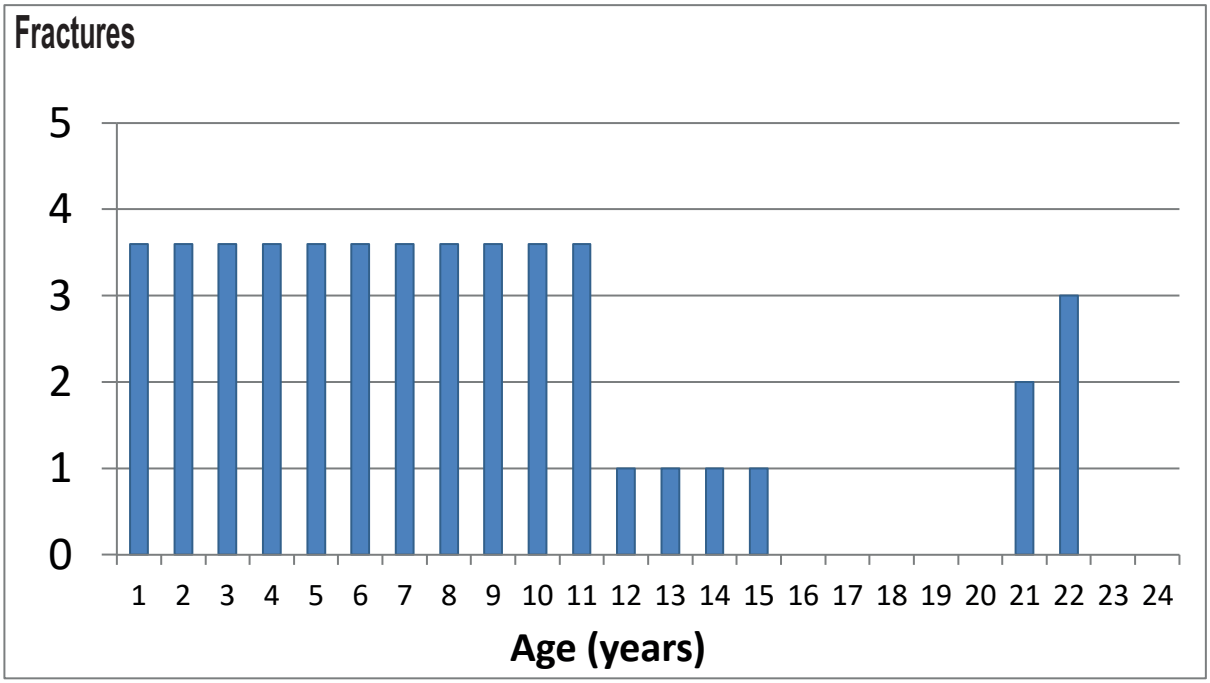

Fig. 1a Changes in the number of low-energy trauma fractures in patient No. 1 The patient suffered 40 fractures until the age of 11 years, i.e. average 3.6 fractrues per year. Alendronate treatment between the age of 12 and 20 years and ibandronate therapy between year 22 and 24, respectively.

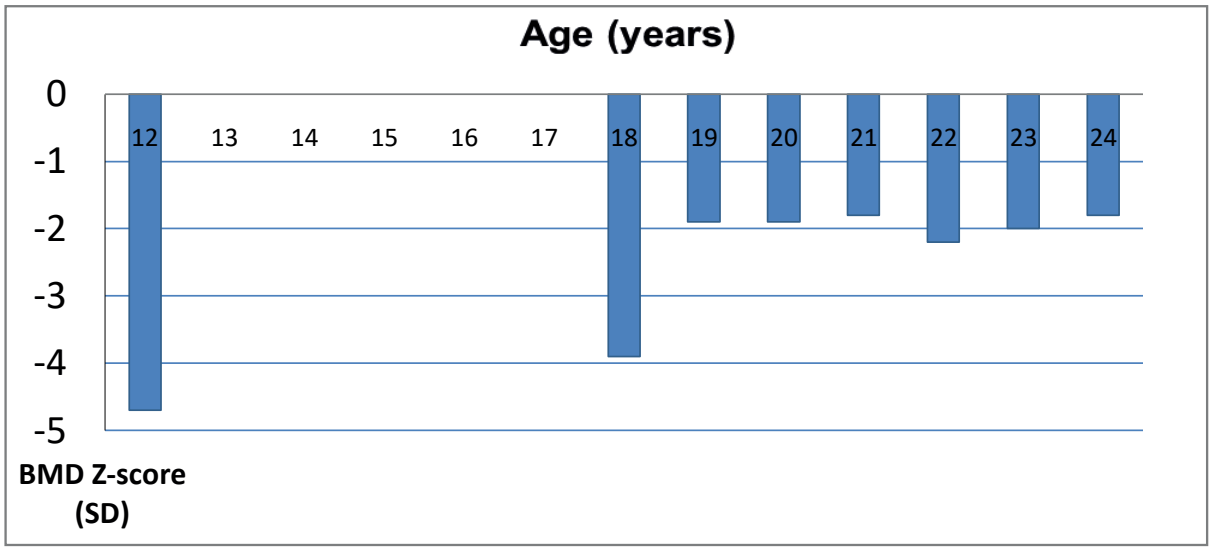

Fig. 1b Changes in spinal (L1–L4) bone mineral density (BMD; Z-score) in patient No. 1 in the course of the alendronate (age 12–20 years) and ibandronate (age 22 onwards) treatment.

CASE REPORT 2

A 14-year old boy with previous history of resolved nephrolithiasis and hypercalciuria in infancy and a low-energy trauma fracture of the second lumbar vertebra at the age of 13 years (Figure 2a). Body height was 154 cm (–1.9 SD Z-score); weight 37 kg (–1.8 SD Z-score); body mass index (BMI) 15.6 (–1.6 SD Z-score). The boy was previously diagnosed with attention deficit hyperactivity disorder (ADHD) and obsessive-compulsive disorder (OCD), and was taking clomipramin and methylphenidate, previous medication included atomoxetine.

He had triangular face, enamel tooth defects, blue sclerae, muscular hypotonia, joint and skin hyperlaxity. L1–L4 BMD was very low (0.553g/cm^2; Z-score –5.1 SD) (Figure 2b). Celiac disease, inflammatory bowel disease, hyperthyroidism, osteomalacia/rickets, parathyroid disorders and renal insufficiency were all ruled out by laboratory assessment. Blood count and biochemical parameters (S-Na, S-K, S-Cl, S-Ca, S-P, S-Mg, S-creatinine, S-PTH, S-ALP, S-AST, S-ALT, U-Ca/U-creat) were all within normal reference ranges. He fulfilled the clinical criteria for OI type I. Informed consent from the patient and his parents was obtained and he was started on once monthly oral ibandronate (150 mg/tablet), at the age of 14 years and 6 months. He was also receiving oral calcium (1000–1500 mg/day) and cholecalciferol 1000–1500 IU/day. The drugs were applied by his parents. After four months his spinal BMD (g/cm^2) increased by 13%, together with an increase in relevant Z-score; (Figure 2b) and after further nine months (i.e. 13 months of treatment) we noticed a dramatic increase in his BMD by 41% (g/cm^2)

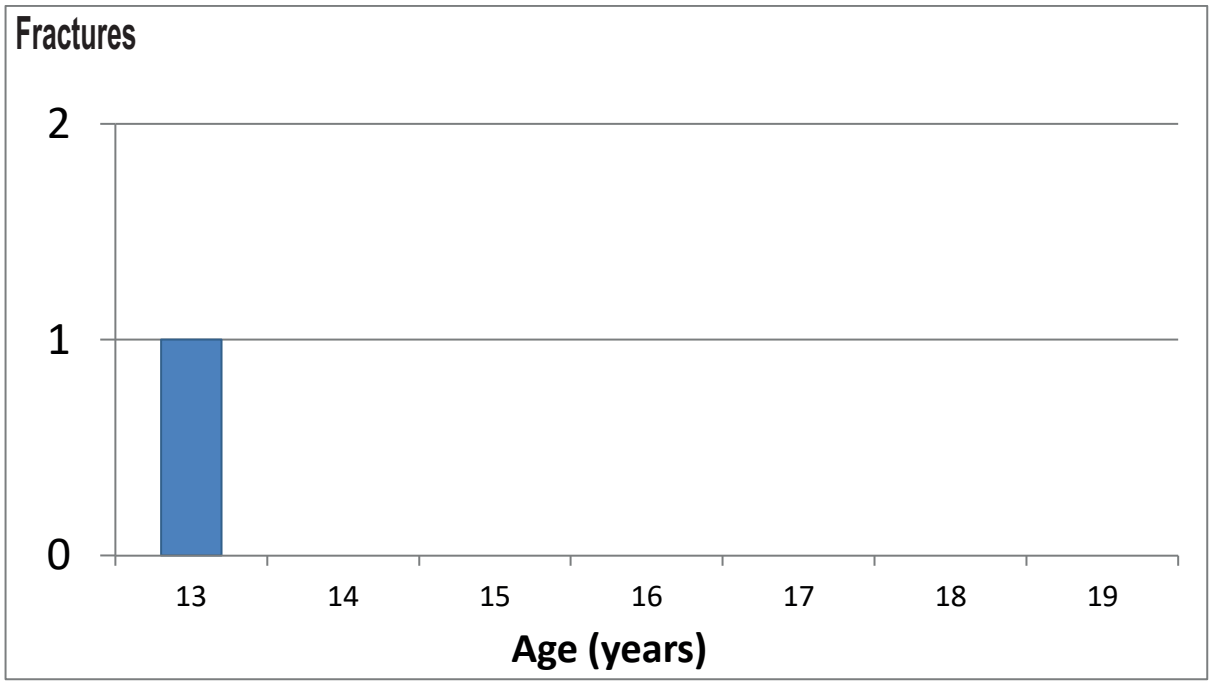

Fig. 2a Number of low-energy trauma fractures in patient No. 2. Ibandronate was administered between the age of 14.5 and 16.8 years.

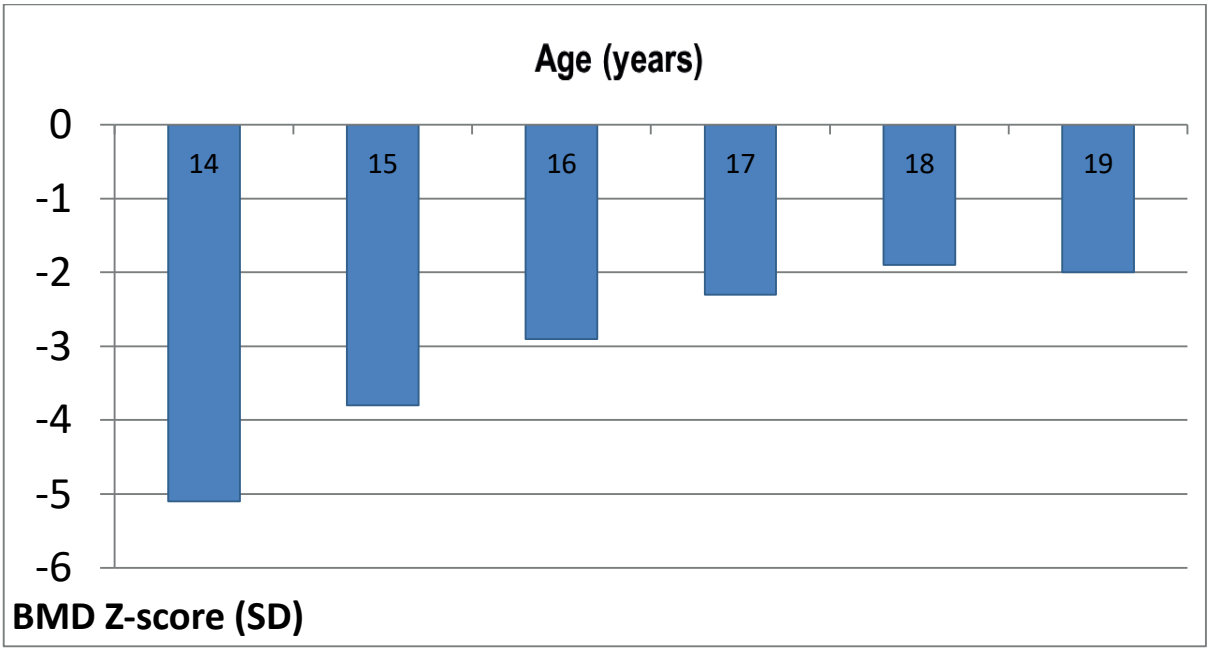

Fig. 2b Changes in L1–L4 BMD (Z-score) in patient No. 2 in the course of the ibandronate treatment. Ibandronate was administered between the age of 14.5 and 16.8 years.

compared to baseline, together with an increase in Z-score (Figure 2b). After another 15 months of ibandronate therapy, there was an additional increase in L1–L4 BMD (g/cm^2) of +13%; in total an increase by +60% and a corresponding increase in Z-score after 28 months of ibandronate treatment, when compared to baseline values (Figure 2b). There were no alterations in the biochemical parameters (S-blood urea nitrogen, S-Na, S-K, S-Cl, S-Ca, S-P, S-Mg, S-creatinine, S-PTH, S-ALP, S-AST, S-ALT, U-Ca/U-creat) that were assessed every three months, and no further occurrence of fractures. However, we noticed mild leukopenia on months 12 and 15 (leukocytes 7.8...5.3...6.74....4.5...3.9...3.8...4.3...4.0 7 × 10^9/L; normal 4–10 × 10^9/L) with a further drop in white blood cells on month 24 and 27, respectively (3.16...2.7 × 10^9/L). Other blood elements were not affected. Therefore, the patient was also followed-up by a pediatric hematologist since month 14. Ibandronate treatment was discontinued on month 28, at the age of 16 years and 10 months. We noticed a tendency toward an improvement in white blood cell number on months 32 and 35 (3.08 and 3.26 × 10^9/L), respectively. One year later, at the age of 18 years, his L1–L4 BMD (g/cm^2) further increased by 9%, with a corresponding increase in Z-score , and at the age of 19 years the L1–L4 BMD remained stable (Figure 2b). He had no new dental problems, neither gastrointestinal irritation. At the age of 19 years his body height was 174 cm (–0.9 SD Z-score) and body weight 57 kg (–1.5 SD Z-score), BMI 18.8 (–1.1 SD Z-score).

CASE REPORT 3

A girl with blue sclerae, skin and joint laxity, muscular hypotonia, who suffered four low-energy trauma fractures of the limbs between the age of six months and four years (Figure 3a). The diagnosis of OI type I was established on basis of phenotype and personal history by the clinical genetist. Between the age of five and eight years no fractures occurred in spite of low BMD Z-score (Figure 3a, b). At the age of nine years she experienced a left wrist fracture after a minor injury. At the age of 11 years and 6 months years she suffered left acetabular fracture and a left elbow fracture, rerspectively. Body height was then 148 cm (–0.3 SD Z-score), body weight 30 kg (–1.2 SD Z-score); BMI 13.7 (–1.5 SD Z-score). L1–L4 BMD at the age of 12 years was low (Figure 3b). Blood count and biochemical parameters (S-Na, S-K, S-Cl, S-Ca, S-P, S-Mg, S-creatinine, S-PTH, S-ALP, S-AST, S-ALT, U-Ca/U-creat) were all within normal reference ranges. Informed consent from the patient and her parents was obtained and she was started on oral ibandronate (150 mg/tablet) once-a-month at 12 years of age. She was also receiving oral calcium (1000–1500 mg/day) and cholecalciferol 1000–1500 IU/day. The drugs were applied by her parents. After one year we noticed a significant L1–L4 BMD (g/cm^2) increase of +31% and a relevant increase in Z-score, and after another year of therapy an additional increase of +23.8%; in total an increase by +62% after two years of ibandronate treatment compared to baseline values. There was also a corresponding increase in Z-score (Figure 3b). There were no alterations in the laboratory parameters (S-blood urea nitrogen, S-Na, S-K, S-Cl, S-Ca, S-P, S-Mg, S-creatinine, S-PTH, S-ALP, S-AST, S-ALT, U-Ca/U-creat) that were assessed every three months and no further occurrence of fractures. At the age of 15 years, there was further increase in L1–L4 BMD (+18% per year, in total +92% compared to the baseline values). A year later (age 16 years), the L1-L4 BMD value (g/cm^2) remained stable and unchanged, however with a decrease in Z-score, fortunately within normal reference range (Figure 3b) and the ibandronate treatment was discontinued. No dental problems occurred, she did not suffer from gastrointestinal irritation. At the age of 16 years her body height was 165 cm (–0.2 SD Z-score) and body weight 47 kg (–0.9 SD Z-score), BMI 17.3 (–1.5 SD Z-score). She is still under close surveillance, her BMD to be assessed once-a-year.

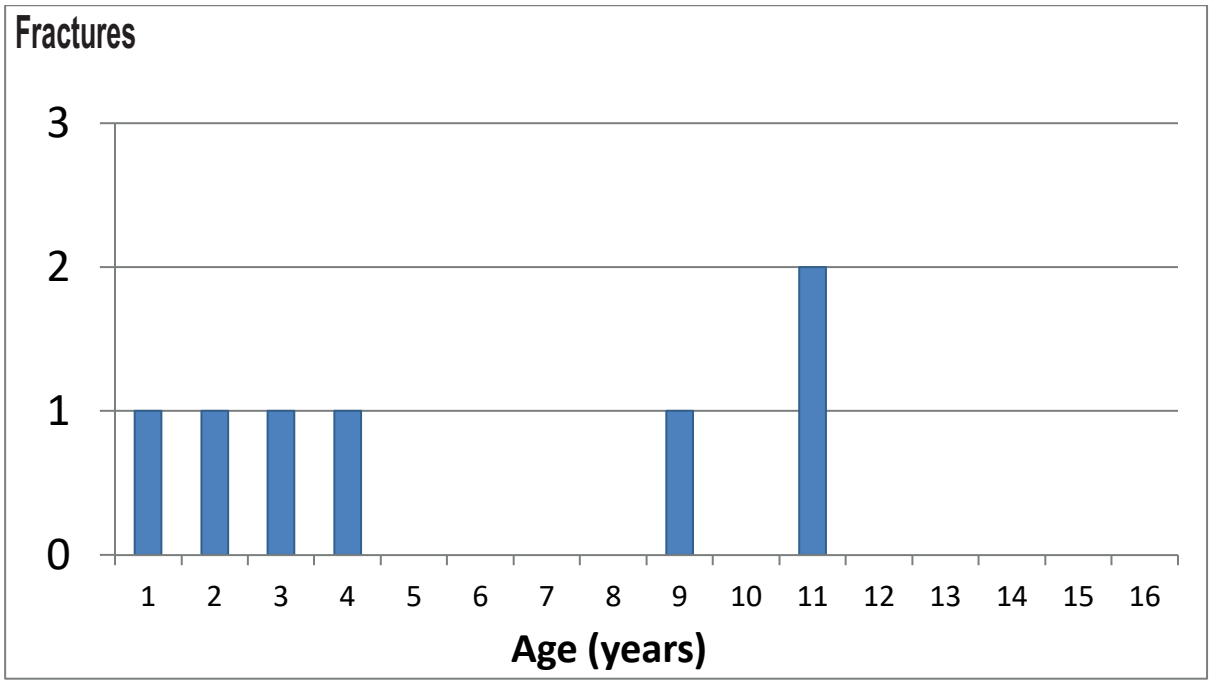

Fig. 3a Number of low-energy trauma fractures in patient No. 3.

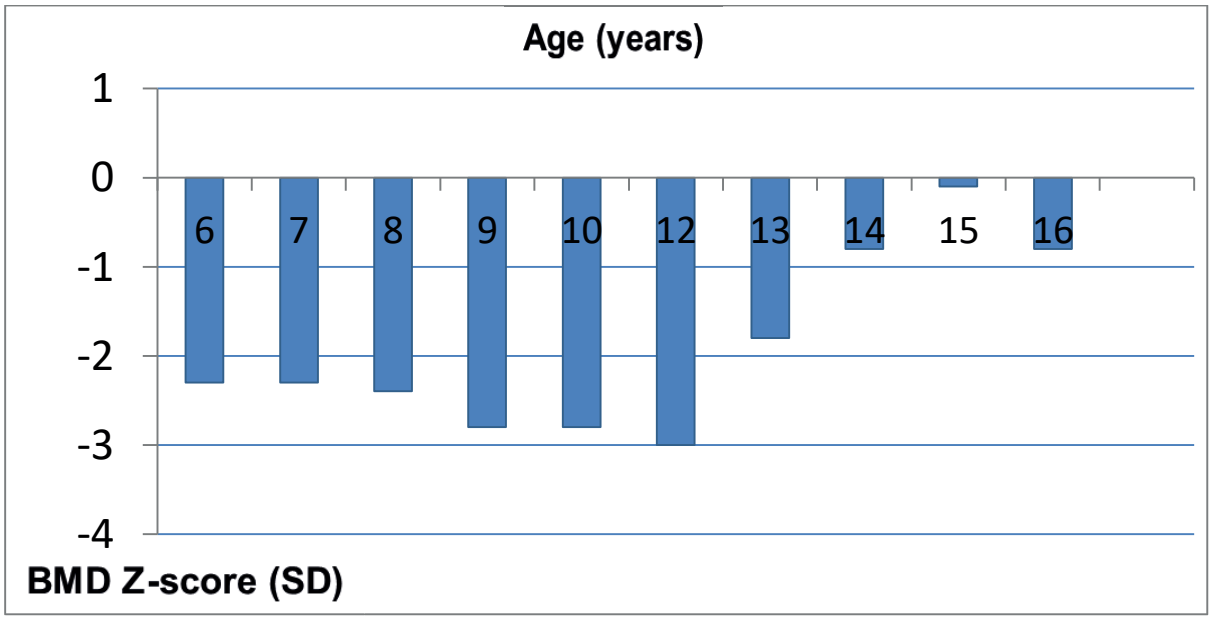

Fig. 3b Changes in L1–L4 BMD (Z-score) in patient No. 3. Ibandronate treatment was started at the age of 12 years, discontinued at the age of 16 years.

DISCUSSION

Ibandronate is an effective drug in the treatment of postmenopausal and male osteoporosis. There is just one report concerning intravenous (i.v.) ibandronate in the therapy of children with OI, where ibandronate was superior to oral calcitriol (7). In a report by Ipach et al. (8), i.v. ibandronate infused every 3 months to 27 patients with OI had an inhibitory effect on bone turnover markers. We have previously published reports on the beneficial effect of once-montly orally administered ibandronate in children and adolescents with osteoporosis, where one to three years treatment increased spinal BMD and resulted in fracture reduction (10–11). In the current report, our three patients with OI benefited from the ibandronate treatment by means of increased spinal BMD and absence of new fractures. The first patient in this report certainly experienced positive effect of alendronate during the first nine years of bisphosphonate therapy. However, discontinuation of antiresorptive therapy resulted in a drop in BMD and recurrence of fractures, where introduction of ibandronate proved to be a rescue therapy, resulting in an increase in spinal BMD, alleviation of pain and absence of fractures. The other two children with OI were treatment-naive and ibandronate therapy dramatically improved their spinal BMD, as evidenced in absolute values and respective Z-scores (Figures 2b, 3b). Surprisingly, there was no corresponding drop in S-ALP in the course

of BMD increase. Both patients 2 and 3 give evidence that better treatment effect with bisphosphonates could be expected in patients with more pronounced bone mineral density deterioration. The fact, that L1–L4 BMD further increased and then remained stable even after discontinuation of ibandronate therapy in patient 2, might confirm the continuous beneficial effect of bisphosphonates on BMD even after the drug withdrawal. Although it is tempting, the impressive increase in L1–L4 BMD can not be solely attributed either to the onset of puberty or the effect of ibandronate. The improvement in BMD is very likely to be the result of bisphosphonate treatment, although puberty must have certainly contributed as well. In patient 3, the L1–L4 BMD value (g/cm^2) at the age of 16 years remained stable and unchanged, but with a decrease in Z-score, however within normal reference range**.** This annual change in BMD Z-score could be explained by the fact that BMD significantly increases in healthy population in this age and the unchanged absolute value in g/cm^2 translated into a decrease in Z-score. However, in spite of this fact, no new fractues occurred in the observed time period. The ibandronate treatment did not adversely affect the patients'growth velocity, as evidenced by the basic anthropometric data.

Leukopenia and agranulocytosis has been observed after intravenously administered zoledronate (12). Concerning leukopenia in patient No. 2, we can't rule out the role of ibandronate therapy in this adverse event, however clomipramin and methylphenidate medication could have contributed as well. Previously, changes in white blood count have been repeatedly reported after clomipramin (13, 14) and methylphenidate medication (15), respectively, but never after ibandronate. Due to safety issues and due to the fact that patient's BMD was steadily improving and almost reached the low-normal level of –2 SD Z-score, we decided to discontinue the ibandronate therapy and opted for drug holiday.

In conclusion, once-monthly oral ibandronate increased BMD and most probably improved bone quality in young patients with OI. Ibandronate, as well as other antiresorptive bone drugs, is an off-label drug and should be used only in the context of an established clinical program with specialist consultation (1, 2, 10, 11).

ACKNOWLEDGEMENTS

This work was presented at The 9th International Conference on Children's Bone Health (ICCBH), June 22–25 2019; Salzburg, Austria.

REFERENCES

1. Sam JE, Dharmalingam M. Osteogenesis imperfecta Indian J Endocr Metab 2017; 21: 903–8.
2. Dwan K, Phillipi CA, Steiner RD, Basel D.Bisphosphonate therapy for osteogenesis imperfecta. Cochrane Database Syst Rev 2016 Oct 19; 10:CD005088
3. Constantino CS, Krzak JJ, Fial AV, et al. Effect of bisphosphonates on function and mobility among children with osteogenesis imperfecta: A systematic review. J Bone Miner Res PLUS 2019; 3/10: e10216.
4. Reginster JY, Adami S, Lakatos P, et al. Efficacy and tolerability of once-monthly oral ibandronate in postmenopausal osteoporosis: 2 year results from the MOBILE study. Ann Rheum Dis 2006; 65: 654–61.
5. Orwoll ES, Binkley NC, Lewiecki EM, Gruntmanis U, Fries MA, Dasic G. Efficacy and safety of monthly ibandronate in men with low bone density. Bone 2010; 46(4): 970–6.
6. Cundy T, Wheadon L, King A. Treatment of idiopathic hyperphosphatasia with intensive bisphosphonate therapy. J Bone Miner Res 2004; 19: 703–11.
7. Li M, Xia WB, Xing XP, et al. Benefit of infusions with ibandronate treatment in children with osteogenesis imperfecta. Chin Med J 2011; 124: 3049–53.
8. Ipach I, Kluba T, Wolf P, Pontz B, Mittag F. The influence of ibandronate treatment on bone density and biochemical bone markers in patients with osteogenesis imperfecta. Orthop Rev (Pavia) 2012; 4: e29.
9. Grenda R, Karczmarewicz E, Rubik J, et al. Bone mineral disease in children after renal transplantation in steroid-free and steroid-treated patients—a prospective study. Pediatr Transplant 2011; 15: 205–13.
10. Kutilek S, Plasilova I, Nemec V. Once-monthly oral ibandronate treatment in an adolescent with recurrent fractures and inadequately low bone mass. J Paediatr Child Health 2012; 48: 622–3.
11. Kutilek S, Plasilova I, Langer J. Ibandronate in the treatment of pediatric osteoporosis. Indian Pediatr 2016; 53: 927.
12. Karahasanovic A, Thorsteinsson AL, Bjarnason NH, Eiken P. Long-term leukopenia in a lung transplanted patient with cystic fibrosis treated with zoledronic acid: a case report. Osteoporos Int 2016; 27: 2621–5.
13. van der Klauw MM, Goudsmit R, Halie MR, van't Veer MB, Herings RM, Wilson JH, Stricker BH. A population-based case-cohort study of drug-associated agranulocytosis. Arch Intern Med 1999; 159: 369–74.
14. Hunt KA, Resnick MP. Clomipramine-induced agranulocytosis and its treatment with G-CSF. Am J Psychiatry 1993; 150: 522–3.
15. Burke MS, Josephson A, Lightsey A. Combined methylphenidate and imipramine complication. J Am Acad Child Adolesc Psychiatry 1995; 34: 403–4.